The transcription factor myocyte enhancer factor-2 (MEF2) in cardiac hypertrophy and heart failure

Ralph J. van Oort

The work described in this thesis was performed at the Hubrecht Laboratory (Netherlands Institute for Developmental Biology), within the framework of the Graduate School of Developmental Biology.

Hubrecht Laboratory, Netherlands Institute for Developmental Biology of the Royal Netherlands Academy of Arts and Sciences (KNAW), Uppsalalaan 8, 3584 CT Utrecht, The Netherlands.

ISBN: 978-90-393-4498-9

The transcription factor myocyte enhancer factor-2 (MEF2) in cardiac hypertrophy and heart failure

De transcriptie factor myocyte enhancer factor-2 (MEF2) in cardiale hypertrofie en hartfalen
(met een samenvatting in het Nederlands)

Proefschrift

ter verkrijging van de graad van doctor aan de Universiteit Utrecht
op gezag van de rector magnificus, prof. dr. W.H. Gispen,
ingevolge het besluit van het college voor promoties
in het openbaar te verdedigen
op dinsdag 24 april 2007 des middags te 2.30 uur

door

Ralph Jeroen van Oort

geboren op 25 april 1977, te Zoelen

Promotor: Prof. Dr. H.C. Clevers
Co-promotor: Dr. L.J. de Windt

Financial support by the Netherlands Heart Foundation for the publication of this thesis is gratefully acknowledged.

CONTENTS

Chapter 1	Introduction	7
Chapter 2	MEF2 activates a genetic program promoting chamber dilation and contractile dysfunction in calcineurin-induced heart failure	17
Chapter 3	MEF2 activates DMPK expression promoting cardiomyocyte elongation and sarcomere degeneration	45
Chapter 4	MEF2 inactivation fails to protect Muscle LIM Protein (MLP) deficient mice from dilated cardiomyopathy	73
Chapter 5	MEF2 transcriptional activity is required for cardiac mitochondrial adaptation in pressure overload and protects against cardiac dysfunction	87
Chapter 6	General discussion	103
Samenvatting		112
Dankwoord		114
Curriculum Vitae		116
List of publications		117

Chapter 1

Introduction

INTRODUCTION

Cardiac hypertrophy and heart failure

Heart failure, defined as the inability of the heart to cope with the metabolic demands of the peripheral tissues, represents the fastest growing subclass of cardiovascular diseases [1-3]. Because of the epidemic proportions it has taken in the past decades, medical and scientific interest in heart failure has been greatly stimulated [4]. Heart failure is the common end-stage for various forms of heart disease with heterogeneous etiologies. The single most powerful predictor of heart failure is sustained cardiac hypertrophy [5, 6]. For this reason, much effort is currently dedicated to elucidate the cellular and molecular determinants underlying hypertrophic remodeling of the heart.

Embryonic growth of the heart occurs primarily through proliferation of cardiac myocytes. Soon after birth, cardiomyocytes withdraw from the cell cycle and cardiac growth can only occur by an increase in size of the individual myocytes (hypertrophy). While this is part of normal postnatal development and thought to initially be a beneficial response of the adult heart in order to adapt to stress stimuli, it is often accompanied by reactivation of a “fetal” cardiac gene program and contributes to heart failure development [7-10]. Clinical conditions that induce cardiac hypertrophy include chronic hypertension, myocardial infarction, coronary artery disease, valvular defects, myocarditis, endocrine disorders and contractile dysfunction from inherited mutations in cardiac structural genes [4, 11-13]. Pathological hypertrophy frequently progresses into dilated cardiomyopathy, a chronic disorder of the heart muscle [6]. In humans, end-stage dilated cardiomyopathy is characterized by poorly contractile and dilated ventricles, accompanied by lengthening of individual cardiomyocytes, cardiomyocyte side-to-side slippage, loss of myofibrils, severe changes in cytoskeletal architecture and accumulation of collagen in perivascular and interstitial spaces (fibrosis) [14, 15].

The genetic underpinnings underlying these pathological myocardial alterations remain largely elusive. The initial hypertrophic response is evoked by activation of several intracellular signaling cascades [11, 16, 17]. These signaling pathways are interconnected and often culminate in the nucleus on only a few transcriptional regulators [18-20]. With the hope of revealing novel therapeutic targets in the treatment of heart failure, much effort is undertaken to unravel the role of these select transcription factors. One of the common downstream targets for several stress cascades in the heart is the transcription factor family known as myocyte enhancer factor-2 (MEF2).

Myocyte enhancer factor-2

MEF2 was originally identified as a DNA binding activity that recognizes conserved A/T-rich elements associated with numerous muscle-specific genes [21]. During the years, four MEF2 genes, *Mef2a*, *-b*, *-c*, and *-d*, have been characterized in vertebrates, with an expression pattern and function that extends beyond striated muscle. MEF2 transcription factors share high homology in an amino-terminal MADS (MCM1, Agamous, Deficiens, and Serum response factor) box and an adjacent MEF2-specific domain, which together mediate dimerization and binding to the consensus DNA sequence $CTA(A/T)_4TA(G/A)$ [22, 23]. Before recognition of the consensus site, MEF2 factors must homo- or hetero-dimerize, but given the extensive alternative splicing that occurs within the four MEF2 isoforms, many associations are possible among these factors [22].

By now, MEF2 factors have been implicated in the embryonic development of cardiac, skeletal, and smooth muscle [24, 25], and several lines of evidence suggest involvement in the progress to postnatal heart disease [18]. In general, *Mef2a-d* genes are widely expressed in the adult vertebrate organism, although a number of specific regulatory functions have been identified in immune, skeletal muscle, cardiac muscle, and neuronal cells [26-28].

MEF2 factors are related to another MADS-box containing transcription factor known as serum response factor (SRF) [29]. In the heart, myocytes undergo developmental and pathophysiological hypertrophy in response to neuro-endocrine-, mitogen- and stress-stimulation. These types of stimulation activate intracellular signal transduction cascades resulting in the modification of transcription factor activity and the reprogramming of cardiac gene expression. Similar to SRF, members of the MEF2 family have been implicated in regulating inducible gene expression in response to such stimuli [22, 29, 30]. A number of lines of evidence suggest that MEF2 factors might regulate gene expression in response to stimuli that underlie the cardiac hypertrophic response.

MEF2 in cardiac hypertrophy

In normal adult myocardium, MEF2 exhibits only basal activity, which is likely required for the maintenance of the cardiomyocyte contractile apparatus and energy metabolism [31, 32]. In cardiac disease, however, circumstantial evidence suggests that MEF2 factors serve as a transcriptional platform for prohypertrophic signaling cascades, including calcineurin, calcium/calmodulin-dependent protein kinase (CaMK), big mitogen-activated protein kinase (MAPK)-1 (BMK-1), and p38 MAPK [33, 34]. Additionally, stress signaling stimulates MEF2 transcriptional activity by causing the nuclear export of class II histone deacetylases (HDACs), which directly interact with MEF2 factors and suppress their activity [35]. Nuclear export of class II HDACs is mediated by stress-responsive protein kinases

including CaMK, protein kinase C (PKC) and protein kinase D (PKD), which promote the dissociation of class II HDACs from MEF2 and de-repress MEF2 activity [32, 36, 37]. In line, mice lacking HDAC9 and/or HDAC5 are hypersensitive to cardiac stress signaling and display excessive cardiac growth and fetal gene induction [38]. Additional evidence that MEF2 regulates stress-responsive signaling derives from the use of a MEF2 β-galactosidase reporter transgene [39], which showed enhanced staining in hypertrophic hearts from calcineurin and CaMK transgenic mice, and in HDAC9 knockout mice [32, 38].

Furthermore, MEF2 has been implicated in a more physiological model for hypertrophy as its DNA binding activity was shown to be increased in hearts of rats subjected to both pressure and volume overload [34, 40]. MEF2 DNA binding activity was also shown to be enhanced in hearts from mdx:Myod$^{-/-}$ mice, a murine model for muscle dystrophy [41].

Moreover, *Mef2c* null mice have altered cardiac gene expression and die during early embryonic development with arrested heart tube morphogenesis, suggesting a critical role in developmental heart growth [28]. Mice expressing a dominant negative mutant of MEF2C in the heart also die during postnatal development with attenuated ventricular growth [41]. Lastly, a portion of *Mef2a* null mice die suddenly during the perinatal period with dilated right ventricles, myofibrillar disorganization, and mitochondrial structural abnormalities [31].

Despite these circumstantial observations that suggest a role for MEF2 factors as transcriptional integrators for cardiac hypertrophic growth, a direct genetic assessment of MEF2 activation in adult cardiac muscle remains to be tested.

OUTLINE OF THIS THESIS

In the present thesis, we report the existence of synergistic interactions between the NFAT and MEF2 transcription factors in the heart triggered by calcineurin (CnA) signaling. To circumvent the embryonic-lethality and mitochondrial deficiency associated with germline null mutations for MEF2C and MEF2A, respectively, we used conditional transgenesis to express a dominant-negative form of MEF2 (DNMEF2) in the murine postnatal heart and combined this with magnetic resonance imaging to investigate MEF2 transcriptional function in Ca^{2+}/CnA induced cardiac remodeling. Surprisingly, end-diastolic and end-systolic ventricular dimensions and contractility were normalized in the presence of severely hypertrophied LV walls upon MEF2 inhibition in calcineurin transgenic mice. In line, we generated lines of transgenic mice expressing MEF2A in the heart, which primarily displayed chamber dilation. Microarray profiling indicated that

MEF2 promotes a gene profile functioning primarily to or at the nucleus, the cytoskeletal and microtubular network, and mitochondria **(Chapter 2)**.

To test the mechanistic underpinnings how MEF2 transcriptional activity may promote features of dilated cardiomyopathy, we reverted to an *in vitro* cardiomyocyte culture system. Cultured ventricular myocytes subjected to adenoviral delivery of wildtype MEF2A or constitutively active MEF2 primarily underwent myocyte elongation, accompanied by sequential loss of myofibrils and redistribution of focal adhesion sites. Genome-wide gene chip analysis in a ventricular muscle cell line with inducible MEF2 activation provided further mechanistic insights into MEF2 function and target genes. Functional clustering of MEF2 target genes revealed an overrepresentation of genes involved in cytoskeletal remodeling and cell-matrix adhesion. We describe myotonic dystrophy protein kinase (DMPK) as a direct transcriptional target for MEF2. By siRNA-mediated knockdown of DMPK expression, we demonstrate the involvement of this gene in the pathological aspects of MEF2 induced cardiomyocyte remodeling **(Chapter 3)**.

Given the resemblance between MEF2 induced cardiac remodeling and the cardiac phenotype of mice lacking Muscle LIM Protein (MLP), an established mouse model for inherited dilated cardiomyopathy, we analyzed MEF2 transcription factor activity in MLP knockout mice by genetic crossbreeding with MEF2 reporter mice. Following confirmation that MEF2 activity was severely upregulated, we used conditional transgenesis to express a dominant-negative form of MEF2 (DNMEF2) in the murine MLP deficient heart and combined this with echocardiographic analysis to examine the effect on cardiac remodeling. Surprisingly, histological and functional analyses indicated that MEF2 inhibition in MLP knockout mice did not have any effect on the genesis of dilated cardiomyopathy **(Chapter 4)**.

Finally, the significance of MEF2 transcriptional activity was assessed in the setting of a more physiological model of biomechanical stress in the form of chronic murine pressure overload using conditional transgenesis to express a dominant-negative form of MEF2 (DNMEF2) in the postnatal heart. Surprisingly, echocardiography indicated that MEF2 inhibition did not improve end-diastolic and end-systolic ventricular dimensions and contractility as observed in calcineurin transgenic hearts with conditional MEF2 inhibition. In fact, cardiac function was significantly worsened in the setting of MEF2 inhibition, which could be correlated with specific defects in mitochondrial adaptation during pressure overload **(Chapter 5)**.

Taken together, in this thesis we demonstrate that MEF2 activation in the heart does not evoke the classic hypertrophic response, yet promotes a gene program primarily involved in processes associated with dilated cardiomyopathy.

Although MEF2 activation is required for maladaptive cardiac remodeling downstream of calcineurin signaling, its activity is not the sole trigger in certain forms of dilated cardiomyopathy, and is even necessary for the adaptive response of the heart during pressure overload.

REFERENCES

1. Braunwald E., Bristow M.R. Congestive heart failure: fifty years of progress. Circulation 2000;102(20 Suppl 4):IV14-23.
2. Lloyd-Jones D.M., Larson M.G., Leip E.P., Beiser A., D'Agostino R.B., Kannel W.B., Murabito J.M., Vasan R.S., Benjamin E.J., Levy D. Lifetime risk for developing congestive heart failure: the Framingham Heart Study. Circulation 2002;106(24):3068-72.
3. Levy D., Kenchaiah S., Larson M.G., Benjamin E.J., Kupka M.J., Ho K.K., Murabito J.M., Vasan R.S. Long-term trends in the incidence of and survival with heart failure. N Engl J Med 2002;347(18):1397-402.
4. Ritter O., Neyses L. The molecular basis of myocardial hypertrophy and heart failure. Trends Mol Med 2003;9(7):313-21.
5. Berenji K., Drazner M.H., Rothermel B.A., Hill J.A. Does load-induced ventricular hypertrophy progress to systolic heart failure? Am J Physiol Heart Circ Physiol 2005;289(1):H8-H16.
6. Hunter J.J., Chien K.R. Signaling pathways for cardiac hypertrophy and failure. N Engl J Med 1999;341(17):1276-83.
7. Grossman W., Jones D., McLaurin L.P. Wall stress and patterns of hypertrophy in the human left ventricle. J Clin Invest 1975;56(1):56-64.
8. Cooper G.t. Basic determinants of myocardial hypertrophy: a review of molecular mechanisms. Annu Rev Med 1997;48:13-23.
9. Olson E.N., Schneider M.D. Sizing up the heart: development redux in disease. Genes Dev 2003;17(16):1937-56.
10. Oka T., Xu J., Molkentin J.D. Re-employment of developmental transcription factors in adult heart disease. Semin Cell Dev Biol 2006.
11. Heineke J., Molkentin J.D. Regulation of cardiac hypertrophy by intracellular signalling pathways. Nat Rev Mol Cell Biol 2006;7(8):589-600.
12. Lips D.J., deWindt L.J., van Kraaij D.J., Doevendans P.A. Molecular determinants of myocardial hypertrophy and failure: alternative pathways for beneficial and maladaptive hypertrophy. Eur Heart J 2003;24(10):883-96.
13. Schwartz K., Mercadier J.J. Molecular and cellular biology of heart failure. Curr Opin Cardiol 1996;11(3):227-36.
14. Beltrami C.A., Finato N., Rocco M., Feruglio G.A., Puricelli C., Cigola E., Sonnenblick E.H., Olivetti G., Anversa P. The cellular basis of dilated cardiomyopathy in humans. J Mol Cell Cardiol 1995;27(1):291-305.
15. Schaper J., Froede R., Hein S., Buck A., Hashizume H., Speiser B., Friedl A., Bleese N. Impairment of the myocardial ultrastructure and changes of the cytoskeleton in dilated cardiomyopathy. Circulation 1991;83(2):504-14.
16. Frey N., Olson E.N. Cardiac hypertrophy: the good, the bad, and the ugly. Annu Rev Physiol 2003;65:45-79.
17. Molkentin J.D., Dorn I.G., 2nd. Cytoplasmic signaling pathways that regulate cardiac hypertrophy. Annu Rev Physiol 2001;63:391-426.

18. Frey N., Katus H.A., Olson E.N., Hill J.A. Hypertrophy of the heart: a new therapeutic target? Circulation 2004;109(13):1580-9.
19. McKinsey T.A., Olson E.N. Toward transcriptional therapies for the failing heart: chemical screens to modulate genes. J Clin Invest 2005;115(3):538-46.
20. Akazawa H., Komuro I. Roles of cardiac transcription factors in cardiac hypertrophy. Circ Res 2003;92(10):1079-88.
21. Gossett L.A., Kelvin D.J., Sternberg E.A., Olson E.N. A new myocyte-specific enhancer-binding factor that recognizes a conserved element associated with multiple muscle-specific genes. Mol Cell Biol 1989;9(11):5022-33.
22. Black B.L., Olson E.N. Transcriptional control of muscle development by myocyte enhancer factor-2 (MEF2) proteins. Annu Rev Cell Dev Biol 1998;14:167-96.
23. McKinsey T.A., Zhang C.L., Olson E.N. MEF2: a calcium-dependent regulator of cell division, differentiation and death. Trends Biochem Sci 2002;27:40-47.
24. Lilly B., Zhao B., Ranganayakulu G., Paterson B.M., Schulz R.A., Olson E.N. Requirement of MADS domain transcription factor D-MEF2 for muscle formation in Drosophila. Science 1995;267(5198):688-93.
25. Olson E.N., Perry M., Schulz R.A. Regulation of muscle differentiation by the MEF2 family of MADS box transcription factors. Dev Biol 1995;172(1):2-14.
26. Lyons G.E., Micales B.K., Schwarz J., Martin J.F., Olson E.N. Expression of mef2 genes in the mouse central nervous system suggests a role in neuronal maturation. J Neurosci 1995;15(8):5727-38.
27. Subramanian S.V., Nadal-Ginard B. Early expression of the different isoforms of the myocyte enhancer factor-2 (MEF2) protein in myogenic as well as non-myogenic cell lineages during mouse embryogenesis. Mech Dev 1996;57(1):103-12.
28. Lin Q., Schwarz J., Bucana C., Olson E.N. Control of mouse cardiac morphogenesis and myogenesis by transcription factor MEF2C. Science 1997;276(5317):1404-7.
29. Shore P., Sharrocks A.D. The MADS-box family of transcription factors. Eur J Biochem 1995;229(1):1-13.
30. Phiel C.J., Gabbeta V., Parsons L.M., Rothblat D., Harvey R.P., McHugh K.M. Differential binding of an SRF/NK-2/MEF2 transcription factor complex in normal versus neoplastic smooth muscle tissues. J Biol Chem 2001;276(37):34637-50.
31. Naya F.J., Black B.L., Wu H., Bassel-Duby R., Richardson J.A., Hill J.A., Olson E.N. Mitochondrial deficiency and cardiac sudden death in mice lacking the MEF2A transcription factor. Nat Med 2002;8(11):1303-9.
32. Passier R., Zeng H., Frey N., Naya F.J., Nicol R.L., McKinsey T.A., Overbeek P., Richardson J.A., Grant S.R., Olson E.N. CaM kinase signaling induces cardiac hypertrophy and activates the MEF2 transcription factor in vivo. J Clin Invest 2000;105(10):1395-406.
33. Lu J., McKinsey T.A., Nicol R.L., Olson E.N. Signal-dependent activation of the MEF2 transcription factor by dissociation from histone deacetylases. Proc Natl Acad Sci U S A 2000;97(8):4070-5.
34. Nadruz W., Jr., Kobarg C.B., Constancio S.S., Corat P.D., Franchini K.G. Load-induced transcriptional activation of c-jun in rat myocardium: regulation by myocyte enhancer factor 2. Circ Res 2003;92(2):243-51.
35. McKinsey T.A., Zhang C.L., Lu J., Olson E.N. Signal-dependent nuclear export of a histone deacetylase regulates muscle differentiation. Nature 2000;408(6808):106-11.
36. Vega R.B., Harrison B.C., Meadows E., Roberts C.R., Papst P.J., Olson E.N., McKinsey T.A. Protein kinases C and D mediate agonist-dependent cardiac hypertrophy through nuclear export of histone deacetylase 5. Mol Cell Biol 2004;24(19):8374-85.
37. Harrison B.C., Kim M.S., van Rooij E., Plato C.F., Papst P.J., Vega R.B., McAnally J.A., Richardson J.A., Bassel-Duby R., Olson E.N., McKinsey T.A. Regulation of cardiac stress signaling by protein kinase d1. Mol Cell Biol 2006;26(10):3875-88.

38. Zhang C.L., McKinsey T.A., Chang S., Antos C.L., Hill J.A., Olson E.N. Class II histone deacetylases act as signal-responsive repressors of cardiac hypertrophy. Cell 2002;110(4):479-88.
39. Naya F.J., Wu C., Richardson J.A., Overbeek P., Olson E.N. Transcriptional activity of MEF2 during mouse embryogenesis monitored with a MEF2-dependent transgene. Development 1999;126(10):2045-52.
40. Molkentin J.D., Markham B.E. Myocyte-specific enhancer-binding factor (MEF-2) regulates alpha-cardiac myosin heavy chain gene expression in vitro and in vivo. J Biol Chem 1993;268(26):19512-20.
41. Kolodziejczyk S.M., Wang L., Balazsi K., DeRepentigny Y., Kothary R., Megeney L.A. MEF2 is upregulated during cardiac hypertrophy and is required for normal post-natal growth of the myocardium. Curr Biol 1999;9(20):1203-6.

Chapter 2

MEF2 activates a genetic program promoting chamber dilation and contractile dysfunction in calcineurin-induced heart failure

Ralph J. van Oort*, Eva van Rooij*, Meriem Bourajjaj, Joost Schimmel, Maurits A. Jansen, Roel van der Nagel, Pieter A. Doevendans, Michael D. Schneider, Cees J. A. van Echteld, Leon J. De Windt

*These authors contributed equally to this work.

Circulation. 2006;114:298-308

ABSTRACT

Hypertrophic growth, a risk factor for mortality in heart disease, is driven by reprogramming of cardiac gene expression. Although the transcription factor myocyte enhancer factor-2 (MEF2) is a common end point for several hypertrophic pathways, its precise cardiac gene targets and function in cardiac remodeling remain to be elucidated.

We report the existence of synergistic interactions between the nuclear factor of activated T cells and MEF2 transcription factors triggered by calcineurin signaling. To circumvent the embryonic lethality and mitochondrial deficiency associated with germ-line null mutations for MEF2C and MEF2A respectively, we used conditional transgenesis to express a dominant-negative form of MEF2 in the murine postnatal heart and combined this with magnetic resonance imaging to assess MEF2 transcriptional function in Ca^{2+}/calcineurin-induced cardiac remodeling. Surprisingly, end-diastolic and end-systolic ventricular dimensions and contractility were normalized in the presence of severely hypertrophied left ventricular walls on MEF2 inhibition in calcineurin transgenic mice. In line, we generated lines of transgenic mice expressing MEF2A in the heart, which displayed primarily chamber dilation. Microarray profiling indicated that MEF2 promotes a gene profile functioning primarily to or at the nucleus, cytoskeletal and microtubular networks, and mitochondria.

These findings assign a novel function to MEF2 transcription factors in the postnatal heart, where they activate a genetic program that minimally affects cardiac growth yet promotes chamber dilation, mechanical dysfunction, and dilated cardiomyopathy.

INTRODUCTION

The heart responds to stress signals by hypertrophic growth, which is accompanied by activation of select transcription factors and reprogramming of cardiac gene expression. Pathological hypertrophy frequently progresses to dilated cardiomyopathy, a chronic disorder of the heart muscle. Dilation of the ventricular chamber and the associated increase in stress on the ventricular wall are often the first irreversible steps toward heart failure [1], but the genetic underpinnings of dilated cardiomyopathy remain largely elusive.

Cytoplasmic members of the Nuclear Factor of Activated T-cells (NFATc1-c4) represent a family of Ca^{2+}/calcineurin-dependent transcription factors [2] that contribute to the development of cardiac hypertrophy [3, 4]. Because DNA binding

by NFAT proteins is quite weak, NFAT family members probably rarely act alone but rather need transcriptional partners to elicit full gene activation. Ca^{2+} responsiveness of a number of muscle promoters/enhancers also has been mapped to another set of response elements recognized by the transcription factor myocyte-enhancer factor-2 (MEF2). In normal adult myocardium, MEF2 exhibits only basal activity, whereas cardiac stress signaling stimulates MEF2 transcriptional activity by causing the nuclear export of class II histone deacetylases (HDACs), which associate with MEF2 and suppress its activity [5]. In line, mice lacking HDAC9 and/or HDAC5 are hypersensitive to cardiac stress signaling and display excessive cardiac growth [6, 7]. MEF2 also serves as a transcriptional platform for several prohypertrophic signaling cascades. Although calcineurin has been reported to promote MEF2 factors by direct dephosphorylation in neurons [8-10] or by promoting ternary complex formation between NFAT and MEF2 in T-lymphocytes [11], the mechanism whereby MEF2 transcription factors are activated downstream of cardiac calcineurin signaling awaits formal experimental demonstration.

Using a multidisciplinary approach, we analyzed the mechanisms whereby MEF2 is activated downstream of calcineurin signaling in heart muscle. We tested the consequences of inactivating the transcription factor MEF2 downstream of calcineurin activation, starting from the premise that MEF2 would be involved primarily in calcineurin-induced hypertrophic remodeling of the heart muscle. The coexistence of multiple MEF2 isoforms in the adult myocardium [12], the embryonic lethal phenotype of a germ-line null mutation for MEF2C [13], and mitochondrial defects and lethal arrhythmias of a germ-line null mutation for MEF2A [14], pose a formidable barrier to using null mutations as a way to test the function of MEF2-dependent transcription in hypertrophy. To circumvent this issue, we used a Cre recombinase activated "Flox-ON" approach to obtain heart-specific overexpression of a dominant-negative form of MEF2 (DNMEF2) in transgenic mice. Surprisingly, crossbreeding of Flox-DNMEF2 mice with calcineurin transgenic mice only modestly repressed cardiac hypertrophy but profoundly reduced chamber dilation and improved contractility. Gene chip analysis of MEF2 target genes downstream of calcineurin activation provided insights into the rescue mechanisms of heart failure. Finally, we generated lines of transgenic mice expressing MEF2A in the heart that primarily displayed dilated cardiomyopathy. Our combined results are consistent with a model wherein MEF2 controls cardiac gene expression by acting as a target for Ca^{2+}-activated NFAT signaling that primarily promotes chamber dilation and loss of contractility in calcineurin-induced heart failure.

MATERIALS AND METHODS

Mice. Details on the generation of transgenic mice expressing a DNMEF2 or wild-type MEF2A are given in the expanded Methods section in the online Data Supplement. Mice expressing Cre recombinase or an activated mutant of calcineurin under control of the 5.5-kb murine cardiac α-myosin heavy chain promoter [15] (MHC-Cre and MHC-CnA transgenic mice, respectively) were described previously [3, 16].

Live cardiac magnetic resonance imaging. Details on magnetic resonance imaging are given in the expanded Methods section (see online-only Data Supplement).

Histological analysis. Hearts were arrested in diastole, perfusion fixed with 4% paraformaldehyde, and embedded in paraffin. Sections (6 μm) were cut and stained with hematoxylin and eosin (H&E).

Recombinant plasmids. All expression vectors used are provided in the expanded Methods section (see online-only Data Supplement).

Coimmunoprecipitation assays. Details on coimmunoprecipitation assays are provided in the expanded Methods section (see online-only Data Supplement).

Chromatin immunoprecipitation. Details on chromatin immunoprecipitation are given in the expanded Methods section (see online-only Data Supplement).

Recombinant Adenoviruses. C-terminal myc-tagged MEF2, encompassing residues 1 to 117 and incorporating the R24L mutation [17] and C-terminal FLAG-tagged full-length human MEF2A, were cloned into the pAdTrack-CMV viral shuttle vector [18] to generate AdDNMEF2 and AdMEF2A. AdGFP was generated as described previously [18]. An adenovirus expressing an activated mutant of calcineurin (AdCnA) was described earlier [19].

Cell culture, transfections, and luciferase assays. Isolation and culture of neonatal rat ventricular cardiomyocytes and COS7 cells were performed as described before in detail [20]. Transient transfections were performed as described [20] with FuGENE 6 reagent (Roche, Basel, Switzerland) according to the manufacturer's recommendations.

Western blot analysis. Sodium dodecyl sulfate-polyacrylamide gel electrophoresis (SDSPAGE) and blotting were performed as described in detail [20]. Antibodies included monoclonal anti-green fluorescent protein (GFP) (Santa Cruz Biotechnology, Inc, Santa Cruz, Calif, 1:500), monoclonal anti-VP16 (Santa Cruz Biotechnology, Inc, 1:500), polyclonal rabbit anti-MEF2A (Upstate Inc, Charlottesville, Va, 1:1000), and monoclonal anti-FLAG (Sigma, St. Louis, Mo, 1:5000), followed by corresponding horseradish peroxidase- conjugated secondary antibodies (Dako, Glostrup, Denmark, 1:5000) and enhanced chemiluminescence detection.

Immunocytochemistry. Neonatal rat cardiomyocyte isolation and preparation for immunofluorescence were performed as described previously in detail [20].

Agilent gene expression profiling and data analysis. RNA extraction, cRNA production, and labeling and hybridization on Agilent 22k mouse microarray slides (Agilent Technologies, Palo Alto, Calif) are described in detail in the expanded Methods section (see online-only Data Supplement). Gene classifications were assigned on the basis of publicly available software and Web sites.

Real-time polymerase chain reaction. RT-RNA material from cardiac tissue from mice was analyzed by real-time polymerase chain reaction (PCR) with the BioRad iCycler (Bio-Rad, Hercules, Calif) using SYBR Green buffer for labeling and detection. Primer sequences are available on request.

Statistical analysis. The results are presented as mean±SEM. Statistical analyses were performed with SPSS and InStat 3.0 software (GraphPad Software, Inc, San Diego, Calif) and consisted of ANOVA, followed by Tukey's posttest when group differences were detected at the 5% significance level or the Student *t* test when 2 experimental groups were compared. The authors had full access to the data and take full responsibility for their integrity. All authors have read and agree to the manuscript as written.

Figure 1. NFAT activates MEF2 transcriptional activity by direct protein-protein interaction. **A.** COS7 cells were transiently transfected with a Gal4 luciferase reporter construct and a Gal4-MEF2C fusion protein either in or not in the presence of NFATc3, activated calcineurin (ΔCnA) and p300. **B.** Transfections using a multimerized MEF2 luciferase reporter showing activation of MEF2 transcriptional activity by NFATc3, ΔCnA and p300. **C.** Protein extracts from COS7 cells transfected with empty vectors (Gal4), FLAG-NFATc3 and/or Gal4-MEF2C deletion constructs were immunoprecipitated with an anti-NFATc3 antibody and subjected to Western blotting using an anti-Gal4 antibody. **D.** Schematic overview of the Gal4-MEF2C deletion constructs and their ability to bind NFATc3 **E.** Protein extracts from COS7 cells transfected with empty vectors (Gal4), Gal4-NFATc3 deletion constructs and/or FLAG-MEF2C were immunoprecipitated using an anti-MEF2 antibody, and subjected to Western blotting with an anti-Gal4 antibody. **F.** Schematic overview of the Gal4-NFATc3 deletion constructs and their ability to bind MEF2C. **G.** Protein extracts from wild-type and calcineurin transgenic mouse hearts were immunoprecipitated with anti-MEF2 antibodies, and subjected to Western blotting using an anti-NFATc3 antibody.

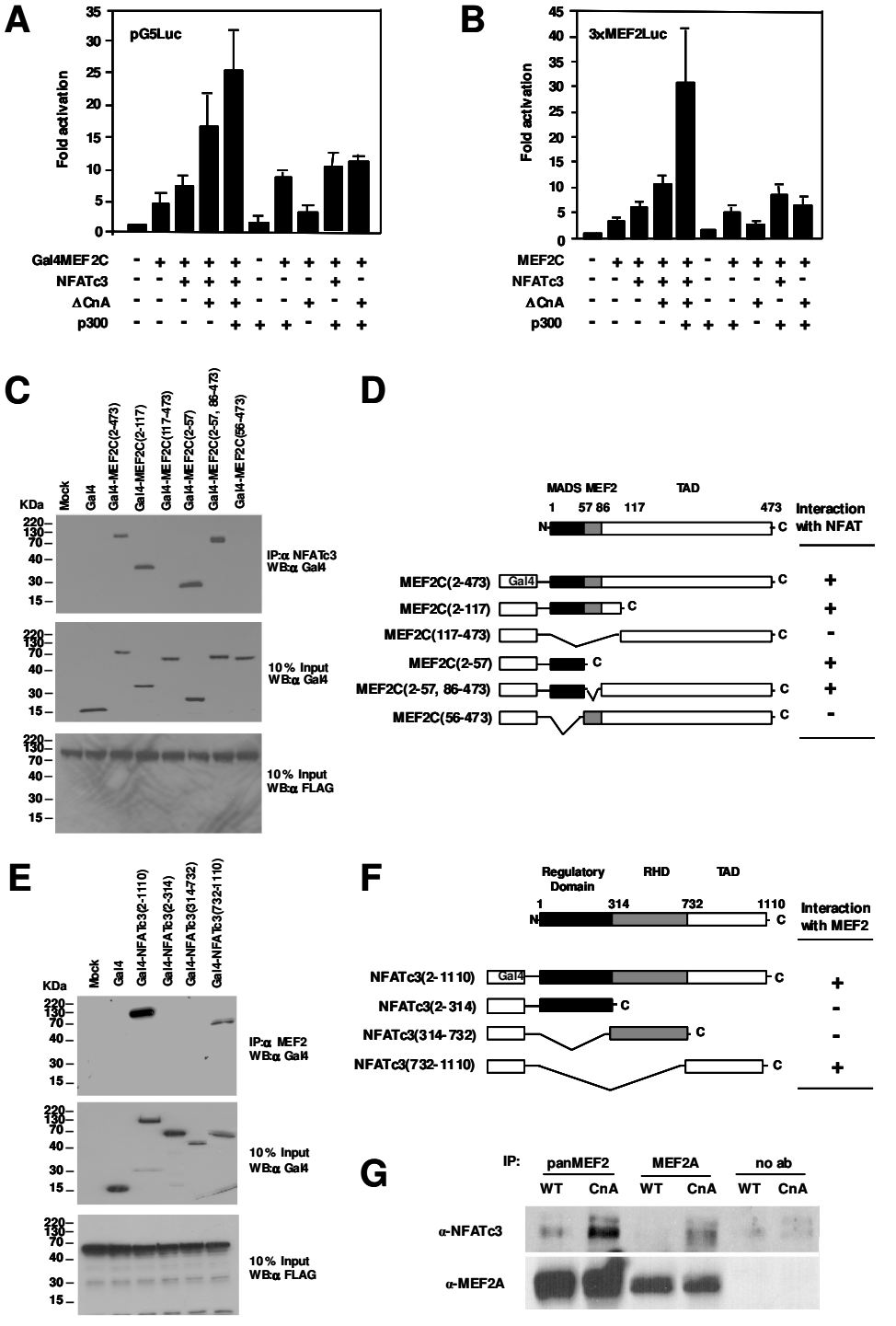
A
pG5Luc
Fold activation
Gal4MEF2C
NFATc3
ΔCnA
p300
B
3xMEF2Luc
Fold activation
MEF2C
NFATc3
ΔCnA
p300
C
KDa
Mock
Gal4
Gal4-MEF2C(2-473)
Gal4-MEF2C(2-117)
Gal4-MEF2C(117-473)
Gal4-MEF2C(2-57)
Gal4-MEF2C(2-57, 86-473)
Gal4-MEF2C(56-473)
IP:α NFATc3
WB:α Gal4
10% Input
WB:α Gal4
10% Input
WB:α FLAG
D
MADS MEF2
TAD
1
57 86
117
473
Interaction with NFAT
MEF2C(2-473)
MEF2C(2-117)
MEF2C(117-473)
MEF2C(2-57)
MEF2C(2-57, 86-473)
MEF2C(56-473)
E
KDa
Mock
Gal4
Gal4-NFATc3(2-1110)
Gal4-NFATc3(2-314)
Gal4-NFATc3(314-732)
Gal4-NFATc3(732-1110)
IP:α MEF2
WB:α Gal4
10% Input
WB:α Gal4
10% Input
WB:α FLAG
F
Regulatory Domain
RHD
TAD
1
314
732
1110
Interaction with MEF2
NFATc3(2-1110)
NFATc3(2-314)
NFATc3(314-732)
NFATc3(732-1110)
G
IP:
panMEF2
MEF2A
no ab
WT
CnA
WT
CnA
WT
CnA
α-NFATc3
α-MEF2A

RESULTS

Calcineurin-induced MEF2 activation is mediated by NFAT

MEF2 transcription factors are activated downstream of calcineurin activity in the heart, but the precise mechanism whereby this class of transcription factors are activated remains to be determined. In T lymphocytes, NFATc2 has been shown to interact directly with MEF2D in a synergistic transcriptional complex to activate the Nur77 gene [11], but the functional significance of NFATc2 in the heart, unlike NFATc3 [21], has not been addressed so far. To test whether an MEF2/NFAT complex is functional in cardiac muscle, we ectopically expressed Gal4-MEF2C, NFATc3, and an active form of calcineurin (ΔCnA) in cultured cardiomyocytes, which gave a 15-fold increase in Gal4-dependent reporter gene activity, whereas addition of p300 further enhanced this level to 25-fold activation (Figure 1A). These findings were confirmed by cotransfecting FLAG-MEF2C, NFATc3, and ΔCnA using a reporter with luciferase under control of multimerized MEF2 binding sites (Figure 1B). Collectively, these data suggest that calcineurin activates MEF2 transcriptional activity by promoting ternary complex formation between NFAT, MEF2, and CBP/p300 chromatin remodeling enzymes.

Recently, interacting domains on MEF2D and NFATc2 were mapped to the MADS-box DNA binding in MEF2D and the C-terminal transactivation domain (C-TAD) of NFATc2 [11]. To test whether these domains were conserved in other MEF2 and NFAT isoforms, various truncation fragments of MEF2C were fused to Gal4. Coexpression of FLAG-NFATc3 and ΔCnA in the presence of the pG5-Luc reporter demonstrated efficient activation only in the presence of full-length MEF2C and deletion fragments harboring the MADS box (Data Supplement Figure IA).

Next, FLAG-NFATc3, ΔCnA, and the Gal4-MEF2C deletion constructs were coexpressed in COS7 cells and immunoprecipitated with an anti-NFATc3 antibody. The presence of Gal4-MEF2C deletion mutants was detected by immunoblotting against Gal4. Among the NFATc3-interacting clones detected were full-length MEF2C (Figure 1C, lane 3) and only mutants that harbored the MADS-box domain (Figure 1C, lanes 4, 6, and 7, and Figure 1D).

To map the domain on NFATc3 that interacts with MEF2, 4 Gal4-NFATc3 fusions were constructed, harboring full-length NFATc3, the N-terminal regulatory domain, the Rel homology domain, or the C-TAD. Cotransfection of Gal4-NFATc3 mutants and FLAG-MEF2C demonstrated efficient transactivation when either full-length NFATc3 or the C-TAD of NFATc3 was linked to Gal4 (Data Supplement Figure IB). Next, FLAG-MEF2C, with distinct Gal4-NFAT mutants, was coimmunoprecipitated with a pan-MEF2 antibody. Among the interacting proteins detected were full-length NFATc3 (Figure 1E, lane 3) and the C-TAD of NFATc3 coupled to Gal4 (Figure 1E, lane 6, and Figure 1F). Collectively, these findings

indicate that specific interactions exist between the MADS box of MEF2C and the C-TAD of NFATc3. To verify whether an NFAT-MEF2 interaction exists in vivo, MEF2 was immunoprecipitated from heart lysate obtained from wild-type and calcineurin transgenic mice. Immunoblotting for NFATc3 readily indicated that endogenous NFAT and MEF2 interacted only in calcineurin transgenic mouse hearts (Figure 1G).

Inhibition of MEF2 reduces calcineurin-induced cardiomyocyte hypertrophy

To begin to assess the requirement of MEF2 downstream of calcineurin-mediated gene expression, we created a DNMEF2 harboring the first 117 amino acid residues from MEF2C with a C-terminal myc-epitope tag under control of the CMV promoter. Additionally, we replaced the arginine residue at position 24 to leucine (R24L), which creates a non-DNA binding mutant form of MEF2 (Data Supplement Figure IIA) [17]. The effectiveness of the DNMEF2 construct was confirmed in cotransfection assays with wild-type MEF2C or MEF2A with increasing amounts of the DNMEF2 construct using 3xMEF2-Luc reporter as a readout, which dose dependently abrogated MEF2-dependent transcription activity (Figure 2A and 2B).

To investigate the requirement of MEF2 in calcineurin-mediated cardiomyocyte hypertrophy, we generated bicistronic adenoviral vectors expressing either the DNMEF2 construct or MEF2A and GFP under separate CMV promoters (AdDNMEF2 and AdMEF2A; see Data Supplement Figure IIA) or only GFP (AdGFP; Figure 2C and 2D). To monitor the change in cell size or sarcomere organization, cardiomyocytes preinfected with the control adenovirus AdGFP or AdDNMEF2 were stained for sarcomeric α-actinin (Figure 2E). After 24 hours, cells were either left untreated (Figure 2E, left) or infected with AdCnA for 24 hours (Figure 2E, right). AdCnA resulted in a >2-fold increase in cell surface area (3478±140 versus 1601±101 μm^2; $P<0.01$ versus AdGFP; Figure 2F). AdDNMEF2 infection modestly abrogated the prohypertrophic effects of AdCnA (2272±76 μm^2; $P<0.05$ versus AdCnA, $P<0.05$ versus AdGFP). The data demonstrate that MEF2 is partially involved in aspects of hypertrophic remodeling of cardiomyocytes after calcineurin activation.

Conversely, cardiomyocytes infected with AdMEF2A demonstrated mild elongation (Figure 2G). Of note, the cells did not display the typical features of hypertrophied cells, including sarcomere assembly, vigorous beating, or ANF positivity (Figure 2G and data not shown), and did not reveal a significant increase in average cell surface area (1924±87 μm^2) compared with AdGFP-infected cultures (1823±83 μm^2; Figure 2H). We next determined the ratio of the length of the major and minor axes of cells in our experimental groups as a measure of cellular elongation. AdGFP-infected cardiomyocytes had a ratio of 2.54±0.13,

whereas AdMEF2A-infected cells displayed a 2-fold increase in the ratio of major to minor axis (5.15±0.43; $P<0.05$) compared with AdGFP-infected cells (Figure 2I). Combined, these data suggest that MEF2 transcriptional activity in cultured cardiomyocytes does not provoke a classic hypertrophic response but rather promotes elongation of cardiomyocytes.

Inhibition of MEF2 reduces biventricular dilation and cardiac dysfunction but minimally affects calcineurin-induced cardiac hypertrophy

To more accurately assess the role of MEF2 transcription factors downstream of cardiac calcineurin signaling, we designed an approach to inhibit MEF2 transcriptional activity in the adult cardiac muscle in vivo. To this end, we generated lines of Flox-DNMEF2 transgenic mice that express DNMEF2 on activation of Cre recombinase and crossed them with MHC-Cre, a transgenic line expressing Cre recombinase in postnatal cardiac muscle [16] (Figure 3A). Three Flox-DNMEF2 founder lines were obtained (lines 29, 32, and 40); lines 29 and 32 expressed the myc-tagged DNMEF2 protein only on activation by Cre recombinase (Figure 3A, bottom). We continued with Flox-DNMEF2 transgenic line 32, which displayed the highest amount of transgenic product in the heart.

Heart size and function of MHC-Cre/Flox-DNMEF2 mice were indistinguishable from nontransgenic and MHC-Cre control mice (Figure 3B and Data Supplement Movies). In line with previous findings [3, 19], MHC-Cre/MHC-CnA mice displayed a 3-fold increase in heart size with severe biventricular dilation. Surprisingly, however, once MHC-Cre/MHC-CnA mice were crossbred with Flox-DNMEF2 mice to generate calcineurin transgenic mice expressing DNMEF2 only in heart muscle cells, gross cardiac morphology analysis indicated reduced biventricular dilation with little effect on heart weight (Figure 3B).

Figure 2. Inhibition of MEF2 modestly attenuates calcineurin-induced cardiomyocyte hypertrophy. **A, B.** COS7 cells were transiently transfected with a multimerized MEF2 reporter in the presence of either MEF2A (A) or MEF2C (B) constructs and increasing amounts of DNMEF2 construct. **C, D.** Western blot analysis with anti-myc, anti-FLAG or anti-GFP antibody on COS7 cell lysates infected with either AdDNMEF2, AdMEF2A or AdGFP. **E.** Representative images of immunostained cardiomyocytes infected with the indicated adenoviruses. **F.** Quantification of cell surface areas of cardiomyocytes pre-infected with AdGFP or AdDNMEF2 and subsequently left uninfected or infected with AdCnA. Data represent the mean ± SEM of 3 independent experiments. **G.** Representative images of immunostained cardiomyocytes infected with the indicated adenoviruses. **H.** Quantification of cell surface areas of cardiomyocytes infected with AdGFP or AdMEF2A. **I.** Quantitative examination of cell-length/cell-width ratios of cardiomyocytes (≥100 per experiment) infected with AdGFP or AdMEF2A. *$P<0.05$, AdCnA infected vs noninfected cells, † $P<0.05$, AdCnA-infected cells preinfected with AdDNMEF2 vs AdCnA-infected cells preinfected with AdGFP control virus.

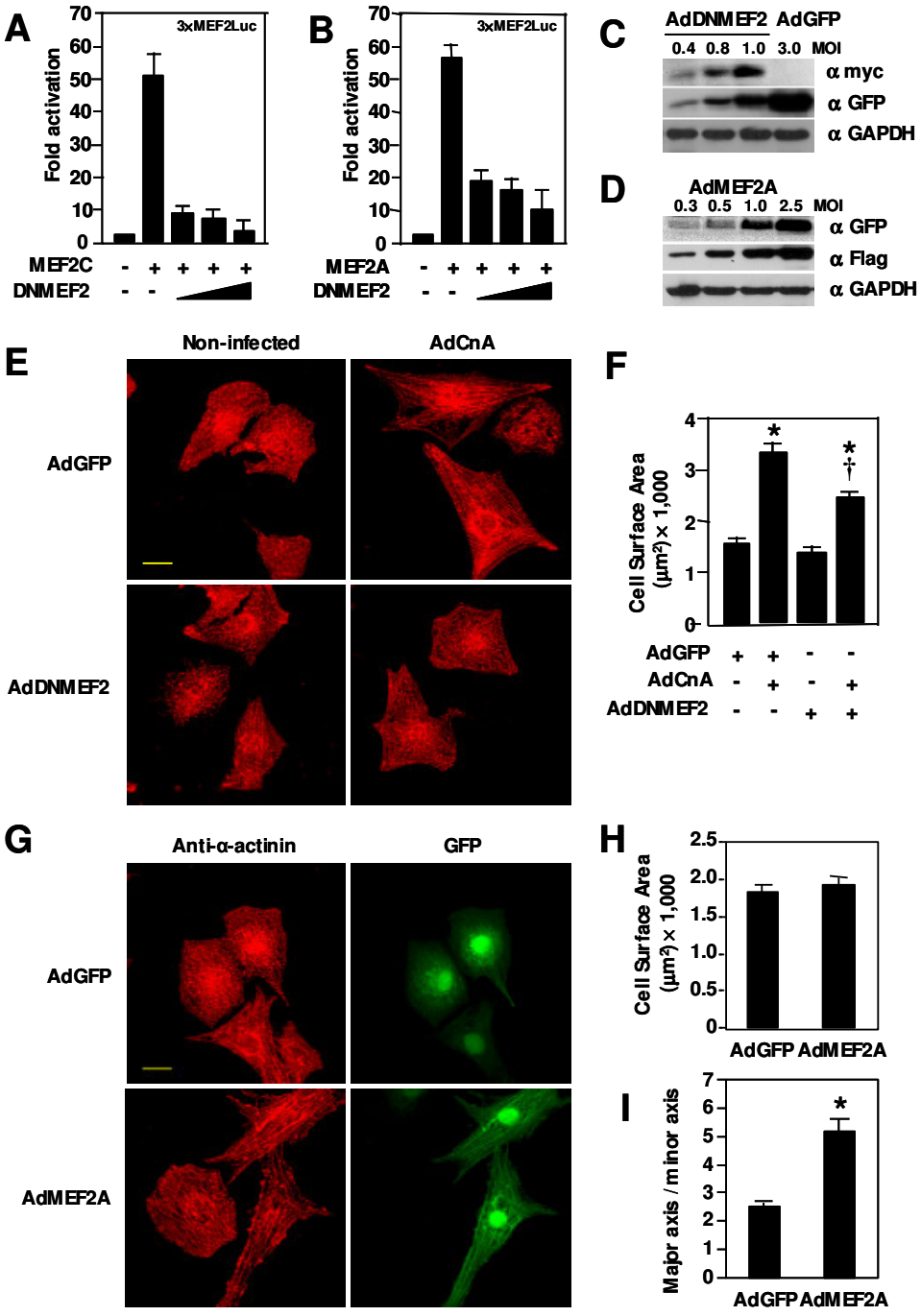
A
3xMEF2Luc
Fold activation
70
60
50
40
30
20
10
0
MEF2C - + + + +
DNMEF2 - - ▲
B
3xMEF2Luc
Fold activation
MEF2A - + + + +
DNMEF2 - - ▲
C
AdDNMEF2 AdGFP
0.4 0.8 1.0 3.0 MOI
α myc
α GFP
α GAPDH
D
AdMEF2A
0.3 0.5 1.0 2.5 MOI
α GFP
α Flag
α GAPDH
E
Non-infected
AdCnA
AdGFP
AdDNMEF2
F
Cell Surface Area (μm²) × 1,000
AdGFP + + - -
AdCnA - + - +
AdDNMEF2 - - + +
G
Anti-α-actinin
GFP
AdGFP
AdMEF2A
H
Cell Surface Area (μm²) × 1,000
AdGFP AdMEF2A
I
Major axis / minor axis
AdGFP AdMEF2A

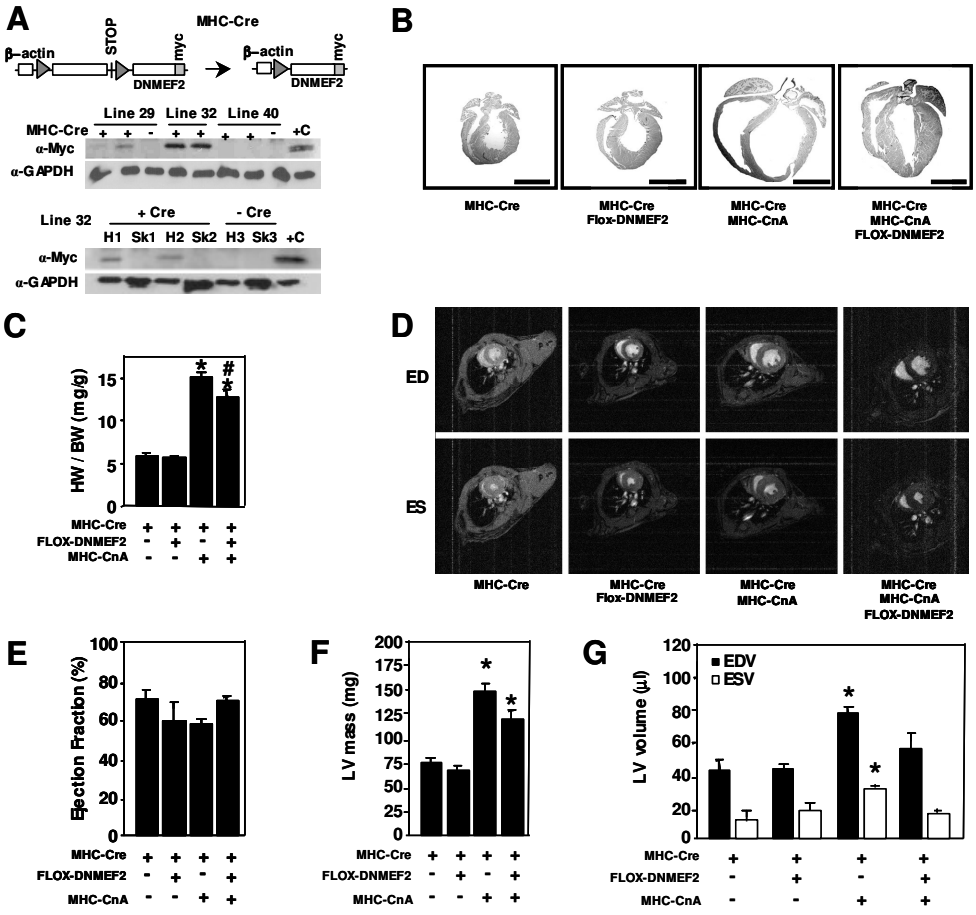

Figure 3. Inhibition of MEF2 reduces calcineurin-induced cardiac dysfunction. **A.** Schematic representation of Flox-DNMEF2 transgenic construct (top panel) before and after Cre induced recombination and Western blot analysis on heart lysate (top blot) and heart (H) and skeletal muscle (Sk) lysate (bottom blot) using an anti-myc antibody to detect DNMEF2 expression. **B.** H&E-stained coronal sections of the 4 experimental genotypes indicating a massive hypertrophic and dilated cardiomyopathy in 8-week-old MHC-Cre/MHC-CnA transgenic mice, and rescue of chamber dilation in MHC-Cre/MHC-CnA/Flox-DNMEF2 transgenic mice. **C.** Ratios of heart weight to body weight (HW/BW) of the indicated genotypes (n=12-17 per group). **D.** NMR images at mid thorax level of living mice of the indicated genotypes at maximal diastole (top panels) and maximal systole (bottom panels) indicating the severe chamber dilation and thickened walls of MHC-Cre/MHC-CnA hearts and less dilation but similar wall thickness of MHC-Cre/MHC-CnA/Flox-DNMEF2 transgenic mice. **E.** Ejection fraction determined from NMR imaging in live mice with the indicated genotypes (n=3 per group). **F.** LV mass determined by NMR imaging in live mice with the indicated genotypes (n=3 per group). **G.** Maximal LV volumes as a measure of chamber dilation calculated at maximal diastole (solid bars) or maximal systole (open bars) determined by NMR imaging in live mice with the indicated genotypes. *P<0.05 vs MHC-Cre control mice. #P<0.05 vs MHC-Cre/MHC-CnA.

Indeed, ratios of heart weight to body weight obtained from all experimental groups indicated only a minimal reduction in heart weight between MHC-Cre/MHC-CnA mice and MHC-Cre/MHC-CnA/Flox-DNMEF2 littermates (heart weight to body weight: MHC-Cre, 5.84±0.32 mg/g; MHC-Cre/Flox-DNMEF2, 5.64±0.33 mg/g; MHC-Cre/MHC-CnA, 15.10±0.56 mg/g; MHC-Cre/MHC-CnA/Flox-DNMEF2, 12.86±0.74 mg/g; $P<0.05$ versus MHC-Cre; $P<0.05$ versus MHC-Cre/MHC-CnA; Figure 3C).

Next, in vivo cardiac morphology and function were analyzed in live mice with magnetic resonance imaging. Cardiac mass, end-diastolic and end-systolic dimensions, and contractility were comparable between MHC-Cre and MHC-Cre/Flox-DNMEF2 transgenic mice (Figure 3D and Data Supplement Movies I and II). In contrast, 8-week-old MHC-Cre/MHC-CnA mice displayed severely increased wall thickness of all ventricular walls, increased end-diastolic and end-systolic intraventricular dimensions, and substantial loss of contractility (Figure 3D and Data Supplement Movie III). Remarkably, MHC-Cre/MHC-CnA/Flox-DNMEF2 littermates displayed biventricular end-diastolic and end-systolic biventricular dimensions and contractility that were comparable to control MHC-Cre mice in the presence of persistently hypertrophied septal and left ventricular (LV) free wall thicknesses (Figure 3D and Data Supplement Movie IV).

Comparison of the images at maximal diastole and systole (Figure 3D) indicated the markedly reduced function in the MHC-Cre/MHC-CnA mice compared with control genotypes and MHC-Cre/MHC-CnA/Flox-DNMEF2 mice, which displayed markedly improved ejection fraction (Figure 3E), a slight reduction in LV mass (Figure 3F), and a striking reduction in biventricular dilation (end-diastolic and end-systolic volume; Figure 3G). LV mass determined at end diastole by nuclear magnetic resonance (NMR) imaging amounted to 75.2±4.2, 67.3±2.5, 146.6±8.1, and 118.6±9.9 mg in MHC-Cre, MHC-Cre/Flox-DNMEF2, MHC-Cre/MHC-CnA, and MHC-Cre/MHC-CnA/Flox-DNMEF2 mice, respectively. End-diastolic volume amounted to 43.3±6.8, 44.5±2.5, 78.4±2.6, and 56.2±9.2 µl in MHC-Cre, MHC-Cre/Flox-DNMEF2, MHC-Cre/MHC-CnA, and MHC-Cre/MHC-CnA/Flox-DNMEF2 mice, respectively. Likewise, ejection fraction was normalized when MEF2 was inhibited in vivo (69±7%, 57±9%, 58±2%, and 70±1% in MHC-Cre, MHC-Cre/Flox-DNMEF2, MHC-Cre/MHC-CnA, and MHC-Cre/MHC-CnA/Flox-DNMEF2 mice, respectively). Taken together, the data indicate that inhibition of MEF2 transcriptional activity downstream of calcineurin signaling rescues biventricular dilation and contractility with a minimal effect on the massive hypertrophy response provoked by transgenic calcineurin activation.

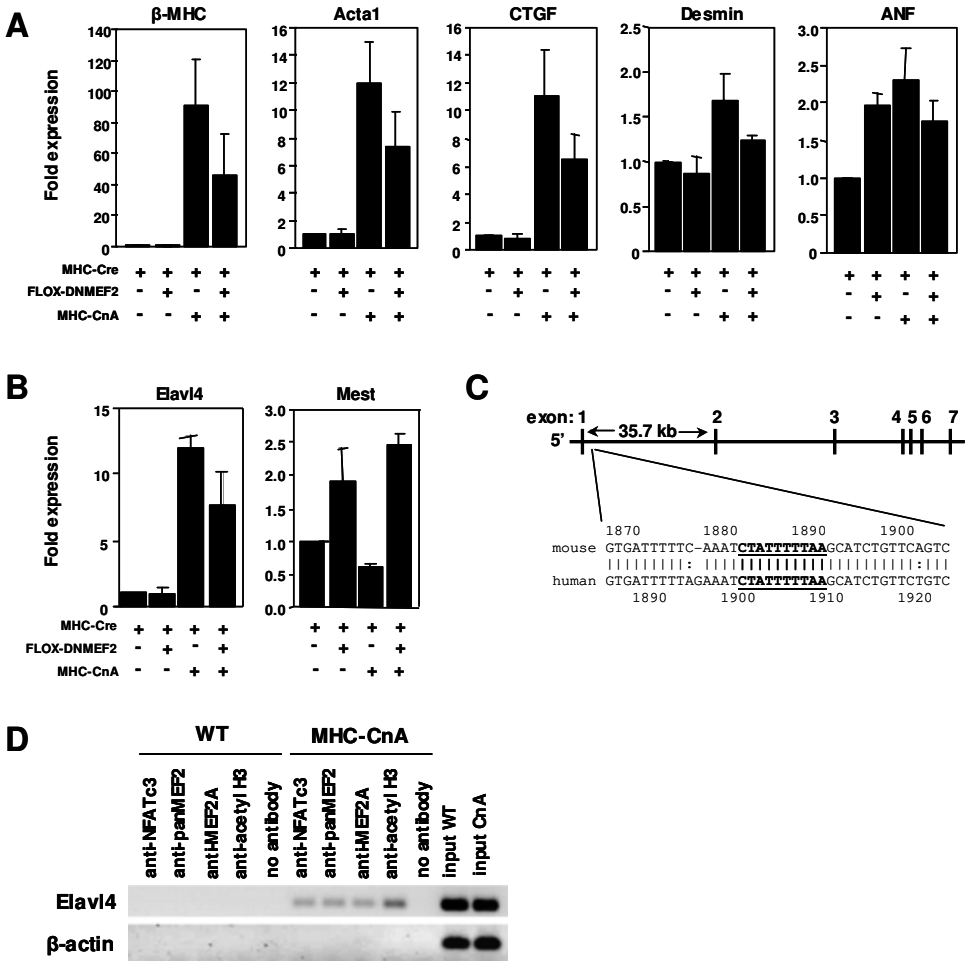

Figure 4. Calcineurin activates MEF2-dependent genes. **A, B.** Verification of transcript levels for β-MHC, Acta1, CTGF, desmin, ANF (A), Elavl4 and Mest (B) by real-time PCR detection in which transcript levels observed in MHC-Cre control mice were set at 1. **C.** Schematic of the intragenic region of *elavl4*, showing the conserved MEF2 binding site. **D.** Chromatin immunoprecipitation demonstrates that NFATc3 associates with MEF2 to form a transcriptionally active complex on A/T-rich motif in the *elavl4* gene in calcineurin transgenic hearts.

Gene expression profiling of calcineurin transgenic mice with or without inhibition of MEF2

We also analyzed hypertrophic marker gene expression, which demonstrated increased levels in MHC-Cre/MHC-CnA transgenic mice and a modestly reduced expression in the presence of the Flox-DNMEF2 transgene (Figure 4A). To provide more insights into the mechanisms underlying the phenotypic rescue evoked by inhibition of MEF2 transcriptional activity downstream of calcineurin, we analyzed the relative gene expression profiles from the indicated experimental groups with Agilent mouse chips (Agilent technologies, Palo Alto, Calif) containing 22,000 genes. One hundred sixty-one gene transcripts (0.7% of all genes) displayed opposite expression between MHC-Cre/MHC-CnA and MHC-Cre/MHC-CnA/Flox-DNMEF2 mice with a fold change in expression ≥1.5 (with $P<0.01$) without a change in abundancy on Cre-mediated activation of Flox-DNMEF2 (the Table). Among these, 108 transcripts were upregulated in MHC-Cre/MHC-CnA double-transgenic mice and oppositely regulated on inhibition of MEF2 transcriptional activity in the setting of cardiac calcineurin signaling. Conversely, 53 transcripts showed decreased expression when calcineurin was activated in the myocardium, with the decrease in expression attenuated when crossbred with Flox-DNMEF2 mice (the Table and Data Supplement Table I). Gene ontology classifications revealed an overrepresentation of gene transcripts in 3 subclasses: signal transducers, cell-matrix adhesion and cytoskeletal architecture, and energy metabolism (Table). On MEF2 inhibition, calcineurin transgenic hearts differentially expressed transcripts for multiple signal transducers (*apln*, *camkk1*, *map3k7*, *pde7a*), transcriptional repressors (*cited2*, *dnajc3*, *rcor2*), cytoskeletal remodeling components (*neb*, *cldn5*, *emilin1*), and ubiquitin-related proteases (*npepp2*, *usp48*). Opposite expression of *elavl4* and *mest* by microarray profiling was confirmed by real-time reverse transcriptase-PCR (RT-PCR) (Figure 4B). Combined, these data indicate that MEF2 activity downstream of calcineurin signaling activates subsets of genes localized primarily to or functioning at the nucleus, the cytoskeletal and microtubular networks, and mitochondria.

To define a regulatory mechanism involving NFAT and MEF2 in the induction of *elavl4*, the mouse and human orthologs were analyzed and aligned for cross-species conservation. A fragment of between 1870 and 1900 bp relative to the transcriptional start site in the murine sequence displayed a remarkable conservation in an A/T-rich MEF2 binding site (^{1883}CTATTTTTAA), which is completely homologous with the consensus MEF2 binding sequence (C/T)TA(T/A)4TA(G/A) (Figure 4C). To determine whether a MEF2/NFAT complex binds to this A/T-rich motif in vivo, we performed ChIP assays using anti-MEF2, anti-NFATc3, and anti–acetylated histone H3 antibodies. No antibody immunoprecipitates (Figure 4D, lanes 5 and 10) were used as negative controls;

input chromatin served as a positive control (Figure 4D, lanes 11 and 12). When immunoprecipitated chromatin was subjected to PCR with primers spanning the A/T-rich motifs in *elavl4*, a specific 209-bp band was obtained only in MHC-CnA transgenic hearts, indicating that a complex consisting of MEF2/NFAT and histone acetyl transferase activity (indicative of p300 presence) occupied the MEF2 binding site. Collectively, these data support the notion that a complex consisting of MEF2, NFAT, and p300 accumulates on selected A/T-rich motifs in genes after calcineurin activity in vivo.

Table. Expression profiling of calcineurin transgenic hearts with or without MEF2 transcriptional activity.

Growth factors, cytokines, receptors (22): Acvrinp1, Akap13, Apln, Arhgap24, Camkk1, Cav1, Dll1, Dok4, Dusp18, Ephb1, Gpr24, Gtpbp4, Map3k7, Olfr566, Pcp2, Pde7a, Plk3, Rassf2, Rgs3, Shank3, Tbc1d4, Wif1
Cytoskeletal architecture, Microtubular system, Cell adhesion (20): Ablim1, Cald1, Dnahc8, Elavl4, Kif1b, Krt1-15, Mtap7, Mtss1, Myo10, Neb, Ofd2, Slmap, A930004K21Rik, Amotl1, Cldn5, Emilin1, Itlna, Mcam, Mest, Mmp15
Transcriptional regulation (14): Ash1l, Bcl6b, Cebpz, Cited2, Dnajc3, Fli1, L3mbtl3, Pou4f1, Ppp1r12b, Rcor2, Six4, Tlx2, Zfpm2, 2310076O14Rik
Proteolysis, Ubiquitin complex (10): Casp7, NE, Nedd4, Npepps, Prp19, Ube2q, Uhrf1, Usp48, 1700095N21Rik, 6430527G18Rik
Energy metabolism, Electron transport (10): Aass, Bpgm, Dbt, Fmo2, Grp58, Lip1, Lpgat1, Pfkp, D2Bwg1356e, 5330438E18Rik
Ion channels (5): Cacna1s, Clic5, Kcnd2, Slc24a3, Slc28a2
Cell cycle (4): Ccng, Mcm6, Rif1, Tlm
Ribosome biogenesis (4): Hnrpa3, Rpl14, Rps26, Rrs1
Intracellular protein transport (3): Rab1b, Rab12, Rab21

One hundred sixty-one transcripts were detected in calcineurin transgenic hearts that were regulated in an opposite manner in the presence of the Flox-DNMEF2 transgene, of which relevant transcripts with a 1.5 fold change in signal intensity are shown. Others include 27 ESTs and 10 transcripts without gene ontology description.

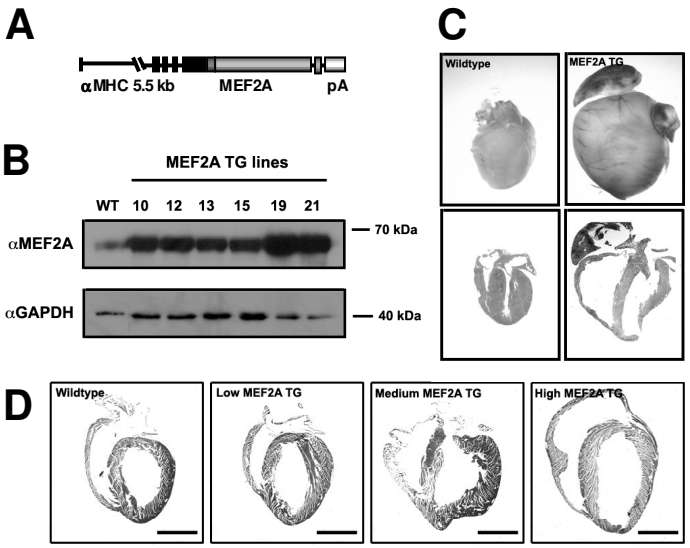

Figure 5. MEF2A transgenic mice display dilated cardiomyopathy. **A.** Schematic of transgenic construct consisting of 5.5 kb αMHC promotor, FLAG-tagged human MEF2A, and human growth hormone polyadenylation signal. **B.** Western blot analysis on nuclear fractions of hearts from wildtype mice and different MEF2A transgenic lines indicates overexpression of MEF2A in cardiac muscle. **C.** Whole-heart image and H&E coronal section of wild-type and a transgenic founder that died suddenly from peripartum dilated cardiomyopathy. **D.** H&E-stained coronal sections of wild-type and low, medium, and high overexpressing MEF2A transgenic mice indicate that with medium and high MEF2A overexpression mild or severe dilated cardiomyopathy, respectively, was observed.

Generation and characterization of MEF2A transgenic mice

To verify whether MEF2 transcriptional function in vivo is restricted primarily to promoting ventricular dilation and contractile loss, we designed a strategy to activate MEF2 transcriptional activity in the postnatal heart. We generated transgenic mice expressing the MEF2A isoform under control of the well-characterized 5.5-kb murine α-myosin heavy chain (*myh6*) promoter (Figure 5A).

Seven independent founders were recovered; 6 produced progeny and established transgenic lines for further characterization. All viable MEF2A transgenic lines overexpressed human MEF2A in the myocardium, albeit at differing levels, varying between 1.5-fold and 4-fold more MEF2A protein at 12 weeks of age, when normalized to glyceraldehyde-3-phosphate dehydrogenase (Figure 5B and data not shown). One female transgenic founder died with an extreme form of peripartum cardiomyopathy and severely dilated ventricular chambers on necropsy (Figure 5C). Low-expressing MEF2A transgenic lines,

characterized by a 1.5-fold to 2-fold increase in MEF2A protein, showed no lethality, no signs of cardiac hypertrophy, and no histological abnormalities of the myocardium on closer inspection (Figure 5D and data not shown). We suspect that the lack of a phenotype in low MEF2 expressers reflects the inability of a low level of MEF2 to overcome HDAC repression. One medium overexpressing MEF2A transgenic line, characterized by 2.5-fold more MEF2A protein, displayed a very mild increase in heart weight (corrected for body weight and tibial length), slightly thickened LV walls, and mild dilation of ventricular walls (Figure 5D and data not shown). Two high-expressor lines, with 4-fold more MEF2A expression, were characterized by substantial dilation of both right ventricular and LV chambers at 12 weeks of age and thinned ventricular walls (Figure 5D). Combined, these data indicate that cardiac MEF2A activation produces a dose-dependent, variable phenotype ranging from no apparent phenotype to slight hypertrophic/dilated remodeling to severe dilated cardiomyopathy characterized by ballooning of the ventricular chambers and thinning of ventricular walls.

DISCUSSION

Here, we demonstrated that cardiac MEF2 transcription factors are activated in an NFAT-dependent fashion by calcineurin, a pivotal mediator of calcium-dependent cardiac growth, and that a Cre/LoxP-dependent approach to antagonize MEF2 transcriptional activity prevented chamber dilation and mechanical dysfunction, with minor effects on cardiac growth. Chronic changes in the cardiac gene program may trigger pathological changes in the myocardium that incite irreversible cellular changes, with chamber dilation and the associated increase in stress on the ventricular wall representing the first irreversible steps toward heart failure. Accordingly, the transcription factors that connect biomechanical forces and the activation of stress pathways to a “fetal” gene program are central to understanding the initiation and progression of heart failure. Multiple signals and transcriptional events suffice to evoke cardiac hypertrophy in cultured myocyte systems and whole-animal gain-of-function models [22], but only a few examples exist in which gene deletion rescues the germane features of heart failure in mice, which are chamber dilation and mechanical dysfunction [23, 24]. Using genetic gain and loss-of-function approaches, we are the first, to the best of our knowledge, to prove the existence of separate genetic programs primary to cardiac growth versus chamber dilation and cardiac dysfunction within the venue of calcium-driven cardiac growth and failure (Figure 6).

The data in this study confirm the existence of a combinatorial MEF2/NFAT regulatory transcriptional pathway controlling gene expression in cardiac muscle

cells. This observation is reminiscent of the cooperative interaction between MEF2 proteins and myogenic basic helix-loop-helix factors in skeletal muscles [25] and between MEF2 proteins and GATA factors in cardiac muscles [26], and it suggests that MEF2 factors interact with a range of transcription factors to optimize gene expression. Calcineurin has been reported to activate the Nur77 promoter in T lymphocytes by promoting nuclear translocation of NFATc2, which in turn forms a ternary complex with MEF2 and CBP/p300 [11]. Given the overlapping expression patterns of MEF2 and NFAT factors in smooth muscle, skeletal muscle, cardiac muscle, and the central nervous system, the NFAT/MEF2-dependent pathway described in this work suggests the existence of this molecular paradigm for Ca^{2+}/calmodulin signaling in excitable tissue.

Using a multidisciplinary approach, we analyzed MEF2 transcription factor function in adult cardiac muscle, starting from the premise that MEF2 would be involved primarily in the initial hypertrophic remodeling phase of the heart muscle [27]. Although transgenic overexpression of (truncated mutants of) transcription factors harbors the risk of unwanted transcriptional squelching, the consistency in opposite phenotypes we observed using our combinatorial dominant-negative versus gain-of-function models for MEF2 transcriptional activity justifies the overall conclusions drawn in this study. To our surprise, MEF2 promotes cardiac disease symptoms that are more compatible with later manifestations of cardiac disease that extends beyond and stems from initial pathological cardiac growth, namely chamber dilation, mechanical dysfunction, and end-stage heart failure. The seeming paradox - that cardiac growth and failure are not mutually inexclusive yet cardiac growth initiates failure - could reflect the limitations of current knowledge on the specificity and convergence of individual characterized stress pathways. Nevertheless, the mere existence of a genetic pathway specifically underlying ventricular dilation will be of fundamental clinical and therapeutic interest.

A large and convincing body of literature demonstrated that cardiac MEF2 activity is under control of HDAC regulation at the onset of cardiac hypertrophy. However, chromatin remodeling is a very general mode of transcription regulation [28], and HDACs have been demonstrated to regulate other transcription factors that have been implicated in promoting cardiomyocyte growth, suggesting that the excessive cardiac growth response observed in HDAC9- or HDAC5-deficient mice [29] may not be limited to derepression of MEF2 activity alone. Indeed, MEF2 LacZ sensor mice injected with prohypertrophic agonists such as isoproterenol, angiotensin II, or thyroid hormone failed to display ventricular MEF2 activity despite an increase in ventricular mass [30]. Given these considerations and the findings with the loss-of-function and gain-of-function analyses for MEF2 in transgenic mice in the present study, it is reasonable to suggest that the function of MEF2 factors in the postnatal myocardium may be more restricted to molecular signals that

promote dilated cardiomyopathy rather than the initial phases of hypertrophic remodeling. Nevertheless, genetic proof that MEF2 is dispensable for developmental or stress-induced postnatal cardiac growth but required for ventricular dilation and mechanical dysfunction suggests the logic of strategies to inhibit this class of transcriptional regulators in forms of heart disease involving calcineurin signaling.

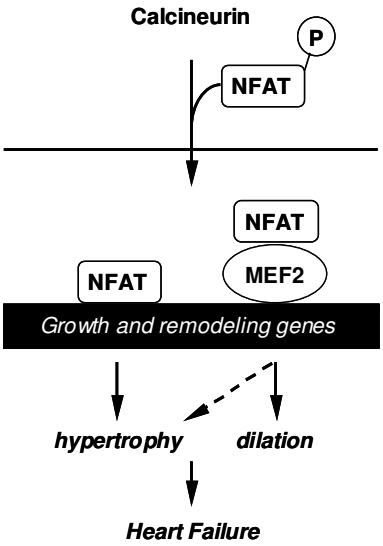

Figure 6. After cardiac calcineurin activation, MEF2 is able to recruit NFAT to activate selected downstream target genes that preferentially drive dilation, whereas NFAT alone or with other transcriptional partners provokes hypertrophy.

The classification profiles of MEF2 target genes secondary to cardiac calcium stress signaling identified in the present study underscore the complexity of genetic events underlying chamber dilation and mechanical dysfunction yet also provide tangible entry points for mechanistic explanations of the findings presented here. First, the gene profiles identified in the present work correlate well with those observed in gene chip analysis of human end-stage idiopathic dilated cardiomyopathy [31] and with the most characteristic pathological features of human end-stage dilated cardiomyopathy, which include a dynamic redistribution of cytoskeletal structures, extensive fibrosis, and extracellular alterations in mitochondria number and morphology [32]. For example, the relative enrichment in transcripts of genes at the cardiomyocyte cytoskeletal network, including *nebulin*, *claudin*, *elastin microfibril interfaces 1 (emilin1), intelectin a* and *microtubule-associated protein 7*, to mention a few, which couple adherens junctions and costameres to myofibrils and the extracellular matrix, underscores the germane role of the cytoskeletal architecture in force transmission. Transcripts for stress signaling components such as *Wnt inhibitory factor 1*, *EphB1*, *apelin*, and *transforming growth factor-β activated kinase 1 (map3k7* or *tak1)* were differentially affected. Tak1 activation suffices to provoke ventricular dilation, mechanical dysfunction, and fulminant heart failure in mice [33]. Finally, ventricular dilation and MEF2 function concur with complex epigenetic effects, as suggested by altered transcript abundance for chromatin remodeling factors, including *cbp/p300-interacting transactivator*, *REST co-repressor 2* and *the DNAJ (Hsp40) homolog*.

The present study provides the first direct approach to studying the biological ramifications of the transcription factor MEF2 in the postnatal heart muscle. Our findings identify distinct gene profiles regulated by MEF2 activity, which suggest that MEF2 promotes multiple cellular changes, each of which may independently or in an interconnected fashion promote changes in the heart muscle that are characteristic of dilated cardiomyopathy.

ACKNOWLEDGEMENTS

We are grateful to Jeffrey Robbins for sharing the α-MHC plasmid, Bert Vogelstein for providing adenoviral plasmids, Eric N. Olson for sharing plasmids and calcineurin transgenic mice, and Marcel G.J. Nederhoff, Melany van Oostrom, and Hamid el Azzouzi for technical support. This work was supported by grant 2000B160 of the Netherlands Heart Foundation (to Dr Doevendans), grants 902-16-275, 912-04-054, and 912-04-017 from the Netherlands Organization for Health Research and Development (ZonMW), and by European Unioncontract LSHM-CT-2005-018833/EUGeneHeart (to Dr De Windt).

REFERENCES

1. Hoshijima M., Chien K.R. Mixed signals in heart failure: cancer rules. J Clin Invest 2002;109(7):849-55.
2. Hogan P.G., Chen L., Nardone J., Rao A. Transcriptional regulation by calcium, calcineurin, and NFAT. Genes Dev 2003;17(18):2205-32.
3. Molkentin J.D., Lu J.R., Antos C.L., Markham B., Richardson J., Robbins J., Grant S.R., Olson E.N. A calcineurin-dependent transcriptional pathway for cardiac hypertrophy. Cell 1998;93(2):215-28.
4. Musaro A., McCullagh K.J., Naya F.J., Olson E.N., Rosenthal N. IGF-1 induces skeletal myocyte hypertrophy through calcineurin in association with GATA-2 and NF-ATc1. Nature 1999;400(6744):581-5.
5. McKinsey T.A., Zhang C.L., Lu J., Olson E.N. Signal-dependent nuclear export of a histone deacetylase regulates muscle differentiation. Nature 2000;408(6808):106-11.
6. Zhang C.L., McKinsey T.A., Chang S., Antos C.L., Hill J.A., Olson E.N. Class II histone deacetylases act as signal-responsive repressors of cardiac hypertrophy. Cell 2002;110(4):479-88.
7. Vega R.B., Harrison B.C., Meadows E., Roberts C.R., Papst P.J., Olson E.N., McKinsey T.A. Protein kinases C and D mediate agonist-dependent cardiac hypertrophy through nuclear export of histone deacetylase 5. Mol Cell Biol 2004;24(19):8374-85.
8. Chin E.R., Olson E.N., Richardson J.A., Yang Q., Humphries C., Shelton J.M., Wu H., Zhu W., Bassel-Duby R., Williams R.S. A calcineurin-dependent transcriptional pathway controls skeletal muscle fiber type. Genes Dev 1998;12(16):2499-509.

9. Flavell S.W., Cowan C.W., Kim T.K., Greer P.L., Lin Y., Paradis S., Griffith E.C., Hu L.S., Chen C., Greenberg M.E. Activity-dependent regulation of MEF2 transcription factors suppresses excitatory synapse number. Science 2006;311(5763):1008-12.
10. Shalizi A., Gaudilliere B., Yuan Z., Stegmuller J., Shirogane T., Ge Q., Tan Y., Schulman B., Harper J.W., Bonni A. A calcium-regulated MEF2 sumoylation switch controls postsynaptic differentiation. Science 2006;311(5763):1012-7.
11. Youn H.D., Chatila T.A., Liu J.O. Integration of calcineurin and MEF2 signals by the coactivator p300 during T-cell apoptosis. Embo J 2000;19(16):4323-31.
12. Kolodziejczyk S.M., Wang L., Balazsi K., DeRepentigny Y., Kothary R., Megeney L.A. MEF2 is upregulated during cardiac hypertrophy and is required for normal post-natal growth of the myocardium. Curr Biol 1999;9(20):1203-6.
13. Lin Q., Schwarz J., Bucana C., Olson E.N. Control of mouse cardiac morphogenesis and myogenesis by transcription factor MEF2C. Science 1997;276(5317):1404-7.
14. Naya F.J., Black B.L., Wu H., Bassel-Duby R., Richardson J.A., Hill J.A., Olson E.N. Mitochondrial deficiency and cardiac sudden death in mice lacking the MEF2A transcription factor. Nat Med 2002;8(11):1303-9.
15. Palermo J., Gulick J., Colbert M., Fewell J., Robbins J. Transgenic remodeling of the contractile apparatus in the mammalian heart. Circ Res 1996;78(3):504-9.
16. Agah R., Frenkel P.A., French B.A., Michael L.H., Overbeek P.A., Schneider M.D. Gene recombination in postmitotic cells. Targeted expression of Cre recombinase provokes cardiac-restricted, site-specific rearrangement in adult ventricular muscle in vivo. J Clin Invest 1997;100(1):169-79.
17. Molkentin J.D., Black B.L., Martin J.F., Olson E.N. Mutational analysis of the DNA binding, dimerization, and transcriptional activation domains of MEF2C. Mol Cell Biol 1996;16(6):2627-36.
18. He T.C., Zhou S., da Costa L.T., Yu J., Kinzler K.W., Vogelstein B. A simplified system for generating recombinant adenoviruses. Proc Natl Acad Sci U S A 1998;95(5):2509-14.
19. De Windt L.J., Lim H.W., Taigen T., Wencker D., Condorelli G., Dorn G.W., 2nd, Kitsis R.N., Molkentin J.D. Calcineurin-mediated hypertrophy protects cardiomyocytes from apoptosis in vitro and in vivo: An apoptosis-independent model of dilated heart failure. Circ Res 2000;86(3):255-63.
20. van Rooij E., Doevendans P.A., de Theije C.C., Babiker F.A., Molkentin J.D., de Windt L.J. Requirement of nuclear factor of activated T-cells in calcineurin-mediated cardiomyocyte hypertrophy. J Biol Chem 2002;277(50):48617-26.
21. Wilkins B.J., De Windt L.J., Bueno O.F., Braz J.C., Glascock B.J., Kimball T.F., Molkentin J.D. Targeted disruption of NFATc3, but not NFATc4, reveals an intrinsic defect in calcineurin-mediated cardiac hypertrophic growth. Mol Cell Biol 2002;22(21):7603-13.
22. Molkentin J.D., Dorn I.G., 2nd. Cytoplasmic signaling pathways that regulate cardiac hypertrophy. Annu Rev Physiol 2001;63:391-426.
23. Minamisawa S., Hoshijima M., Chu G., Ward C.A., Frank K., Gu Y., Martone M.E., Wang Y., Ross J., Jr., Kranias E.G., Giles W.R., Chien K.R. Chronic phospholamban-sarcoplasmic reticulum calcium ATPase interaction is the critical calcium cycling defect in dilated cardiomyopathy. Cell 1999;99(3):313-22.
24. Minamino T., Yujiri T., Terada N., Taffet G.E., Michael L.H., Johnson G.L., Schneider M.D. MEKK1 is essential for cardiac hypertrophy and dysfunction induced by Gq. Proc Natl Acad Sci U S A 2002;99(6):3866-71.
25. Molkentin J.D., Olson E.N. Combinatorial control of muscle development by basic helix-loop-helix and MADS-box transcription factors. Proc Natl Acad Sci U S A 1996;93(18):9366-73.
26. Morin S., Charron F., Robitaille L., Nemer M. GATA-dependent recruitment of MEF2 proteins to target promoters. Embo J 2000;19(9):2046-55.

27. Olson E.N., Schneider M.D. Sizing up the heart: development redux in disease. Genes Dev 2003;17(16):1937-56.
28. Kouzarides T. Histone acetylases and deacetylases in cell proliferation. Curr Opin Genet Dev 1999;9(1):40-8.
29. Chang S., McKinsey T.A., Zhang C.L., Richardson J.A., Hill J.A., Olson E.N. Histone deacetylases 5 and 9 govern responsiveness of the heart to a subset of stress signals and play redundant roles in heart development. Mol Cell Biol 2004;24(19):8467-76.
30. Zhao X.S., Gallardo T.D., Lin L., Schageman J.J., Shohet R.V. Transcriptional mapping and genomic analysis of the cardiac atria and ventricles. Physiol Genomics 2002;12(1):53-60.
31. Grzeskowiak R., Witt H., Drungowski M., Thermann R., Hennig S., Perrot A., Osterziel K.J., Klingbiel D., Scheid S., Spang R., Lehrach H., Ruiz P. Expression profiling of human idiopathic dilated cardiomyopathy. Cardiovasc Res 2003;59(2):400-11.
32. Schaper J., Froede R., Hein S., Buck A., Hashizume H., Speiser B., Friedl A., Bleese N. Impairment of the myocardial ultrastructure and changes of the cytoskeleton in dilated cardiomyopathy. Circulation 1991;83(2):504-14.
33. Zhang D., Gaussin V., Taffet G.E., Belaguli N.S., Yamada M., Schwartz R.J., Michael L.H., Overbeek P.A., Schneider M.D. TAK1 is activated in the myocardium after pressure overload and is sufficient to provoke heart failure in transgenic mice. Nat Med 2000;6(5):556-63.

Supplemental table I.

Gene	Description	Cre-CnA vs Cre	P-value	Cre-CnA-DNMEF2 vs Cre-CnA	P-value
Elavl4	ELAV (embryonic lethal, abnormal vision, Drosophila)-like 4 (Hu antigen D)	**12.6**	1,82E-24	**-1.5**	7,23E-04
Itlna	intelectin a	**9.1**	4,57E-19	**-10.1**	8,55E-26
2210407C18Rik	RIKEN cDNA 2210407C18 gene	**8.2**	1,96E-27	**-3.1**	5,46E-16
Dnahc8	dynein, axonemal, heavy chain 8	**5.6**	3,07E-09	**-2.4**	9,26E-09
Sprr2b	small proline-rich protein 2B	**4.9**	1,89E-22	**-1.7**	2,37E-05
Clic5	chloride intracellular channel 5	**4.4**	5,1E-20	**-1.6**	3,95E-05
Pam	peptidylglycine alpha-amidating monooxygenase	**3.9**	3,11E-19	**-4.4**	6,78E-21
Wif1	Wnt inhibitory factor 1	**3.1**	5,44E-12	**-1.9**	2,39E-07
Sprr2k	small proline-rich protein 2K	**3.1**	1,44E-15	**-1.7**	8,96E-06
Krt1-15	keratin complex 1, acidic, gene 15	**3.0**	1,89E-09	**-1.8**	1,02E-05
Pde7a	phosphodiesterase 7A	**2.9**	1,76E-12	**-1.7**	3,66E-05
A930014K01Rik	RIKEN cDNA A930014K01 gene	**2.9**	5,84E-06	**-2.4**	1,12E-06
1200008A14Rik	RIKEN cDNA 1200008A14 gene	**2.8**	8,6E-06	**-2.5**	5,96E-09
Slc24a3	solute carrier family 24 (sodium/potassium/calcium exchanger), member 3	**2.8**	6,48E-10	**-1.8**	8,36E-06
NE	neutrophil elastase	**2.7**	0,000909	**-2.6**	1,89E-05
Hnrpa0	RIKEN full-length enriched library, clone:3010025E17 HETEROGENEOUS NUCLEAR RIBONUCLEOPROTEIN A0	**2.7**	8,81E-08	**-2.2**	8,49E-09
BY417443	BY417443 RIKEN full-length cDNA clone I920026M11 3	**2.7**	2,48E-13	**-1.6**	9,94E-05
Cyfip2	cytoplasmic FMR1 interacting protein 2	**2.7**	2,45E-13	**-2.9**	7,59E-15
Cited2	Cbp/p300-interacting transactivator, with Glu/Asp-rich carboxy-terminal domain, 2	**2.7**	9,95E-13	**-1.6**	1,64E-02
2310076O14Rik	RIKEN full-length enriched library, clone:2310076O14 product:hypothetical Bacterial regulatory protein, LysR family containing protein	**2.6**	1,8E-12	**-1.9**	5,11E-07
Ddit4	DNA-damage-inducible transcript 4	**2.5**	4,12E-12	**-1.9**	1,92E-07
Igsf1	immunoglobulin superfamily, member 1 (Igsf1), transcript variant 1	**2.5**	6,52E-12	**-3.1**	9,08E-16
Loxl2	lysyl oxidase-like 2 (Loxl2)	**2.4**	0,003694	**-2.3**	5,94E-06
2310043K02Rik	RIKEN cDNA 2310043K02 gene	**2.4**	2,83E-09	**-2.1**	1,12E-08
2210010L05Rik	RIKEN cDNA 2210010L05 gene	**2.4**	2,27E-06	**-2.4**	2,53E-10
Kif1b	kinesin family member 1B (Kif1b), transcript variant 1	**2.3**	6,93E-11	**-2.4**	1,21E-11
Nedd4	neural precursor cell expressed, developmentally down-regulted gene 4	**2.3**	5,96E-11	**-2.2**	3,30E-10
Hsp105	heat shock protein 105	**2.3**	2,02E-10	**-1.5**	2,43E-04
Acvrinp1	activin receptor interacting protein 1	**2.2**	1,45E-09	**-1.9**	3,34E-07
Six4	Mouse mRNA for AREC3, partial cds. [D50418]	**2.2**	0,000458	**-1.8**	7,62E-05
1110018M03Rik	RIKEN cDNA 1110018M03 gene	**2.2**	4,24E-10	**-1.5**	2,85E-04
Gtpbp4	GTP binding protein 4	**2.2**	0,001235	**-2.1**	3,38E-05
Arhgap24	Rho GTPase activating protein 24	**2.2**	3,24E-09	**-1.5**	4,52E-04
Ubxd2	UBX domain containing 2	**2.2**	1,05E-08	**-3.3**	1,59E-16
Cacna1s	dihydropyridine sensitive skeletal muscle calcium channel	**2.2**	3,72E-09	**-1.6**	2,06E-04
4732473B16Rik	RIKEN cDNA 4732473B16 gene	**2.2**	2,07E-08	**-2.2**	2,48E-09
Aass	aminoadipate-semialdehyde synthase	**2.1**	7,14E-05	**-1.7**	3,39E-04
AA960436	expressed sequence AA960436	**2.1**	0,000153	**-2.2**	1,19E-06
Rrs1	RRS1 ribosome biogenesis regulator homolog (S. cerevisiae)	**2.1**	3,4E-08	**-1.7**	7,93E-06
Akap13	type II cAMP-dependent protein kinase anchoring protein Ht31	**2.1**	5,56E-09	**-1.7**	1,05E-05
Slmap	sarcolemma associated protein	**2.0**	1,5E-07	**-3.0**	1,27E-10
Myo10	myosin X	**2.0**	0,000112	**-1.5**	1,52E-03
Laptm5	lysosomal-associated protein transmembrane 5	**2.0**	0,000864	**-1.5**	2,37E-03
Gpr24	G protein coupled receptor 24	**2.0**	1,42E-05	**-3.0**	4,39E-14
Mtap7	microtubule-associated protein 7	**2.0**	0,001924	**-2.0**	3,79E-06
Itih5	inter-alpha (globulin) inhibitor H5	**1.9**	1,02E-07	**-2.1**	9,63E-09

A930004K21Rik	RIKEN cDNA A930004K21 gene	**1.9**	1,03E-07	**-1.5**	3,10E-04
Tlx2	T-cell leukemia, homeobox 2	**1.9**	1,98E-05	**-2.2**	2,22E-09
Glt25d1	glycosyltransferase 25 domain containing 1	**1.9**	1,51E-07	**-2.1**	7,63E-09
Ablim1	actin-binding LIM protein 1	**1.9**	0,000138	**-1.6**	5,00E-04
L3mbtl3	l(3)mbt-like 3 (Drosophila)	**1.9**	0,00087	**-2.2**	3,72E-07
Neb	Nebulin	**1.9**	0,001613	**-2.5**	2,31E-08
Rab12	RAB12, member RAS oncogene family	**1.9**	1,59E-05	**-1.9**	8,41E-05
Rif1	Rap1 interacting factor 1 homolog (yeast)	**1.9**	7,28E-06	**-2.4**	1,09E-03
Amotl1	RIKEN full-length enriched library, clone:4932416D09 product:B-MOTIN (FRAGMENT) homolog [Homo sapiens]	**1.9**	0,003484	**-2.4**	7,75E-13
Rps26	ribosomal protein S26	**1.8**	4,73E-07	**-1.6**	1,54E-04
Tbc1d4	RIKEN full-length enriched library, clone:5930406J04 product:hypothetical Phosphotyrosine interaction (PID or PI) containing protein	**1.8**	0,003133	**-1.6**	1,13E-03
Dnajc3	DnaJ (Hsp40) homolog, subfamily C, member 3	**1.8**	1,13E-06	**-1.6**	3,70E-05
Cald1	caldesmon 1	**1.8**	1,01E-05	**-1.9**	3,04E-07
A930013K19	hypothetical protein A930013K19	**1.8**	4,32E-06	**-1.6**	1,13E-04
Fmo2	flavin containing monooxygenase 2	**1.8**	6,04E-06	**-3.0**	5,13E-15
Ppp1r12b	RIKEN full-length enriched library, clone:B230333M12 product:MYOSIN PHOSPHATASE TARGETING/REGULATORY SUBUNIT (MYOSIN PHOSPHATASE TARGET SUBUNIT 2) homolog [Homo sapiens]	**1.8**	4,63E-06	**-4.1**	1,13E-19
Kcnd2	potassium voltage-gated channel, Shal-related family, member 2	**1.7**	0,001631	**-4.4**	1,11E-16
5330438E18Rik	RIKEN cDNA 5330438E18 gene	**1.7**	1,85E-05	**-1.6**	1,87E-04
Lip1	lysosomal acid lipase 1	**1.7**	2,46E-05	**-2.1**	1,49E-08
Mt1	metallothionein 1	**1.7**	4,55E-06	**-2.2**	4,28E-10
4832420M10	hypothetical protein 4832420M10	**1.7**	0,000252	**-1.9**	1,57E-06
Zfpm2	zinc finger protein, multitype 2	**1.7**	0,000347	**-2.6**	1,85E-10
Emilin1	elastin microfibril interfacer 1	**1.7**	6,55E-06	**-2.9**	1,70E-14
Pola1	polymerase (DNA directed), alpha 1	**1.7**	0,00243	**-1.7**	8,67E-05
MGC5739	similar to hypothetical protein FLJ20010	**1.7**	0,000128	**-1.5**	5,85E-04
Dbt	dihydrolipoamide branched chain transacylase E2	**1.7**	2,86E-05	**-2.1**	5,54E-09
Gclc	glutamate-cysteine ligase, catalytic subunit	**1.7**	0,000247	**-1.5**	5,54E-04
5033405K12Rik	mRNA for mKIAA1458 protein. [AK129365]	**1.7**	1,65E-05	**-3.3**	9,54E-17
Rab21	RAB21, member RAS oncogene family	**1.7**	0,000396	**-2.8**	1,72E-12
Abhd1	abhydrolase domain containing 1, mRNA (cDNA clone MGC:19172 IMAGE:4224364)	**1.7**	1,94E-05	**-2.9**	1,91E-14
6430527G18Rik	RIKEN cDNA 6430527G18 gene	**1.7**	3,88E-05	**-1.5**	3,34E-04
D830029A09Rik	RIKEN full-length enriched library, clone:D830029A09 product:similar to BA56H7.1.2 (NEBULETTE PROTEIN (NEBL, ACTIN-BINDING Z-DISC PROTEIN)) [Homo sapiens]	**1.7**	2,05E-05	**-5.0**	1,05E-22
Ccng1	cyclin G1	**1.7**	2,34E-05	**-1.6**	6,73E-05
Nol8	nucleolar protein 8	**1.6**	8,27E-05	**-2.8**	5,52E-14
Inpp4b	inositol polyphosphate-4-phosphatase, type II	**1.6**	0,003276	**-1.7**	7,12E-05
Pou4f1	POU domain, class 4, transcription factor 1	**1.6**	0,000636	**-2.2**	1,08E-08
Dusp18	dual specificity phosphatase 18	**1.6**	0,000283	**-1.5**	4,18E-04
Als2cr3	amyotrophic lateral sclerosis 2 (juvenile) chromosome region, candidate 3 homolog(human)	**1.6**	0,000106	**-2.7**	2,92E-13
Grp58	glucose regulated protein	**1.6**	6,71E-05	**-1.6**	3,41E-05
D2Bwg1356e	RIKEN full-length enriched library, clone:5530400J02 product:similar to DJ971N18.2.1 (NOVEL PROTEIN (ISOFORM 1)) [Homo sapiens]	**1.6**	0,008107	**-3.2**	8,45E-14
Pcp2	Purkinje cell protein 2 (L7)	**1.6**	0,00454	**-1.9**	4,74E-06
Usp48	ubiquitin specific protease 48	**1.6**	0,000457	**-3.7**	4,05E-17
Olfr566	olfactory receptor 566	**1.6**	0,001564	**-2.0**	1,29E-06
Hist1h4d	histone 1, H4d	**1.6**	0,002042	**-2.8**	5,35E-12
Prp19	PRP19/PSO4 homolog (S. cerevisiae)	**1.6**	0,000117	**-1.5**	4,75E-04
1110031B06Rik	RIKEN full-length enriched library, clone:C330024G07 product:hypothetical Target SNARE coiled-coil domain containing protein	**1.6**	0,00012	**-1.5**	2,70E-04

Npepps	aminopeptidase puromycin sensitive	**1.6**	0,000132	**-1.6**	5,62E-05
Cebpz	CCAAT/enhancer binding protein zeta	**1.6**	0,000517	**-1.5**	2,82E-04
BC017133	cDNA sequence BC017133	**1.6**	0,000693	**-1.5**	4,63E-04
Camkk1	calcium/calmodulin-dependent protein kinase kinase 1, alpha	**1.6**	0,000461	**-1.5**	5,10E-04
BC059729	cDNA clone MGC:74331 IMAGE:6601702	**1.6**	0,000176	**-2.0**	5,43E-08
Lpgat1	lysophosphatidylglycerol acyltransferase 1	**1.6**	0,000837	**-2.2**	3,91E-10
Ash1l	ash1 (absent, small, or homeotic)-like (Drosophila)	**1.5**	0,007414	**-2.6**	4,89E-09
Tlm	T lymphoma oncogene	**1.5**	0,000393	**-2.2**	5,15E-10
Dicer1	Dicer1, Dcr-1 homolog (Drosophila)	**1.5**	0,001582	**-2.5**	8,53E-11
Amac1	acyl-malonyl condensing enzyme 1	**1.5**	0,007737	**-1.6**	4,18E-04
Hnrpa3	heterogeneous nuclear ribonucleoprotein A3 (Hnrpa3), transcript variant b	**1.5**	0,002668	**-1.6**	6,51E-05
0610007H07Rik	RIKEN cDNA 0610007H07 gene	**1.5**	0,000575	**-1.6**	7,22E-05
BC006965	cDNA sequence BC006965	**1.5**	0,001723	**-2.4**	4,61E-09
2610301F02Rik	RIKEN full-length enriched library, clone:B230207H03 product:hypothetical Spectrin repeat containing protein	**1.5**	0,001759	**-3.3**	1,79E-15
Map3k7	mitogen activated protein kinase kinase kinase 7	**1.5**	0,001619	**-1.6**	5,63E-05
1700008O03Rik	RIKEN full-length enriched library, clone:1700008O03	**1.5**	0,007567	**-1.7**	2,22E-05
R3hdm	R3H domain (binds single-stranded nucleic acids)	**-1.5**	0,004149	**2.2**	3,11E-09
2610005L07Rik	RIKEN cDNA 2610005L07 gene	**-1.6**	0,003843	**1.9**	1,01E-05
C1qtnf6	C1q and tumor necrosis factor related protein 6 (C1qtnf6), mRNA [NM_028331]	**-1.6**	0,001599	**2.2**	4,29E-09
Rshl2	radial spokehead-like 2	**-1.6**	7,37E-05	**2.2**	4,16E-08
Cldn5	claudin 5	**-1.6**	0,000124	**1.8**	1,49E-06
Mmp15	matrix metalloproteinase 15	**-1.6**	0,000228	**1.6**	1,01E-04
AU041783	expressed sequence AU041783	**-1.6**	0,00471	**1.7**	5,43E-05
Rab1b	RAB1B, member RAS oncogene family	**-1.6**	5,2E-05	**1.6**	8,73E-05
Znrf1	zinc and ring finger 1	**-1.6**	0,000759	**1.7**	1,50E-05
Dok4	docking protein 4	**-1.6**	0,000337	**1.6**	2,24E-04
BC022623	cDNA sequence BC022623	**-1.6**	5,54E-05	**1.5**	4,20E-04
Fli1	Friend leukemia integration 1	**-1.6**	5,37E-05	**1.7**	2,50E-05
Cav1	caveolin, caveolae protein 1	**-1.6**	0,000295	**1.5**	9,55E-04
Isg20	interferon-stimulated protein	**-1.7**	0,007916	**1.8**	1,59E-05
Tyms	thymidylate synthase	**-1.7**	0,000161	**1.6**	5,06E-04
Odf2	outer dense fiber of sperm tails 2	**-1.7**	1,38E-05	**2.7**	2,80E-04
Tnfsf13	tumor necrosis factor (ligand) superfamily, member 13	**-1.7**	0,008822	**1.6**	1,92E-03
Shank3	SH3/ankyrin domain gene 3	**-1.7**	0,000823	**2.1**	4,44E-01
Rcor2	REST co-repressor 2	**-1.7**	8,71E-06	**2.0**	1,08E-08
6230427J02Rik	RIKEN cDNA 6230427J02 gene	**-1.8**	0,00193	**2.0**	1,08E-08
Plk3	polo-like kinase 3 (Drosophila)	**-1.8**	0,000552	**1.7**	3,74E-04
Mcm6	minichromosome maintenance deficient 6 (MIS5 homolog, S. pombe) (S. cerevisiae)	**-1.8**	2,06E-06	**1.6**	4,17E-05
4632428N05Rik	RIKEN cDNA 4632428N05 gene	**-1.8**	9,95E-06	**1.5**	6,38E-04
Dll1	delta-like 1 (Drosophila)	**-1.8**	0,002979	**1.7**	2,89E-03
Ubp1	upstream binding protein 1	**-1.8**	7,78E-06	**1.6**	1,17E-04
Mcam	melanoma cell adhesion molecule	**-1.8**	2,57E-06	**1.7**	1,70E-05
Ube2q	ubiquitin-conjugating enzyme E2Q (putative)	**-1.8**	2,59E-06	**2.7**	1,59E-10
Pogz	pogo transposable element with ZNF domain	**-1.9**	0,00013	**1.7**	6,75E-05
Bpgm	2,3-bisphosphoglycerate mutase	**-1.9**	0,009424	**1.9**	5,22E-05
Chd3	chromodomain helicase DNA binding protein 3	**-1.9**	4,85E-06	**1.6**	1,62E-10
1700095N21Rik	RIKEN cDNA 1700095N21 gene	**-1.9**	7,36E-06	**1.6**	5,37E-05
Rgs3	regulator of G-protein signaling 3	**-2.0**	7,27E-08	**2.5**	2,01E-07
Igsf4c	immunoglobulin superfamily, member 4C	**-2.0**	0,002422	**1.6**	2,41E-03
Casp7	caspase 7 (Casp7)	**-2.0**	1,35E-07	**2.1**	1,31E-08
Ifi44	interferon-induced protein 44	**-2.0**	0,004425	**1.7**	1,78E-03
BI079946	BI079946 602875955F1 NCI_CGAP_Mam2 cDNA clone IMAGE:5007924 5	**-2.1**	0,004431	**2.8**	2,42E-10
Slc28a2	solute carrier family 28 (sodium-coupled nucleoside transporter), member 2	**-2.1**	3,15E-07	**1.8**	7,03E-06
Mtr	RIKEN full-length enriched library, clone:D830038K18 product:hypothetical Vitamin B12 dependent methionine synthase activation domain containing protein, full insert sequence	**-2.1**	0,006907	**1.7**	4,29E-03

Rpl14	ribosomal protein L14	**-2.2**	3,28E-07	**1.9**	1,17E-06
AK028934	RIKEN full-length enriched library, clone:4732471N16 product:weakly similar to FAS B (FRAGMENT)	**-2.3**	0,005365	**1.7**	7,33E-03
BC003277	cDNA sequence BC003277	**-2.3**	1,27E-09	**2.4**	1,70E-11
Mx2	myxovirus (influenza virus) resistance 2	**-2.3**	8,25E-05	**1.7**	8,20E-04
2310075M15Rik	mRNA for mKIAA0230 protein	**-2.4**	2,08E-09	**2.0**	9,52E-08
Pfkp	phosphofructokinase, platelet (Pfkp)	**-2.4**	1,48E-08	**1.6**	4,43E-04
4932425I24Rik	RIKEN cDNA 4932425I24 gene	**-2.4**	0,009367	**1.9**	1,69E-03
Rassf2	Ras association (RalGDS/AF-6) domain family 2	**-2.4**	4,01E-09	**1.6**	1,44E-04
Ephb1	Eph receptor B1	**-2.6**	0,000645	**1.7**	2,01E-06
Bcl6b	B-cell CLL/lymphoma 6, member B	**-2.7**	4,74E-12	**1.8**	2,01E-06
Mtss1	metastasis suppressor 1	**-2.7**	4,49E-05	**1.7**	4,49E-05
Uhrf1	ubiquitin-like, containing PHD and RING finger domains, 1	**-2.7**	0,000276	**2.2**	4,07E-05
4930555G01Rik	RIKEN cDNA 4930555G01 gene	**-2.9**	2,27E-05	**2.6**	6,39E-09
Mest	mesoderm specific transcript	**-3.5**	3,33E-17	**2.2**	1,20E-09
Apln	Apelin	**-3.6**	6,49E-14	**2.5**	3,18E-11

Indicated are the fold increase or decrease with which gene transcripts differ between MHC-Cre vs MHC-Cre/MHC-CnA hearts (column Cre-CnA vs Cre). Likewise, indicated are the fold increase or decrease with which gene transcripts are differentially expressed between MHC-Cre/MHC-CnA vs MHC-Cre/MHC-CnA/Flox-DNMEF2 transgenic hearts (column Cre-CnA-DNMEF2) vs Cre-CnA. For each gene product the P value is indicated, and only gene transcripts with P value <0.01 were considered. Gene, indicates symbolic name of gene transcript; Description, indicates a description of the symbolic short namen of the gene transcript.

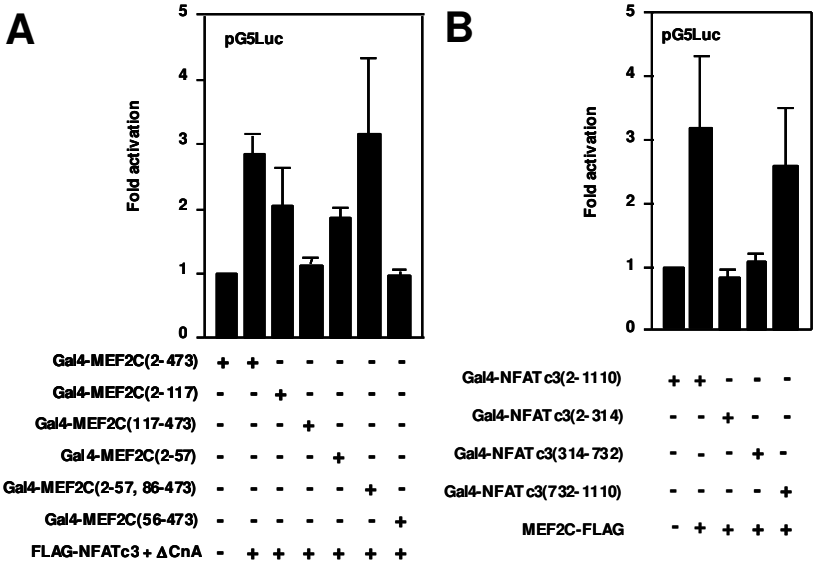

Supplemental figure I. Mapping of NFATc3 and MEF2C interacting domains. **A.** COS7 cells were transfected with deletion mutants of Gal4-MEF2C fusion proteins with or without NFATc3 and activated calcineurin. **B.** COS7 cells were transfected with deletion mutants of Gal4-NFATc3 fusion proteins with or without MEF2C.

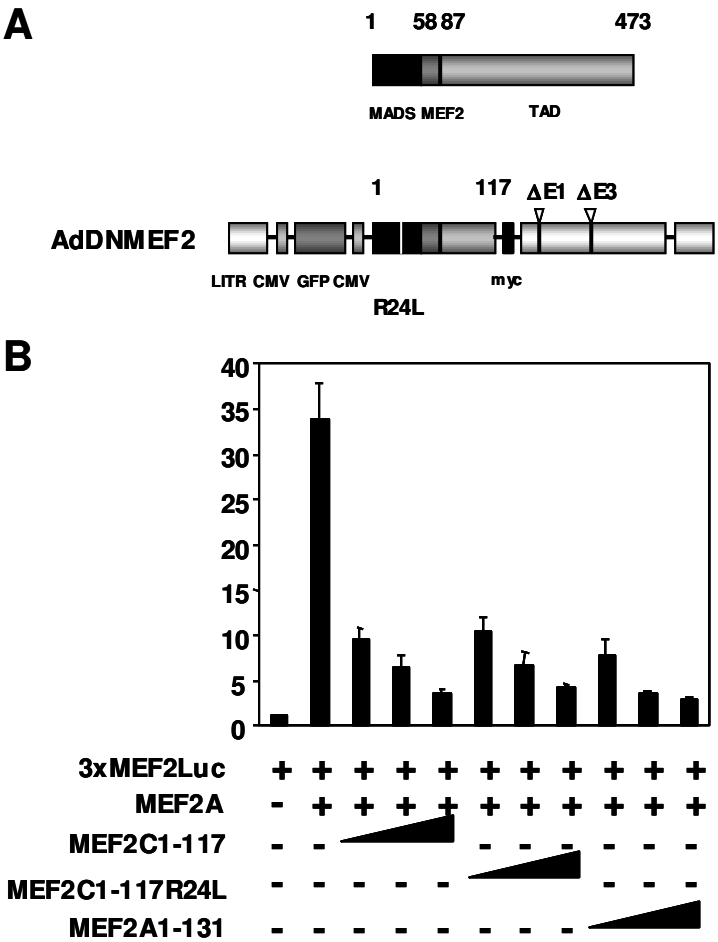

Supplemental figure II. A. Schematic representation of human MEF2C and dominant negative MEF2 virus. **B.** COS7 cells were transiently transfected with a multimerized MEF2 reporter in the presence of expression plasmids containing MEF2A with or without increasing amounts of MEF2C1-117, MEF2C1-117(R24L) or MEF2A1-131. All dominant negative constructs dose-dependently inhibited transcriptional activation of the MEF2 reporter construct.

Chapter 3

MEF2 activates DMPK expression promoting cardiomyocyte elongation and sarcomere degeneration

Ralph J. van Oort, Meriem Bourajjaj, Joost Schimmel, Melany C. van Oostrom, Roel van der Nagel, Igor I. Rybkin, Rhonda Bassel-Duby, Eric N. Olson, Elisabeth Ehler, Leon J. De Windt

Submitted

ABSTRACT

The heart responds to stress signals by hypertrophic growth, which is accompanied by activation of select transcription factors and reprogramming of cardiac gene expression. Although the transcription factor myocyte enhancer factor-2 (MEF2) is known to be a common endpoint for several hypertrophic pathways, its precise gene targets and role in myocardial remodeling remain to be elucidated. To this end, we pursued comprehensive gain-of-function approaches to activate MEF2 transcriptional activity in cultured cardiomyocytes. Adenoviral delivery of wildtype MEF2A or constitutively active MEF2 to cultured ventricular myocytes primarily induced myocyte elongation and myofibril degeneration, instead of concentric hypertrophy and sarcomere assembly, which one would expect for a hypertrophic effector.

To facilitate the identification of early MEF2 target genes underlying this cellular remodeling process, we combined an inducible gene expression system in a cardiac cell line with genome wide gene chip analyses, and found 75 MEF2 target genes at 24 hrs after inducible MEF2 activation. Gene ontology classification revealed an overrepresentation of genes involved in energy metabolism, cytoskeletal remodeling, and cell-matrix adhesion. Confocal analyses indicated that MEF2-induced myocyte elongation was accompanied by a redistribution of focal adhesions. SiRNA mediated knockdown of the MEF2 target gene myotonic dystrophy protein kinase (DMPK) was sufficient to inhibit MEF2 induced cardiomyocyte elongation.

Thus, these findings assign a novel function to MEF2 transcription factors in postnatal heart muscle, where they activate a gene program that promotes myocyte elongation, myofibril degeneration, and focal adhesion distribution in a DMPK-dependent fashion.

INTRODUCTION

The myocyte enhancer factor-2 (MEF2) transcription factor was originally defined as a muscle-specific DNA binding activity that recognizes conserved A/T-rich elements associated with numerous muscle-specific genes [1]. To date, four MEF2 genes, *mef2a*, *-b*, *-c*, and *-d*, have been characterized in vertebrates, with an expression pattern and function that extends beyond striated muscle. MEF2 transcription factors share high homology in an amino-terminal MADS (MCM1, Agamous, Deficiens, and Serum response factor) box and an adjacent MEF2-specific domain, which together mediate dimerization and binding to the consensus

DNA sequence CTA(A/T)$_4$TA(G/A) [2, 3]. MEF2 factors have been implicated in the embryonic development of cardiac, skeletal, and smooth muscle [4], and in postnatal heart disease [5, 6].

Soon after birth, cardiomyocytes withdraw from the cell cycle and heart growth occurs only by an increase in size of the individual myocytes. While this is a part of normal development and initially beneficial it can run out of control and the response to stress signals can lead to pathological hypertrophy and activation of a "fetal" cardiac gene program. Clinical stress signals that induce cardiac hypertrophy include hypertension, endocrine disorders, myocardial infarction, and contractile dysfunction from inherited mutations in cardiac structural genes. Pathological hypertrophy frequently progresses to dilated cardiomyopathy (DCM), a chronic disorder of the heart muscle. In humans, end-stage DCM is characterized by poorly contractile and dilated ventricles, accompanied by lengthening of myocytes, myocyte side-to-side slippage, loss of myofibrils, severe changes in cytoskeletal architecture and accumulation of collagen in perivascular and interstitial spaces [7, 8]. The genetic underpinnings underlying the cellular alterations in DCM remain largely elusive.

Thus far, MEF2 transcription factors have been postulated to play a role in the development of cardiac hypertrophy. In line with this premise, in normal adult myocardium, MEF2 exhibits only basal activity, likely required for the maintenance of contractile protein gene expression and energy metabolism [9, 10]. In cardiac disease, however, circumstantial evidence suggests that MEF2 factors serve as a transcriptional platform for prohypertrophic signaling cascades, including calcineurin, calcium/calmodulin-dependent protein kinase (CaMK), big mitogen-activated protein kinase (MAPK)-1 (BMK-1), and p38 MAPK [6, 11, 12].

In contrast, we and others have recently demonstrated that overexpression of MEF2 in the postnatal heart minimally triggers the hypertrophic growth response, but induces dilated cardiomyopathy [6, 13].

To further investigate the role of MEF2 in cardiomyocyte remodeling, we generated adenoviruses expressing either wildtype MEF2A or a constitutively active mutant of MEF2. Cultured ventricular myocytes infected with these viruses primarily underwent myocyte elongation, accompanied by sequential loss of myofibrils. A genome-wide gene chip analysis of early MEF2 target genes in a ventricular muscle cell line with inducible MEF2 activation provided mechanistic insights into the diverse cardiomyopathic consequences associated with MEF2 activation. Functional clustering of MEF2 target genes revealed an overrepresentation of genes involved in cytoskeletal remodeling and cell-matrix adhesion. In line, MEF2-induced myocyte elongation was accompanied by focal adhesion redistribution. One of the genes found to be upregulated by MEF2 activation was myotonic dystrophy protein kinase (DMPK). Inhibition of the MEF2

induced increase of DMPK protein levels resulted in partial rescue of the elongated phenotype, suggesting a primary role for DMPK in myocyte elongation and the genesis of dilated cardiomyopathy.

Table 1. List of oligonucleotide primers used for RT-PCR.

Gene	Accession number	Forward	Reverse
Acta1	NM_009606	5'-GCATGCAGAAGGAGATCACA	5'-ACATCTGCTGGAAGGTGGAC
CTGF	NM_010217	5'-AGACATACAGGGCTAAGTTCTG	5'-CACTGGCAGAGTGGTGGTTCT
DMPK	S60315	5'-GGACAAGTATGTGGCCGACT	5'-CATCTTCACCACCGCTACCT
Gsta1	NM_008181	5'-CGCCACCAAATATGACCTCT	5'-CAAGGCAGTCTTGGCTTCTC
Itga7	NM_008398	5'-AACAGCACCTTTCTGGAGGA	5'-GGATGCATCTCTGAGCAACA
Itgb4	BC059192	5'-CCTTCGAGCAGCCTGAATAC	5'-CTCCCTCCACAGGGACATAA
L7	BC086786	5'-GAAGCTCATCTATGAGAAGGC	5'-AAGACGAAGGAGCTGCAGAAC
Muc5b	NM_028801	5'-CTCTTCAACTCACGCATGGA	5'-TACACAGGCCTGACAGTTGC
Myl9	BC055439	5'-CAGAACCGAGATGGCTTCAT	5'-CCCCAAACATTGTGAGGAAC
Nexn	NM_199465	5'-AGAGGAAGAACGCAGGCATA	5'-GCTTGAATTGAGCCACTCCT
Sgca	NM_009161	5'-AGGCCCAGCAGACAACTTTA	5'-GGTGAGCGTGGTAGGTGAGT
Sgcb	NM_011890	5'-TGCTGAGGTTCAAGCAAGTG	5'-CTGGAAGACAATTGGCTGGT

MATERIALS AND METHODS

Recombinant adenoviruses. MEF2VP16, a fusion between amino acids (aa) 1-91 of human MEF2D and aa 412-490 of the viral transcriptional activator VP16, was cloned into the pAdTrack-CMV viral shuttle vector (generously provided by Bert Vogelstein, Johns Hopkins University) and recombined in BJ5183 bacteria (Stratagene) to obtain E1-E3-deleted adenoviral bicistronic vectors to generate AdMEF2VP16, which expresses MEF2VP16 and GFP under separate CMV promoters. AdMEF2A, an adenovirus expressing both C-terminal FLAG-tagged human MEF2A and GFP, and AdGFP, a control virus expressing only GFP, were generated as described previously [6, 14]. Virus titers were determined in neonatal rat cardiomyocytes based upon GFP fluorescence and used at a multiplicity of infection (moi) of 1.0 or less when indicated.

Cell culture and transient transfection assays. Isolation and culture of neonatal rat ventricular cardiomyocytes was performed as described before in detail [15]. Low passage COS7 and HEK293 cells were grown in Dulbecco's modified Eagle's medium (Invitrogen) supplemented with 10% fetal bovine serum. NkL-TAg cells were cultured as described previously [16]. For transfection assays, cells were

grown in 48-well plates and transiently transfected using the indicated expression and reporter vectors with FuGENE 6 reagent (Roche) at 1.5 µl FuGENE:1 µg DNA ratios, and measured using the Dual Luciferase assay system (Promega), where *firefly* luciferase activity is normalized for *Renilla* luciferase activity to control for variations in transfection efficiency. For siRNA experiments, cardiomyocytes were transfected with control siRNAs or siRNAs specific for DMPK (Ambion) in a final concentration of 100 nM, using Oligofectamine (Invitrogen). Twenty-four hours after transfection, cells were washed in PBS and further treated as described.

Immunofluorescence and confocal microscopy. Cultured cardiomyocytes were fixed for 10 min in 4% paraformaldehyde and permeabilized with 0.2% Triton X-100 in PBS for 5 minutes. Primary and secondary antibodies were diluted using 1% BSA in TBS and incubations were carried out at room temperature for 1 hour. Cells were washed 3 times with PBS for 5 minutes, mounted with coverslips in 0.1 M Tris-HCl (pH 9.5)-glycerol (3:7) including 50 mg/ml *n*-propylgallate as anti-fading reagent, and analyzed by confocal microscopy using a Zeiss LSM 510 META instrument. Antibodies used included mouse anti α-actinin (Sigma, 1:500); rabbit anti α-actinin [17] (1:200), monoclonal anti-myomesin [17] (1:50), monoclonal anti-titin T12 [17]; rabbit anti-titin M8 [18] (1:50); monoclonal anti-EH-myomesin [19] (1:500); monoclonal anti-vinculin (Sigma, 1:50); Cy5 goat anti-rabbit and Cy3 goat anti-mouse (Jackson Immuno Research, 1:100 and 1:500, respectively); DAPI (1:100). Cell surface areas and cell length-width ratios were determined using SPOT-imaging software (Diagnostic Instruments).

RT-PCR. Total RNA was isolated from the indicated cell types using TRIzol reagent (Invitrogen). Three µg RNA was used as template for Superscript reverse transcriptase II (Gibco) using the indicated primer combinations (Table 1).

Western blot analysis. Protein was isolated from cells by lysis in extraction buffer (20 mM Tris (pH7.5), 150 mM NaCl, 1 mM EDTA, 1 mM EGTA, 1% Triton X-100, and complete protease inhibitor cocktail (Roche). Total protein from centrifuged lysate was separated by electrophoresis on a 10% SDS-PAGE gel and transferred to polyvinylidene difluoride membranes (Amersham Pharmacia Biotech). Antibodies used included mouse monoclonal anti-GFP (Santa Cruz, 1:500), mouse monoclonal anti-VP16 (Santa Cruz, 1:500), mouse monoclonal anti-FLAG (Sigma, 1:5000), and rabbit polyclonal anti-DMPK (Zymed, 1:500) in 10% non-fat dry milk, followed by corresponding horseradish peroxidase (HRP)-conjugated secondary antibodies (DAKO, 1:5000) and processed for chemiluminescent detection as described by the manufacturer (Amersham).

Generation of stable cardiac cell lines. NkL-TAg cells were cultured as described previously [16]. Double stable, MEF2VP16-inducible cells were generated using the T-REX system (Invitrogen) with modifications. Briefly, NkL-TAg cells were transfected using FuGENE 6 reagent (Roche) with 8 µg pCAgβTrs-

hygro, a vector expressing the Tet-repressor (TR) under control of a β-actin promoter (generously provided by Hans Clevers, Hubrecht Laboratory) and stable clones selected with 250 µg/µl hygromycin. Selected colonies were transiently transfected using FUGENE 6 reagent (Roche) with 0.2 µg pcDNA4/TO-luciferase (generously provided by Hans Clevers) to test their responsiveness to doxycyclin (Dox) using the Dual Luciferase assay system (Promega). Two different Tet-repressor clones (TR1 and TR4), showing high luciferase activity and low background, were subsequently transfected with 8.5 µg pcDNA4/TO-MEF2VP16 using FUGENE 6 reagent (Roche) and cultured in the presence of hygromycin and 750 µg/µl zeocin to generate double stable cell lines. Zeocin/hygromycin resistant clones were transiently transfected with a MEF2-luciferase reporter (3xMEF2-Luc [9]) to test their DOX-inducible MEF2 activation profile.

Agilent gene expression profiling and data analysis. TR1-194 and TR4-39 inducible MEF2VP16-NkL-TAg clones were maintained in parallel cultures, mortalized by overnight AdCre infection, cultured for an additional 3 days in serum-free media either in the presence or absence of 24 h Dox-treatment. Three corresponding cultures were pooled, total RNA extracted using TRIzol (Invitrogen) and cleaned with Qiagen RNeasy Mini Kits (Qiagen). RNA quantity was measured with a NanoDrop® ND-1000 UV-Vis Spectrophotometer (Wilmington), and RNA quality was monitored using an Agilent 2100 bioanalyzer. Agilent 44k mouse whole genome microarray slides (Palo Alto) were used and a dye-swap experimental design applied. RNA samples (500 ng each) acquired from the clones were amplified and labeled with Cy5- and Cy3-CTP (Perkin Elmer) to produce labeled cRNA using Agilent low RNA input fluorescent linear amplification kits following the manufacturer's protocol. After amplification and labeling, the dye-incorporation ratio was determined with NanoDrop® ND-1000 UV-Vis Spectrophotometer (Wilmington). For hybridization, the guidelines for 44k format arrays with cRNA targets were strictly followed. Briefly, 750 ng of Cy3-labeled cRNA and 750 ng Cy5-labeled cRNA were mixed and incubated with an Agilent microarray slide for 17 hours using an Agilent *in situ* hybridization kit following SSC buffer washing. The washed slides were immediately dried, and scanned using Agilent DNA Microarray Scanner (G2565BA). Raw data were generated using Agilent's Feature Extraction software (FE v7.1). Gene classifications were assigned based upon publicly available software and websites, including FATIGO Data mining with Ontology (www.fatigo.org), Mouse Genome Informatics (MGS; www.informatics.jax.org), GenBank and Medline.

Chromatin immunoprecipitation. Chromatin immunoprecipitation was carried out using the Upstate Biotechnology ChIP assay kit according to the manufacturer's instructions using anti-acetylated histone H3 antibody (Upstate Biotechnology) and pan-MEF2 polyclonal antibody (Santa Cruz). Equal amounts of soluble chromatin

from each sample were immunoprecipitated with 1 µg of the above mentioned antibodies. Following immunoprecipitation of immunocomplexes, the lysates were put at 65°C for four hours to reverse the formaldehyde crosslinking. Associated DNA was purified by phenol/chloroform extraction. PCR was carried out using specific primers to the promoter region of rat *dmpk* (FW: 5'- gagctattttggggtctctt, REV: 5'- cttcttcgtgactcagcaat).

Statistical analysis. The results are presented as means ± SEM. Statistical analyses were performed using INSTAT 3.0 software (GraphPad, San Diego) and Student's t-test or ANOVA followed by Tukey's post-test when appropriate. Statistical significance was accepted at a P value < 0.05.

RESULTS

Activation of MEF2 induces elongation in cultured cardiomyocytes

To address the role of MEF2 in cardiomyocyte remodeling, we first tested the efficiency of two different expression vectors of MEF2, one expressing wildtype MEF2A, and one expressing a constitutively active mutant of MEF2, MEF2VP16, using a luciferase reporter with 3 multimerized MEF2 binding sites upstream of a minimal TATA box (3xMEF2-Luc) as a readout in cotransfection experiments. Cotransfection of the reporter with MEF2A produced an approximate 12 ± 3-fold increase in luciferase activity. Even double amounts of MEF2A produced a similar activation profile of the reporter (15 ± 3) (Fig. 1A). In contrast, the MEF2VP16 expression vector resulted in a 134 ± 28-fold higher MEF2 transcriptional activity (Fig. 1A). These findings indicate that overexpression of wildtype MEF2A or MEF2VP16 will provide means to mimic either mild (MEF2A) or strong (MEF2VP16) activation of MEF2 transcription factors in cultured cardiomyoctes.

Figure 1. MEF2 induces eccentric cardiac hypertrophy. **A.** Cotransfection of 3xMEF2-Luc reporter with expression vectors for MEF2A (0.1 and 0.2 µg) and MEF2VP16 (0.1 µg) in COS7 cells, indicate that transcription is robustly activated by MEF2VP16. **B.** Schematic representation of the bicistronic adenoviral vectors expressing MEF2A and GFP or MEF2VP16 and GFP. **C.** Western blot analysis with either anti-FLAG and anti-GFP antibodies (upper panel) or anti-VP16 and anti-GFP antibodies (lower panel) on lysates of COS7 cells infected with AdMEF2A, or AdMEF2VP16 and AdGFP, respectively. **D.** Representative confocal images of immunostained cardiomyocytes infected with the indicated adenoviruses. Sarcomeric α-actinin staining demonstrates both hypertrophied (AdMEF2A and AdMEF2VP16) and thin and elongated (AdMEF2VP16) cells. Bar, 50 µm. **E.** Surface area measurements of cardiomyocytes (≥ 100 per experiment) infected with AdGFP, AdMEF2A and AdMEF2VP16. **F.** Quantitative examination of cell-length/cell-width ratios of cardiomyocytes (≥ 100 per experiment) infected with AdGFP, AdMEF2A and AdMEF2VP16. *Indicates P<0.05 compared to AdGFP infected cells.

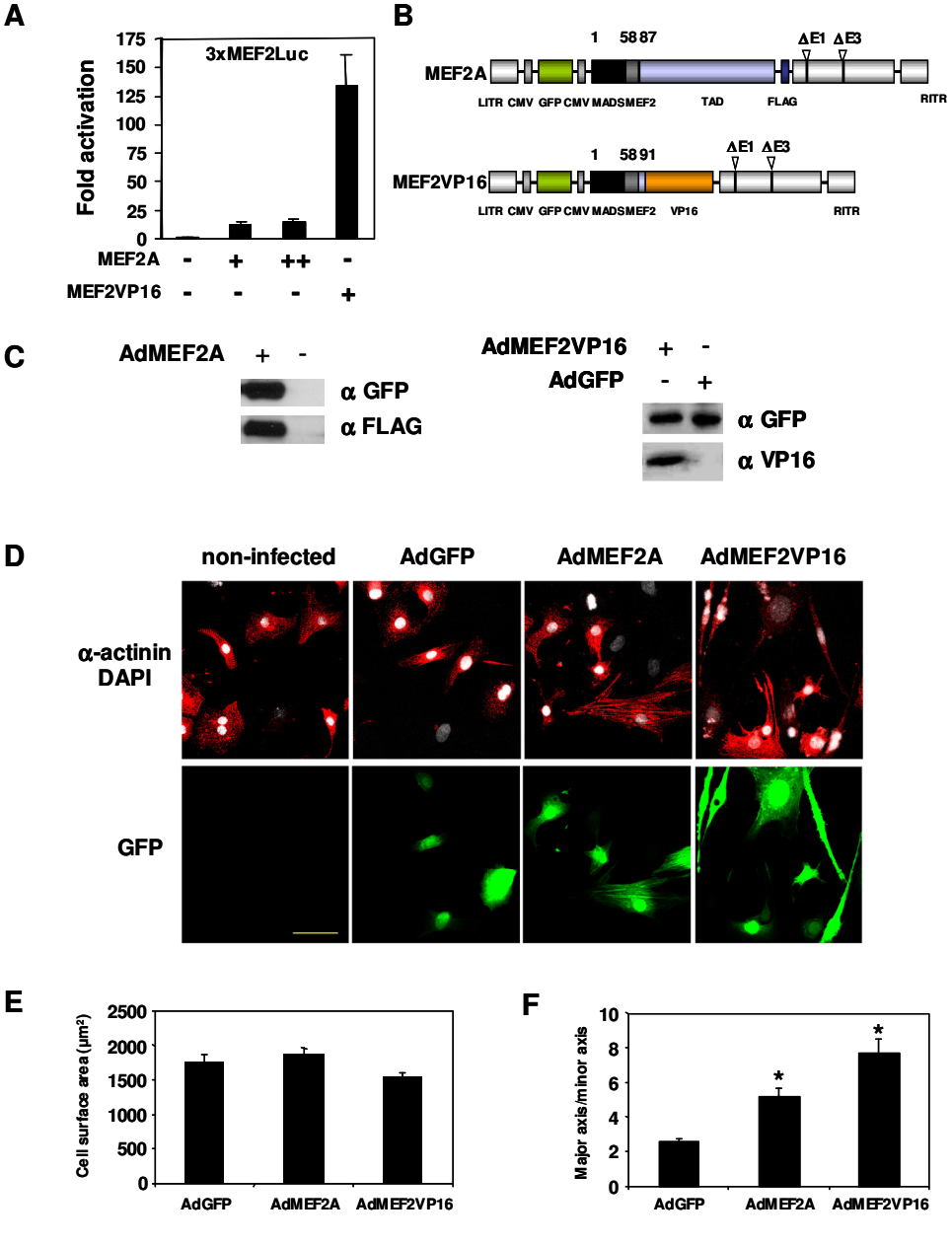
A
Fold activation
175
150
125
100
75
50
25
0
3xMEF2Luc
MEF2A - + ++ -
MEF2VP16 - - - +
B
MEF2A
1 58 87
ΔE1 ΔE3
LITR CMV GFP CMV MADS MEF2 TAD FLAG RITR
MEF2VP16
1 58 91
ΔE1 ΔE3
LITR CMV GFP CMV MADS MEF2 VP16 RITR
C
AdMEF2A + -
α GFP
α FLAG
AdMEF2VP16 + -
AdGFP - +
α GFP
α VP16
D
non-infected
AdGFP
AdMEF2A
AdMEF2VP16
α-actinin
DAPI
GFP
E
Cell surface area (μm²)
2500
2000
1500
1000
500
0
AdGFP
AdMEF2A
AdMEF2VP16
F
Major axis/minor axis
10
8
6
4
2
0
*
*
AdGFP
AdMEF2A
AdMEF2VP16

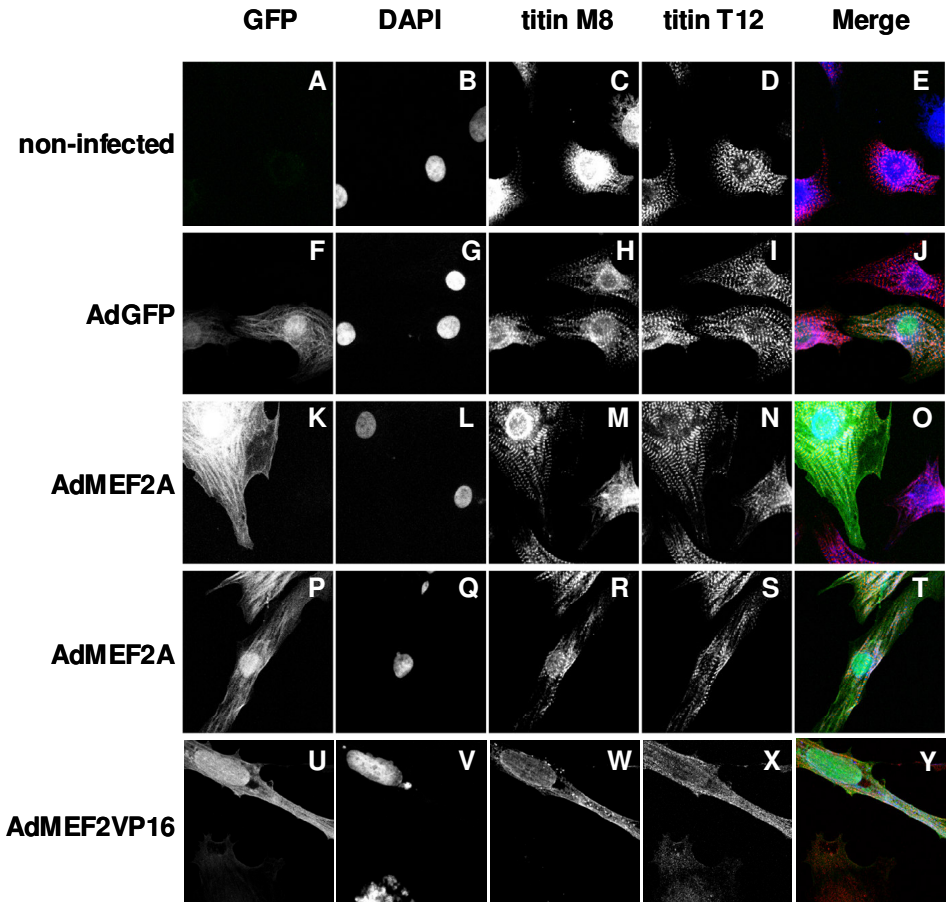

Figure 2. MEF2 activation promotes cardiomyocyte elongation. Confocal immunocytochemistry of cultured neonatal rat cardiomyocytes using antibodies raised against titin epitopes located in the Z-disc (titin T12) and in the M-band (titin M8), demonstrates that MEF2 stimulation preferentially stimulates myocyte elongation.

To overcome the low transfection efficiency of cultured cardiomyocytes, we generated adenoviral vectors to overexpress the two MEF2 constructs. Two replication-deficient, bicistronic adenoviruses were generated expressing either MEF2A and GFP or MEF2VP16 and GFP under control of separate CMV promoters (Fig. 1B). Western blotting with anti-GFP, anti-FLAG, and anti-VP16 antibodies confirmed that the viruses expressed proteins of the correct size (Fig. 1C). In contrast, the control AdGFP adenovirus only displayed immunoreactivity for GFP and not for FLAG (data not shown) or VP16 (Fig. 1C). The viruses were then

used to infect cultured neonatal rat ventricular myocytes. Following infection, cells were serum starved for 48 h, fixed and stained for α-actinin to identify cardiomyocytes and visualize myofibrils, and counterstained with DAPI to visualize nuclei (Fig. 1D). Control cells (uninfected or AdGFP infected) showed no signs of hypertrophy. Surprisingly, cardiomyocytes infected with AdMEF2A demonstrated different phenotypes: the majority of GFP-positive cells were elongated when compared to control cells, and less than 10% of GFP-positive cells were visibly larger than control cells. Of note, the larger cells did not display the typical features of hypertrophied cells, including sarcomere assembly, vigorous beating, or ANF positivity (data not shown). AdMEF2VP16-infected cells showed a more pronounced elongation by 48 hours, and larger cells were only sporadically detected in these cultures. In line, AdMEF2A- and AdMEF2VP16-infected cultures did not reveal a significant increase in average cell surface area (1870 ± 93 μm^2 and 1539 ± 74 μm^2, respectively), a measure of hypertrophy, as compared to AdGFP-infected cultures (1778 ± 94 μm^2) (Fig. 1E). We next determined the ratio of the length of the major and minor axis of cells in our experimental groups, as a measure of cellular elongation. AdGFP-infected cardiomyocytes had a ratio of 2.57 ± 0.16, while AdMEF2A- and AdMEF2VP16-infected cells displayed a 2- and 3 fold increase in major to minor axis ratios (5.20 ± 0.50 and 7.70 ± 0.77, respectively; $P < 0.05$) compared to AdGFP-infected cells (Fig. 1F). Combined, these data suggest that neither a mild increase in MEF2 transcriptional activity in cultured cardiomyocytes, accomplished by AdMEF2A infection, nor a high increase in transcriptional activity of MEF2, by AdMEF2VP16 infection, provoke a classical hypertrophic response, but rather promotes elongation of cardiomyocytes.

MEF2 activation in cardiomyocytes causes loss of myofibril architecture

To more accurately analyze the phenotypes we observed upon AdMEF2A and AdMEF2VP16 infection, we immunostained for specific intracellular components of cardiomyocytes and performed confocal microscopy at higher magnification (Fig. 2). Cells were either left uninfected (Fig. 2A-E), infected with AdGFP (Fig. 2F-J), AdMEF2A (Fig. 2K-T), or AdMEF2VP16 (Fig 2. U-Y) at moi's <1, to be able to identify infected cells (GFP-positive) adjacent to non-infected cells within the same cultures. Fluorescence for GFP was used to track the individual cells infected with AdGFP, AdMEF2A or AdMEF2VP16 (Fig. 2, Panels A, F, K, P and U). DAPI staining was used to visualize nuclei (Fig. 2, Panels B, G, L, Q, V). We immunostained cells for either titin at the M-band (titin M8; Fig. 2, Panels C, H, M, R, W) or titin at the Z-disc (titin T12; Fig. 2, Panels D, I, N, S, X), and finally merged the different channels (Fig. 2, Panels E, J, O, T, Y).

AdGFP-infected cells cultured under serum free conditions displayed a regular pattern of myofibril staining, with a regular spacing between the M-band and the Z-

disc (Fig. 2J), which was indistinguishable from non-infected cells (Fig. 2E and J). As discussed above, upon AdMEF2A infection two different phenotypes were distinguishable, either elongated cells or enlarged cells that did not show signs of classical cardiomyocyte hypertrophy. Fig. 2O displays a representative example of an AdMEF2A-infected enlarged myocyte, with adjacent, non-infected, significantly smaller cardiomyocytes in the same culture. In the larger AdMEF2A-infected cells, myofibril structures were less well organized (Fig. 2M, N, O). In elongated AdMEF2A-infected myocytes, the organization of M-band and Z-disc structures were even less apparent (Fig. 2R, S), resulting in overall poorly defined myofibrils (Fig. 2T). The most dramatic loss of sarcomeres was evident in AdMEF2VP16-infected cultures, with only remnants of M-band (Fig. 2W) and Z-disc structures (Fig. 2X).

Next, we inspected cardiomyocyte cultures with altered MEF2 transcriptional activity for other myofibril components; α-actinin at the Z-disc, and myomesin located at the M-band (Fig. 3). Cells were left uninfected (Fig. 3A-E), infected with AdGFP (Fig. 3F-J), AdMEF2A (Fig. 3K-T), or AdMEF2VP16 (Fig. 3U-Y). Fluorescence for GFP was used to track the individual cells infected with AdGFP, AdMEF2A or AdMEF2VP16 (Fig. 3, Panels A, F, K, P, and U). DAPI staining was used to visualize nuclei (Fig. 3, Panels B, G, L, Q, and V). Examples of cells immunostained for either α -actinin at the Z-disc (Fig. 3, Panels C, H, M, R, W) or myomesin at the M-band (Fig. 3, Panels D, I, N, S, X), and merged channels (Fig. 3, Panels E, J, O, T, Y) are presented. Uninfected or AdGFP-infected cultures demonstrated a regular pattern of sarcomere staining (Fig. 3E, J). Enlarged AdMEF2A-infected cells demonstrated slightly less well-defined myofibril integrity (Fig. 3O) or more severely affected organization of myomesin (Fig. 3T), while elongated AdMEF2VP16-infected cells showed only remnants of either myofibril structure (arrows in Fig. 3S, W, X).

In conclusion, these data demonstrate that increased MEF2 transcriptional activity in cultured cardiomyocytes provokes myocyte elongation, accompanied by a progressive loss of myofibrillar structures.

Inducible activation of MEF2 in cardiac cell lines

To begin to understand the mechanisms underlying the characteristic phenotypic alterations presumably evoked by MEF2 transcriptional activity and activation of its downstream target genes, we generated a cellular system to inducibly activate MEF2 target genes in NkL-TAg cells, a previously described ventricular muscle cell line [16]. To this end, NkL-TAg cells were stably transfected with an expression vector harboring the Tet-repressor (TR) under control of a β-actin promoter using hygromycin as selectable marker (Fig 4A). About 80 clones were obtained and tested for Dox-inducibility after transient transfection of a

luciferase reporter construct downstream of two Tet-operator (TetO) sites (Fig. 4B). We continued with 2 NkL-TAg-TR clones (designated TR1 and TR4), which showed at least a 100-fold increase of luciferase activity in the presence of Dox and background luciferase in the absence of Dox (Fig. 4B).

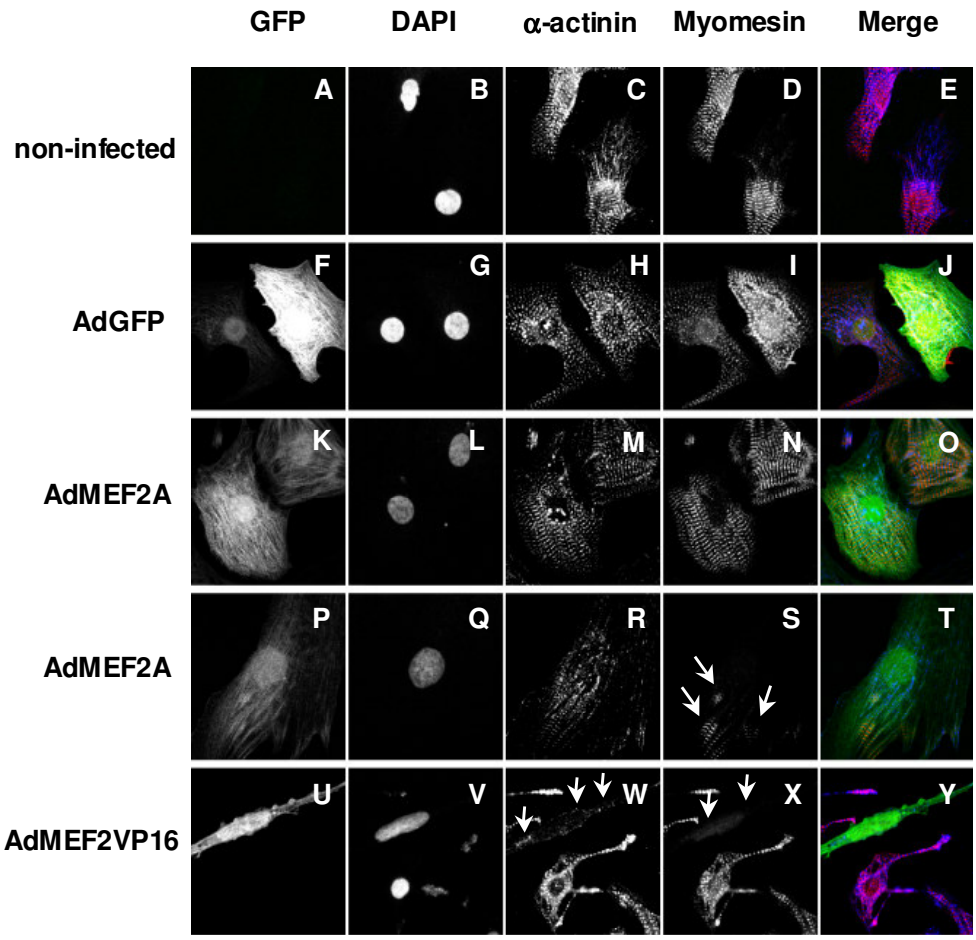

Figure 3. MEF2 activation promotes sarcomere degeneration. Confocal immunocytochemistry of cultured neonatal rat cardiomyocytes, using anti-sarcomeric α-actinin (Z-disc) and anti-myomesin (M-band) antibodies, demonstrates that MEF2-induced myocyte elongation is accompanied with myofibril degeneration. Arrows in Panels S, W and X point to residual α-actinin immunoreactivity.

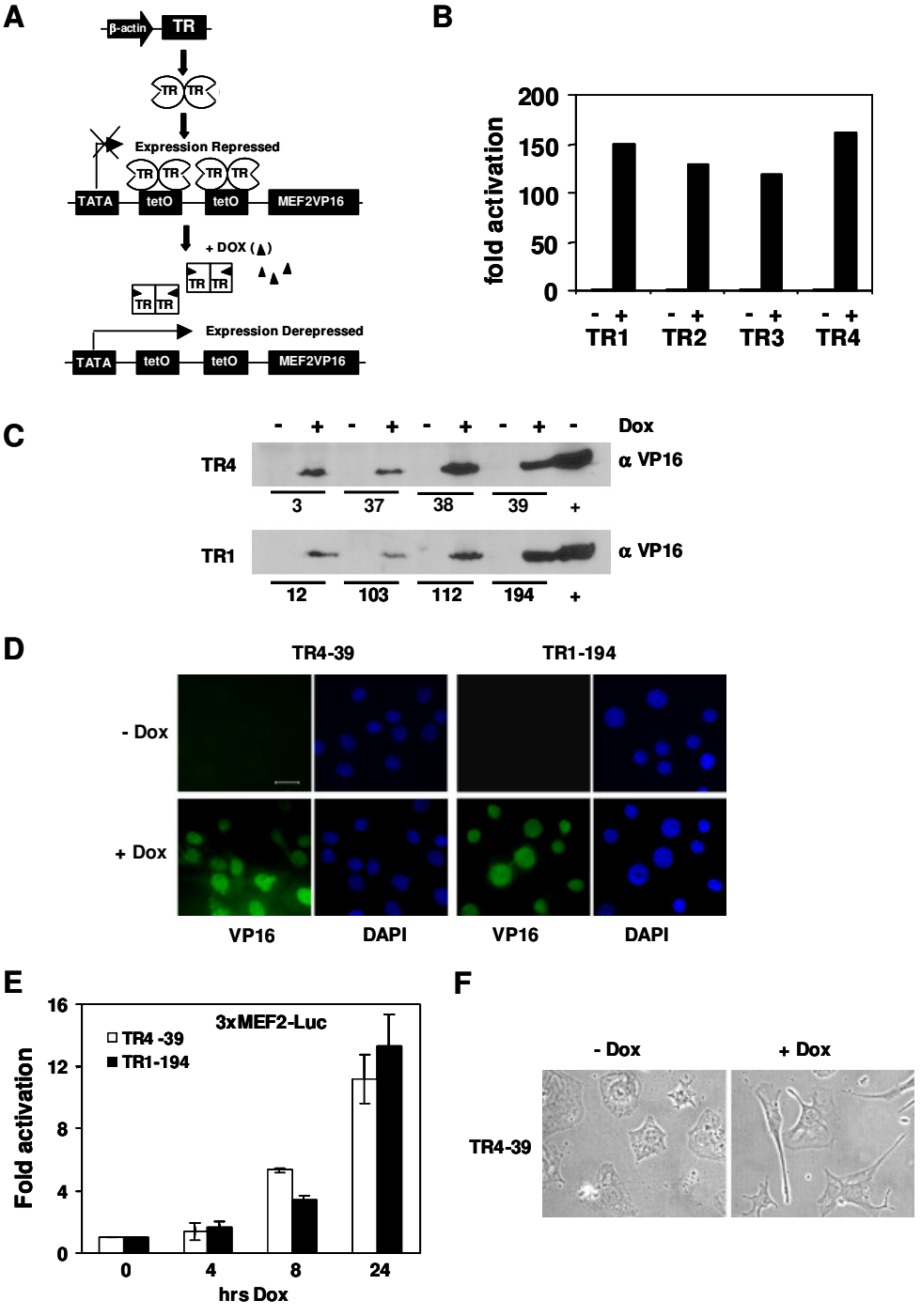
A
β-actin
TR
TR TR
Expression Repressed
TR TR TR TR
TATA
tetO
tetO
MEF2VP16
+ DOX (▲)
TR TR
TR TR
Expression Derepressed
TATA
tetO
tetO
MEF2VP16
B
fold activation
200
150
100
50
0
- + - + - + - +
TR1 TR2 TR3 TR4
C
- + - + - + - + -
Dox
TR4
α VP16
3 37 38 39 +
TR1
α VP16
12 103 112 194 +
D
TR4-39
TR1-194
- Dox
+ Dox
VP16 DAPI VP16 DAPI
E
Fold activation
16
12
8
4
0
3xMEF2-Luc
TR4 -39
TR1-194
0 4 8 24
hrs Dox
F
- Dox
+ Dox
TR4-39

Next, we stably transfected TR1 and TR4 clones with a construct harboring MEF2VP16 under transcriptional control of 2 TetO sites (Fig. 4A), using zeocin as a selectable marker. Up to 200 clones were obtained and tested for inducible MEF2 transcriptional activity following Dox stimulation using a 3xMEF2-Luc reporter (data not shown). For both TR1 and TR4, 4 double-stable clones were obtained which only expressed MEF2VP16 after Dox stimulation, as demonstrated by Western blotting using an antibody against VP16 (Fig. 4C). To control for cell-based variations, we selected two TR-MEF2VP16 clones, designated TR1-194 and TR4-39, for further analysis.

Immunofluorescent staining showed absence of VP16 immunofluorescence in the absence of Dox, and homogenous MEF2VP16 expression after 24 h induction with Dox, which was exclusively localized to the nucleus, as expected for a constitutively active MEF2 transcription factor (Fig. 4D). Finally, both clones were transiently transfected with 3xMEF2-Luc, mortalized with AdCre infection [16], cultured for 72 hrs in serum free media to allow to adopt a ventricular muscle cell fate, and exposed to Dox for varying periods to establish at which time-course elevated MEF2 transcriptional activity was evident. In both clones, an approximate 5-fold increase of MEF2 transcriptional activity was evident at 8 h, compared to TR1-194 and TR4-39 clones cultured in the absence of Dox (Fig. 4E). After 24 h Dox exposure, both clones demonstrated an approximate 10-fold increase in MEF2 transcriptional activity (Fig. 4E). Both TR1-194 and TR4-39 cell lines elongated after Cre-induced mortalization and Dox stimulation (Fig. 4F, and data not shown).

In conclusion, we established a novel system that allows inducible activation of MEF2 transcriptional activity in ventricular muscle cells by addition of doxycyclin to the culture medium.

Figure 4. Generation of cardiac cell lines inducibly expressing MEF2VP16. **A.** Schematic representation of double-stable cell line expressing MEF2VP16 after Dox stimulation. **B.** Stable cell lines expressing the Tet repressor (TR) were tested for Dox-inducibility, using a luciferase reporter downstream of Tet operators. **C.** Western blot analysis, using anti-VP16 antibody, on lysate of different double stable TR-MEF2VP16 clones, which are either untreated or stimulated with Dox for 24 h. All clones express MEF2VP16 only after stimulation with Dox. Pos.ctrl, Western blot positive control for VP16 antibody **D.** Immunofluorescent staining of TR4-39 and TR1-194 cells show homogenous expression of MEF2VP16 after induction with Dox. Note that MEF2VP16 is localized primarily to the nuclei of cells. Bar, 20 µm. **E.** Luciferase measurements on TR4-39 and TR1-194 cells, transiently transfected with 3xMEF2Luc reporter, indicate a time-dependent increase in MEF2 transcriptional activity after stimulation with Dox. **F.** Bright field microscopic images showing elongation of TR4-39 cells after Dox stimulation.

Cardiac genes regulated by MEF2

Both inducible MEF2VP16 ventricular myocyte cell lines were used for a genome-wide microarray analysis using Agilent mouse chips containing 44,000 genes, to identify the earliest gene expression pattern regulated by the transcription factor MEF2, as the morphological alterations in AdMEF2VP16-infected cardiomyocytes were already evident by 24-48 hrs. TR1-194 and TR4-39 cells were plated in parallel cultures, mortalized by overnight infection with AdCre, cultured in SF medium for 72 hrs, and cultured for an additional 24 hrs in the absence or presence of Dox. 75 genes (0.2% of all genes) were differentially expressed in both TR1-194 and TR4-39 cells with a fold change in expression ≥ 2 ($P < 0.01$) (Table 2). Among these 75 genes, 43 showed an increase in expression, 32 genes a decreased expression. We were interested to identify genes that may provide explanations for the dramatic change in morphology we observed in cultured cardiomyocytes with altered MEF2 transcriptional activity. Gene ontology classifications revealed an overrepresentation of genes in three specific subclasses: cell-matrix adhesion, cytoskeletal remodeling, and energy metabolism (Table 2, Fig. 5A). We picked 10 genes from the most interesting classifications to verify differential expression by RT-PCR (Fig. 5B). For example*, integrin alpha-7* (Itga7), *nexilin* (Nexn), *connective tissue growth factor* (CTGF), *regulatory myosin light chain 9* (Myl9), *myotonic dystrophy protein kinase* (DMPK), *sarcoglycan alpha* (Sgca) and *sarcoglycan beta* (Sgcb) were each significantly upregulated upon MEF2VP16 expression in TR1-194 and TR4-39 clones (Fig. 5B). In contrast, *integrin beta 4* (Itgb4), *glutathione S-transferase alpha 1* (gsta1) and *mucin 5* (muc5b) were significantly downregulated. Another gene class differentially regulated by MEF2 transcription factors included genes involved in energy metabolism and mitochondrial energy production. This is in line with previous reports suggesting a direct or indirect role for MEF2 to control cardiac energy production [10, 20]. Combined, these data indicate that MEF2 activity activates subsets of genes primarily localized to or functioning at the cytoskeleton, focal adhesion sites, the extracellular matrix, and energy metabolism/mitochondrial energy production.

Figure 5. Classification of MEF2 target genes. **A.** Bar graph indicating the number of differentially expressed genes in different functional classifications. **B.** Semi-quantitative RT-PCR for mRNA levels of indicated genes in TR1-194 and TR4-39 clones in absence or presence of Dox. Ribosomal protein L7 mRNA levels were determined as control for equal amplification and loading. **C-V.** Confocal immunocytochemistry of cultured neonatal rat cardiomyocytes, using anti-EH-myomesin and anti-vinculin antibodies, demonstrates that MEF2 activation alters the distribution of focal adhesion sites. Arrows in Panel S point to residual myomesin immunoreactivity.

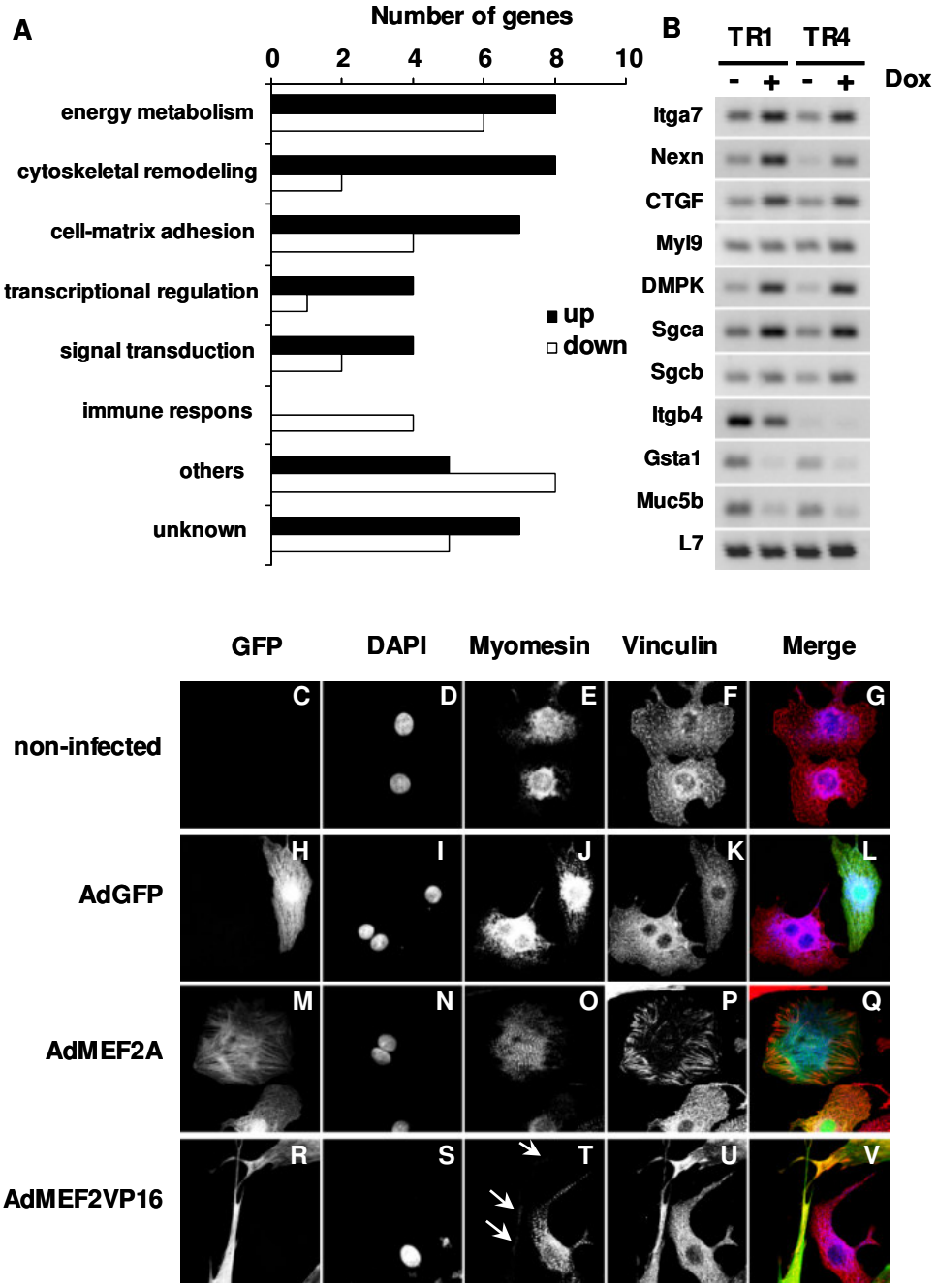
A
Number of genes
0
2
4
6
8
10
energy metabolism
cytoskeletal remodeling
cell-matrix adhesion
transcriptional regulation
signal transduction
immune respons
others
unknown
up
down
B
TR1
TR4
- + - +
Dox
Itga7
Nexn
CTGF
Myl9
DMPK
Sgca
Sgcb
Itgb4
Gsta1
Muc5b
L7
GFP
DAPI
Myomesin
Vinculin
Merge
non-infected
AdGFP
AdMEF2A
AdMEF2VP16
C
D
E
F
G
H
I
J
K
L
M
N
O
P
Q
R
S
T
U
V

Table 2. Functional clustering of genes regulated by MEF2.

Accesion Number	Gene	Description	Fold Change TR1-194	Fold Change TR4-39
Cell-matrix adhesion (11)				
NM_010217	CTGF	connective tissue growth factor	10,5	3,6
NM_008398	Itga7	integrin alpha 7	7,3	4,1
NM_199465	Nexn	nexilin	4,8	4,4
NM_009621	Adamts1	disintegrin-like and metalloprotease (reprolysin type) with thrombospondin type 1 motif, 1	3,9	5,0
NM_013494	Cpe	carboxypeptidase E	2,1	3,7
NM_011580	Thbs1	thrombospondin 1	2,9	2,2
NM_144862	Lims2	LIM and senescent cell antigen like domains 2	2,5	2,3
BC059192	Itgb4	integrin beta 4	-2,6	-2,2
NM_011595	Timp3	tissue inhibitor of metalloproteinase 3	-2,6	-2,5
NM_054077	Prelp	proline arginine-rich end leucine-rich repeat	-4,1	-2,7
AF064749	Col6a3	type VI collagen alpha 3 subunit	-4,0	-4,3
Cytoskeleton (10)				
BC055439	Myl9	myosin, light polypeptide 9, regulatory	10,2	7,0
NM_009606	Acta1	actin, alpha 1, skeletal muscle	13,4	2,6
S60315	DMPK	myotonic dystrophy kinase	3,9	4,0
NM_011619	Tnnt2	troponin T2, cardiac	2,9	3,3
NM_009161	Sgca	sarcoglycan, alpha (dystrophin-associated glycoprotein)	3,5	2,5
NM_011890	Sgcb	sarcoglycan, beta (dystrophin-associated glycoprotein)	2,7	2,9
NM_013560	Hspb1	heat shock protein 1	3,0	2,5
NM_008800	Pde1b	phosphodiesterase 1B, Ca2+-calmodulin dependent	2,4	2,2
AK034012	Synpo	RIKEN clone:9330140I15	-2,1	-2,3
U72681	Vill	EF-6	-2,2	-2,2
Energy metabolism (14)				
NM_009943	Cox6a2	cytochrome c oxidase, subunit VI a, polypeptide 2	13,8	3,9
NM_021273	Ckb	creatine kinase, brain	3,0	3,3
NM_007431	Akp2	alkaline phosphatase 2, liver	3,0	3,3
NM_008509	Lpl	lipoprotein lipase	2,5	3,2
NM_024188	Oxct1	3-oxoacid CoA transferase 1	2,8	2,8
NM_026619	1700020F09Rik	RIKEN cDNA 1700020F09 gene	2,5	2,5
NM_007382	Acadm	acetyl-Coenzyme A dehydrogenase, medium chain	2,3	2,4
NM_007808	Cycs	cytochrome c, somatic	2,0	2,2
NM_010795	Mgat3	mannoside acetylglucosaminyltransferase 3	-2,7	-2,1
NM_010358	Gstm1	glutathione S-transferase, mu 1	-2,8	-2,6
NM_010359	Gstm3	glutathione S-transferase, mu 3	-3,5	-2,3
NM_011921	Aldh1a7	aldehyde dehydrogenase family 1, subfamily A7	-3,6	-2,4
NM_007436	Aldh3a1	aldehyde dehydrogenase family 3, subfamily A1	-5,5	-6,6
NM_008181	Gsta1	glutathione S-transferase, alpha 1 (Ya)	-8,7	-8,0
Signal transduction (6)				
AK004534	Rasl11b	RIKEN clone:1190017B18	2,7	3,3
AK033726	Map3k5	mitogen activated protein kinase kinase kinase 5	2,9	2,2
XM_355574	Gnai1	guanine nucleotide binding protein, alpha inhibiting 1	2,1	2,9
NM_026505	Bambi	BMP and activin membrane-bound inhibitor	2,5	2,4
NM_009368	Tgfb3	transforming growth factor, beta 3	-3,2	-2,1
NM_181748	Gpr120	G protein-coupled receptor 120	-2,7	-2,8
Transcriptional regulation (5)				
NM_017373	Nfil3	nuclear factor, interleukin 3, regulated	3,4	3,2
NM_025926	Dnajb4	DnaJ (Hsp40) homolog, subfamily B, member 4	2,4	3,4
NM_011600	Tle4	transducin-like enhancer of split 4	2,5	2,5
NM_011542	Tcea3	transcription elongation factor A (SII), 3	2,3	2,2
NM_010495	Idb1	inhibitor of DNA binding 1	-3,6	-2,9

Immune response (4)				
NM_010741	Ly6c	lymphocyte antigen 6 complex, locus C	-2,4	-2,3
NM_010779	Mcpt4	mast cell protease 4	-3,9	-3,0
NM_011333	Ccl2	chemokine (C-C motif) ligand 2	-7,0	-2,7
NM_020519	1110021N19Rik	RIKEN cDNA 1110021N19 gene	-4,9	-5,3
Others (13)				
NM_008871	Serpine1	serine (or cysteine) proteinase inhibitor, clade E, member 1	2,5	3,3
NM_153098	Cd109	CD109 antigen (Cd109)	2,0	3,8
NM_024185	2310047O13Rik	RIKEN cDNA 2310047O13 gene	2,0	2,9
NM_029508	0610009F02Rik	RIKEN cDNA 5830443C21 gene	2,0	2,3
NM_146194	Picalm	phosphatidylinositol binding clathrin assembly protein (Picalm)	2,1	2,1
NM_009115	S100b	S100 protein, beta polypeptide, neural	-2,9	-2,2
NM_030261	Sesn3	sestrin 3	-3,2	-2,0
NM_013568	Kcna6	potassium voltage-gated channel, shaker-related, subfamily, member 6	-3,4	-2,8
AK041604	Dact2	RIKEN clone:A630024E20	-3,9	-2,5
NM_030127	Htra3	RIKEN cDNA 9530081K03 gene	-5,2	-2,1
NM_008597	Mglap	matrix gamma-carboxyglutamate (gla) protein	-5,0	-3,5
NM_019414	Selenbp2	selenium binding protein 2	-5,9	-4,9
NM_028801	Muc5b	mucin 5, subtype B, tracheobronchial	-13,5	-11,9
Unknown (12)				
AK086025	4631423F02Rik	RIKEN clone:D830045N18	6,9	2,3
AK017206	5033430I15Rik	RIKEN clone:5033430I15	4,6	3,2
NM_026931	1810011O10Rik	RIKEN cDNA 1810011O10 gene	4,3	3,2
NM_145980	8430408G22Rik	RIKEN cDNA 8430408G22 gene	2,2	4,2
NM_173752	1110067D22Rik	RIKEN cDNA 1110067D22 gene	2,8	2,9
AK008679	2210008N01Rik	RIKEN clone:2210008N01	2,7	2,4
AK01525	4930431B09Rik	RIKEN clone:4930431B09	2,2	2,6
AK021294	2810416G20Rik	RIKEN clone:D530019O13	-2,2	-2,2
NM_178642	AU040576	expressed sequence AU040576	-2,5	-2,0
NM_027950	1700012B18Rik	RIKEN cDNA 1700012B18 gene	-2,2	-2,9
NM_026821	D4Bwg0951e	DNA segment, Chr 4	-2,8	-2,4
AA726875	AA726875	cDNA clone IMAGE:1193490	-4,5	-2,3

MEF2 activation alters focal adhesion structures in cardiomyocytes

To verify whether alterations in cellular adhesion indeed correlated with the elongation of cultured cardiomyocytes upon MEF2 activation, we infected cardiomyocytes with AdMEF2A and AdMEF2VP16 and immunostained cultures for EH-myomesin and vinculin, a component of cardiac focal adhesion sites. Cells were left uninfected (Fig. 5C-G), infected with AdGFP (Fig. 5H-L), AdMEF2A (Fig. 5M-Q), or AdMEF2VP16 (Fig. 5R-V). Fluorescence for GFP was used to track the individual cells infected with AdGFP, AdMEF2A or AdMEF2VP16 (Fig. 5, Panels C, H, M, and R). DAPI staining was used to visualize nuclei (Fig. 5, Panels D, I, N, S). Examples of cells immunostained for either EH-myomesin at the M-band (Fig. 5, Panels E, J, O, T) or vinculin to visualize the localization of focal adhesions (Fig. 5, Panels F, K, P, U), and merged channels (Fig. 5, Panels G, L, Q, V) are presented. Uninfected or AdGFP-infected cultures demonstrated a regular pattern of sarcomere staining (Fig. 5D, I) and a punctuate distribution of vinculin at the focal

adhesions (Fig. 5E, J). Enlarged AdMEF2A-infected cells with modestly impaired myofibril integrity, displayed a redistribution of vinculin towards the outer borders of cells (Fig. 5N). Highly elongated AdMEF2VP16-infected cells with only remnants of myofibrillar structure (Arrows in Fig. 5S), demonstrated intense vinculin staining at the most distal tips of their cellular structure.

Thus, increased MEF2 transcriptional activity in cultured cardiomyocytes activates a gene program associated with a gradual loss of myofibrillar structure, which is accompanied by an increase and redistribution of focal adhesion sites.

DMPK is a cardiac MEF2 target gene

Of all genes found to be upregulated by MEF2 activation, DMPK was of specific interest. DMPK has initially been implicated in myotonic dystrophy (DM), an inherited degenerative neuromuscular disorder [21-24]. DM patients suffer from skeletal muscle myotonia, muscle weakness, and cardiac conduction defects. Furthermore, transgenic mice overexpressing DMPK display a heart failure phenotype, with extensive myocyte disarray and interstitial fibrosis [25].

To verify that DMPK represents a direct transcriptional target of MEF2, rat, mouse and human orthologs were aligned and analyzed for conserved MEF2 binding sites. One conserved MEF2 binding sequence (CTAAATTTAA) was detected 513 bp upstream of the transcriptional start site of the rat *dmpk* gene (Fig. 6A). We performed ChIP analysis to determine whether MEF2 binds to this A/T rich motif (Fig. 6B). Chromatin was immunoprecipitated from rat neonatal cardiomyocytes infected with either AdGFP or AdMEF2A, using antibodies directed against MEF2 and acetylated histone H3. No antibody immunoprecipitates were used as negative control. PCR amplification of the immunoprecipitated material using primers flanking the MEF2 site, demonstrate MEF2 binding to the *dmpk* promoter in cardiomyoctes infected with the MEF2A expressing adenovirus (Fig. 6B).

Figure 6. MEF2 induces cardiomyocyte elongation via DMPK. **A.** Sequence alignment of rat, mouse, and human *dmpk* promoter regions. The gray box indicates the conserved -513 MEF2 site. **B.** ChIP analysis was performed by PCR using primers flanking the MEF2 site on chromatin immunoprecipitated using either a MEF2 or an acetylated histone H3 antibody. No antibody immunoprecipitations serve as negative control, non-immunoprecipitated DNA was used as input control. **C.** Western blot analysis for DMPK expression in cardiomyocytes pre-transfected with either control or DMPK specific siRNAs and infected with the indicated adenoviruses. Immunoreactivity for GAPDH serves as loading control. **D.** Graph indicating the percentage of cardiomyocytes, pre-transfected with either control or DMPK specific siRNAs and infected with the indicated adenoviruses, with a major axis/minor axis ratio <2.5, between 2.5 and 5, or >5. **E.** Confocal immunocytochemistry of cultured neonatal rat cardiomyocytes, using an anti-α-actinin antibody, demonstrates that knockdown of DMPK inhibits MEF2 induced cardiomyocyte elongation. Arrows point to residual α-actinin immunoreactivity.

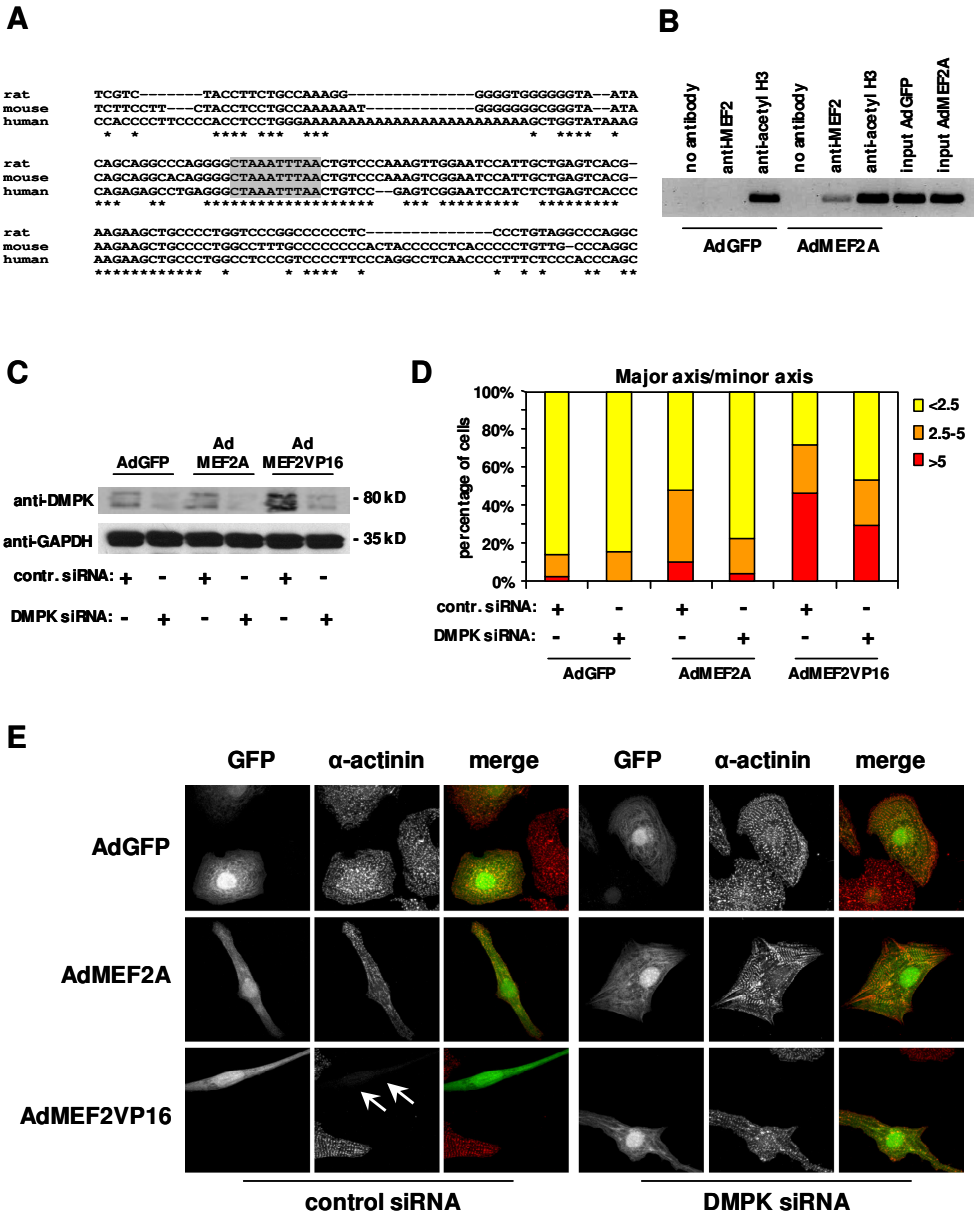
A
rat TCGTC-------TACCTTCTGCCAAAGG----------GGGGTGGGGGGTA--ATA
mouse TCTTCCTT---CTACCTCCTGCCAAAAAAT----------GGGGGGGCGGGTA--ATA
human CCACCCCTTCCCCACCTCCTGGGAAAAAAAAAAAAAAAAAAAAAAAAAGCTGGTATAAAG
rat CAGCAGGCCCAGGGGCTAAATTTAACTGTCCCAAAGTTGGAATCCATTGCTGAGTCACG-
mouse CAGCAGGCACAGGGGCTAAATTTAACTGTCCCAAAGTCGGAATCCATTGCTGAGTCACG-
human CAGAGAGCCTGAGGGCTAAATTTAACTGTCC--GAGTCGGAATCCATCTCTGAGTCACCC
rat AAGAAGCTGCCCCTGGTCCCGGCCCCCCTC----------CCCTGTAGGCCCAGGC
mouse AAGAAGCTGCCCCTGGCCTTTGCCCCCCCCACTACCCCCTCACCCCCTGTTG-CCCAGGC
human AAGAAGCTGCCCTGGCCTCCCGTCCCCTTCCCAGGCCTCAACCCCTTTCTCCCACCCAGC
B
no antibody
anti-MEF2
anti-acetyl H3
no antibody
anti-MEF2
anti-acetyl H3
input AdGFP
input AdMEF2A
AdGFP
AdMEF2A
C
AdGFP
Ad MEF2A
Ad MEF2VP16
anti-DMPK
- 80 kD
anti-GAPDH
- 35 kD
contr. siRNA: + - + - + -
DMPK siRNA: - + - + - +
D
Major axis/minor axis
percentage of cells
100%
80%
60%
40%
20%
0%
<2.5
2.5-5
>5
contr. siRNA: + - + - + -
DMPK siRNA: - + - + - +
AdGFP
AdMEF2A
AdMEF2VP16
E
GFP
α-actinin
merge
GFP
α-actinin
merge
AdGFP
AdMEF2A
AdMEF2VP16
control siRNA
DMPK siRNA

DMPK upregulation is required for MEF2-induced myocyte elongation

In order to assess the potential role of DMPK in MEF2 induced cardiomyocyte remodeling, we evaluated the effect of DMPK siRNA knockdown during this remodeling process. As determined by Western blotting, we established significant knockdown of DMPK expression levels by transfecting cardiomyocytes with siRNAs directed against DMPK (Fig. 6C). Infection with AdMEF2A and especially AdMEF2VP16 enhanced DMPK protein levels in cardiomyocytes pre-transfected with control siRNA. This increase in expression, however, was inhibited in cardiomyocytes pre-transfected with siRNA targeting DMPK, where DMPK expression levels were comparable to the basal expression level (Fig. 6C).

Next, we investigated the effect of DMPK inhibition on MEF2 induced cardiomyocyte elongation by determination of the ratio of the length of the major and minor axis of the cells. Pre-transfection with control siRNA had no effect on cellular morphology (data not shown). MEF2 activation induced elongation of cardiomyocytes transfected with control siRNA as the percentage of GFP positive cells with a major axis/minor axis ratio >5 amounted to 10.4% and 46% after infection with AdMEF2A and AdMEF2VP16, compared to 2.5% for AdGFP infected control cells (Fig. 6D). Cardiomyocytes pre-transfected with DMPK siRNA showed a significant attenuation of the elongation response, as the percentage of GFP positive cells with a major axis/minor axis ratio >5, declined to 3.5%, 28.9%, and 0%, for AdMEF2A, AdMEF2VP16, and AdGFP infected cells, respectively (Fig. 6D). Representative images of cardiomyocytes pre-transfected with either control or DMPK siRNA and infected with AdGFP, AdMEF2A, or AdMEF2VP16, and immunostained for α-actinin are given in Figure 6E. Noteworthy, sarcomeric degeneration seemed to be less pronounced after knockdown of DMPK expression. Conclusively, DMPK is a direct cardiac target gene of MEF2 and promotes elongation of cardiomyocytes.

DISCUSSION

One pivotal observation of this study is that MEF2 activity in postnatal cardiac muscle promotes changes that are consistent with the development of dilated cardiomyopathy. The activation of a “fetal” gene program is a highly conserved feature of the hypertrophic response and has been extensively studied as a means to identify physiological regulators of hypertrophy. Although the initial steps of the induction of embryonic genes are reversible, chronic changes in the cardiac gene program may trigger pathological changes in the myocardium that can be irreversible in nature and promote cardiac dysfunction. Dilation of the ventricular chamber and the associated increase in stress on the ventricular wall are often the

first irreversible steps towards heart failure [26]. Accordingly, the transcription factors and their target genes that connect biomechanical forces and the activation of stress pathways to morphological changes of the myocardium are central to understanding the initiation and progression of heart failure.

Using a multidisciplinary approach, we analyzed the consequences of activating the transcription factor MEF2 in cardiac muscle. As described earlier, MEF2 promotes cardiomyopathic alterations that are fundamentally different from myocyte hypertrophy [6, 13]. Concordantly, the classification profiles of MEF2 target genes identified in the present study, revealed surprisingly little overlap with those observed with massive hypertrophic remodeling in early pressure overload (http://cardiogenomics.med.harvard.edu). In contrast, our gene profiles correlate well with those observed in gene chip analysis of human end-stage idiopathic dilated cardiomyopathy [27] and with the most characteristic pathological features of human end-stage dilated cardiomyopathy, which include myocyte lengthening (elongation), myofibril degeneration, a dynamic redistribution of cytoskeletal structures, alterations in mitochondria number and morphology (energy metabolism), and extensive fibrosis [7, 8].

One of the striking observations in the present study included the elongated morphology of cardiomyocytes and the sequential disassembly of myofibril components upon increasing MEF2 transcriptional activity, which affected both M-band and Z-disc components. Many cardiomyopathic conditions share the common characteristic of myofibril degeneration, which contrasts the promotion of sarcomere organization during early phases of cardiac hypertrophy. Loss of myofibrils is the most obvious structural change in dilated cardiomyopathy [28] and sarcomeric disarray is characteristic of end-staged failing human hearts [8]. Features of human dilated cardiomyopathy include increased myocardial mass and biventricular chamber dilation, myocyte and myofibril disarray, and loss of contractile material [7].

Another striking observation was the redistribution of focal adhesions sites that accompanied elongated cardiomyocytes upon MEF2 activation. Cardiomyocytes from MLP knockout mice and tropomodulin-overexpressing transgenic mice [29], two models with severe chamber dilation, present striking alterations of their cell-matrix as well as their cell-cell contacts. Isolated myocytes from these cardiomyopathic models elicit a more irregular shape compared with their wild-type counterparts [30], which may serve to increase the number of focal contacts between neighboring cells. Specifically, the costameric protein vinculin showed patchy staining near the plasma membranes in MLP null cardiomyocytes compared with the regular well-ordered striations that are observed at the membrane of wildtype cardiomyocytes [30]. These differences in vinculin subcellular distribution mimic the changes observed in our study on vinculin

localization in hypertrophic and elongated myocytes following MEF2 activation. Increased expression of extracellular matrix components, as found in our gene profiles, and a general upregulation of vinculin was described in patients with DCM [8, 31], suggesting that this phenomenon might not be restricted to mouse models for this disease.

In this study, microarray analysis provided mechanistic insights into the cardiomyopathic remodeling processes, as many of the genes activated by MEF2 are involved in cytoskeletal remodeling and focal adhesion assembly. We further demonstrated that one of these genes, DMPK, is a direct target of MEF2. More importantly, knockdown of DMPK expression sufficiently inhibited cardiomyocyte elongation and sarcomere disassembly in response to elevated MEF2 activity. Myotonic dystrophy 1 is associated with expansion of untranslated CTG repeats in the 3 prime UTR of *dmpk*, which is believed to result in a pathological accumulation of RNA in the nucleus [23, 32]. In the heart, however, the DM1 cardiac pathology may be more directly due to increased DMPK expression, rather than RNA toxicity [33]. Indeed, transgenic mice overexpressing DMPK display a heart failure phenotype, with extensive myocyte disarray and interstitial fibrosis [25].

Findings in several other studies underline the potential role of DMPK in myocyte remodeling. The *dmpk* gene encodes a protein kinase related to the Rho family of protein kinases, which are associated with actin cytoskeletal remodeling [34-37]. DMPK shares a high homology with myotonic dystrophy kinase-related Cdc42 binding kinases (MRCKs) [34]. MRCK and Cdc42 colocalize at the cell periphery inducing actin and myosin reorganization and focal adhesion complex formation [38]. Cdc42 has been described to play a critical role in sarcomere assembly and elongation of cardiomyocytes [39]. DMPK is also known to interact with Rac-1 [40], and both DMPK and Rac-1 are able to phosphorylate and inhibit myosin phosphatase [41]. Inhibition of myosin phosphatase and associated increase in myosin phosphorylation leads to an increase in stress fibers and focal adhesion sites and is important for sarcomere organization [37, 42]. Expression of constitutively activated Rac1 in the heart induces focal adhesion redistribution and cardiac dilation [43]. We observed localization of focal adhesion complexes to the most distal ends of elongated cardiomyocytes upon MEF2 activation. Interestingly, overexpression of human DMPK in yeast resulted in polarized elongated cell growth [44]. Furthermore, during differentiation of human skeletal muscle cells DMPK localizes towards the terminal parts of elongating cells [45].

In conclusion, our findings identify DMPK as a direct transcriptional target of MEF2, promoting myocyte elongation, myofibril degeneration and polarized focal adhesion redistribution, changes of the heart muscle, which are characteristic of dilated cardiomyopathy.

ACKNOWLEDGEMENTS

The authors would like to thank Marc van de Wetering and Hans Clevers for reagents and advice with the generation of stable cell lines. This work was supported by grants 902-16-275, 912-04-054 and 912-04-017 from the Netherlands Organization for Health Research and Development (ZonMW), grant 2003B258 of the Netherlands Heart Foundation, and by the European Union Contract No. LSHM-CT-2005-018833/EUGeneHeart (to L.J.D.W.).

REFERENCES

1. Gossett L.A., Kelvin D.J., Sternberg E.A., Olson E.N. A new myocyte-specific enhancer-binding factor that recognizes a conserved element associated with multiple muscle-specific genes. Mol Cell Biol 1989;9(11):5022-33.
2. Black B.L., Olson E.N. Transcriptional control of muscle development by myocyte enhancer factor-2 (MEF2) proteins. Annu Rev Cell Dev Biol 1998;14:167-96.
3. McKinsey T.A., Zhang C.L., Olson E.N. MEF2: a calcium-dependent regulator of cell division, differentiation and death. Trends Biochem Sci 2002;27:40-47.
4. Olson E.N., Perry M., Schulz R.A. Regulation of muscle differentiation by the MEF2 family of MADS box transcription factors. Dev Biol 1995;172(1):2-14.
5. Frey N., Katus H.A., Olson E.N., Hill J.A. Hypertrophy of the heart: a new therapeutic target? Circulation 2004;109(13):1580-9.
6. van Oort R.J., van Rooij E., Bourajjaj M., Schimmel J., Jansen M.A., van der Nagel R., Doevendans P.A., Schneider M.D., van Echteld C.J., De Windt L.J. MEF2 activates a genetic program promoting chamber dilation and contractile dysfunction in calcineurin-induced heart failure. Circulation 2006;114(4):298-308.
7. Beltrami C.A., Finato N., Rocco M., Feruglio G.A., Puricelli C., Cigola E., Sonnenblick E.H., Olivetti G., Anversa P. The cellular basis of dilated cardiomyopathy in humans. J Mol Cell Cardiol 1995;27(1):291-305.
8. Schaper J., Froede R., Hein S., Buck A., Hashizume H., Speiser B., Friedl A., Bleese N. Impairment of the myocardial ultrastructure and changes of the cytoskeleton in dilated cardiomyopathy. Circulation 1991;83(2):504-14.
9. Passier R., Zeng H., Frey N., Naya F.J., Nicol R.L., McKinsey T.A., Overbeek P., Richardson J.A., Grant S.R., Olson E.N. CaM kinase signaling induces cardiac hypertrophy and activates the MEF2 transcription factor in vivo. J Clin Invest 2000;105(10):1395-406.
10. Naya F.J., Black B.L., Wu H., Bassel-Duby R., Richardson J.A., Hill J.A., Olson E.N. Mitochondrial deficiency and cardiac sudden death in mice lacking the MEF2A transcription factor. Nat Med 2002;8(11):1303-9.
11. Lu J., McKinsey T.A., Nicol R.L., Olson E.N. Signal-dependent activation of the MEF2 transcription factor by dissociation from histone deacetylases. Proc Natl Acad Sci U S A 2000;97(8):4070-5.
12. Nadruz W., Jr., Kobarg C.B., Constancio S.S., Corat P.D., Franchini K.G. Load-induced transcriptional activation of c-jun in rat myocardium: regulation by myocyte enhancer factor 2. Circ Res 2003;92(2):243-51.
13. Xu J., Gong N.L., Bodi I., Aronow B.J., Backx P.H., Molkentin J.D. Myocyte enhancer factors 2A and 2C induce dilated cardiomyopathy in transgenic mice. J Biol Chem 2006;281(14):9152-62.

14. He T.C., Zhou S., da Costa L.T., Yu J., Kinzler K.W., Vogelstein B. A simplified system for generating recombinant adenoviruses. Proc Natl Acad Sci U S A 1998;95(5):2509-14.
15. Taigen T., De Windt L.J., Lim H.W., Molkentin J.D. Targeted inhibition of calcineurin prevents agonist-induced cardiomyocyte hypertrophy. Proc Natl Acad Sci U S A 2000;97(3):1196-201.
16. Rybkin, II, Markham D.W., Yan Z., Bassel-Duby R., Williams R.S., Olson E.N. Conditional expression of SV40 T-antigen in mouse cardiomyocytes facilitates an inducible switch from proliferation to differentiation. J Biol Chem 2003;278(18):15927-34.
17. Ehler E., Rothen B.M., Hammerle S.P., Komiyama M., Perriard J.C. Myofibrillogenesis in the developing chicken heart: assembly of Z-disk, M-line and the thick filaments. J Cell Sci 1999;112 (Pt 10):1529-39.
18. Obermann W.M., Gautel M., Steiner F., van der Ven P.F., Weber K., Furst D.O. The structure of the sarcomeric M band: localization of defined domains of myomesin, M-protein, and the 250-kD carboxy-terminal region of titin by immunoelectron microscopy. J Cell Biol 1996;134(6):1441-53.
19. Agarkova I., Schoenauer R., Ehler E., Carlsson L., Carlsson E., Thornell L.E., Perriard J.C. The molecular composition of the sarcomeric M-band correlates with muscle fiber type. Eur J Cell Biol 2004;83(5):193-204.
20. Czubryt M.P., McAnally J., Fishman G.I., Olson E.N. Regulation of peroxisome proliferator-activated receptor gamma coactivator 1 alpha (PGC-1 alpha) and mitochondrial function by MEF2 and HDAC5. Proc Natl Acad Sci U S A 2003;100(4):1711-6.
21. Brook J.D., McCurrach M.E., Harley H.G., Buckler A.J., Church D., Aburatani H., Hunter K., Stanton V.P., Thirion J.P., Hudson T., et al. Molecular basis of myotonic dystrophy: expansion of a trinucleotide (CTG) repeat at the 3' end of a transcript encoding a protein kinase family member. Cell 1992;68(4):799-808.
22. Tsilfidis C., MacKenzie A.E., Mettler G., Barcelo J., Korneluk R.G. Correlation between CTG trinucleotide repeat length and frequency of severe congenital myotonic dystrophy. Nat Genet 1992;1(3):192-5.
23. Mahadevan M., Tsilfidis C., Sabourin L., Shutler G., Amemiya C., Jansen G., Neville C., Narang M., Barcelo J., O'Hoy K., et al. Myotonic dystrophy mutation: an unstable CTG repeat in the 3' untranslated region of the gene. Science 1992;255(5049):1253-5.
24. Fu Y.H., Pizzuti A., Fenwick R.G., Jr., King J., Rajnarayan S., Dunne P.W., Dubel J., Nasser G.A., Ashizawa T., de Jong P., et al. An unstable triplet repeat in a gene related to myotonic muscular dystrophy. Science 1992;255(5049):1256-8.
25. O'Cochlain D.F., Perez-Terzic C., Reyes S., Kane G.C., Behfar A., Hodgson D.M., Strommen J.A., Liu X.K., van den Broek W., Wansink D.G., Wieringa B., Terzic A. Transgenic overexpression of human DMPK accumulates into hypertrophic cardiomyopathy, myotonic myopathy and hypotension traits of myotonic dystrophy. Hum Mol Genet 2004;13(20):2505-18.
26. Hoshijima M., Chien K.R. Mixed signals in heart failure: cancer rules. J Clin Invest 2002;109(7):849-55.
27. Grzeskowiak R., Witt H., Drungowski M., Thermann R., Hennig S., Perrot A., Osterziel K.J., Klingbiel D., Scheid S., Spang R., Lehrach H., Ruiz P. Expression profiling of human idiopathic dilated cardiomyopathy. Cardiovasc Res 2003;59(2):400-11.
28. Mann D.L., Urabe Y., Kent R.L., Vinciguerra S., Cooper G.t. Cellular versus myocardial basis for the contractile dysfunction of hypertrophied myocardium. Circ Res 1991;68(2):402-15.

29. Sussman M.A., Welch S., Cambon N., Klevitsky R., Hewett T.E., Price R., Witt S.A., Kimball T.R. Myofibril degeneration caused by tropomodulin overexpression leads to dilated cardiomyopathy in juvenile mice. J Clin Invest 1998;101(1):51-61.
30. Ehler E., Horowits R., Zuppinger C., Price R.L., Perriard E., Leu M., Caroni P., Sussman M., Eppenberger H.M., Perriard J.C. Alterations at the intercalated disk associated with the absence of muscle LIM protein. J Cell Biol 2001;153(4):763-72.
31. Wilke A., Schonian U., Herzum M., Hengstenberg C., Hufnagel G., Brilla C.G., Maisch B. [The extracellular matrix and cytoskeleton of the myocardium in cardiac inflammatory reaction]. Herz 1995;20(2):95-108.
32. Davis B.M., McCurrach M.E., Taneja K.L., Singer R.H., Housman D.E. Expansion of a CUG trinucleotide repeat in the 3' untranslated region of myotonic dystrophy protein kinase transcripts results in nuclear retention of transcripts. Proc Natl Acad Sci U S A 1997;94(14):7388-93.
33. Mahadevan M.S., Yadava R.S., Yu Q., Balijepalli S., Frenzel-McCardell C.D., Bourne T.D., Phillips L.H. Reversible model of RNA toxicity and cardiac conduction defects in myotonic dystrophy. Nat Genet 2006;38(9):1066-70.
34. Wansink D.G., van Herpen R.E., Coerwinkel-Driessen M.M., Groenen P.J., Hemmings B.A., Wieringa B. Alternative splicing controls myotonic dystrophy protein kinase structure, enzymatic activity, and subcellular localization. Mol Cell Biol 2003;23(16):5489-501.
35. Amano M., Chihara K., Nakamura N., Kaneko T., Matsuura Y., Kaibuchi K. The COOH terminus of Rho-kinase negatively regulates rho-kinase activity. J Biol Chem 1999;274(45):32418-24.
36. Amano M., Fukata Y., Kaibuchi K. Regulation and functions of Rho-associated kinase. Exp Cell Res 2000;261(1):44-51.
37. Kaibuchi K., Kuroda S., Amano M. Regulation of the cytoskeleton and cell adhesion by the Rho family GTPases in mammalian cells. Annu Rev Biochem 1999;68:459-86.
38. Leung T., Chen X.Q., Tan I., Manser E., Lim L. Myotonic dystrophy kinase-related Cdc42-binding kinase acts as a Cdc42 effector in promoting cytoskeletal reorganization. Mol Cell Biol 1998;18(1):130-40.
39. Nagai T., Tanaka-Ishikawa M., Aikawa R., Ishihara H., Zhu W., Yazaki Y., Nagai R., Komuro I. Cdc42 plays a critical role in assembly of sarcomere units in series of cardiac myocytes. Biochem Biophys Res Commun 2003;305(4):806-10.
40. Shimizu M., Wang W., Walch E.T., Dunne P.W., Epstein H.F. Rac-1 and Raf-1 kinases, components of distinct signaling pathways, activate myotonic dystrophy protein kinase. FEBS Lett 2000;475(3):273-7.
41. Muranyi A., Zhang R., Liu F., Hirano K., Ito M., Epstein H.F., Hartshorne D.J. Myotonic dystrophy protein kinase phosphorylates the myosin phosphatase targeting subunit and inhibits myosin phosphatase activity. FEBS Lett 2001;493(2-3):80-4.
42. Aoki H., Sadoshima J., Izumo S. Myosin light chain kinase mediates sarcomere organization during cardiac hypertrophy in vitro. Nat Med 2000;6(2):183-8.
43. Sussman M.A., Welch S., Walker A., Klevitsky R., Hewett T.E., Price R.L., Schaefer E., Yager K. Altered focal adhesion regulation correlates with cardiomyopathy in mice expressing constitutively active rac1. J Clin Invest 2000;105(7):875-86.
44. Sasagawa N., Kino Y., Takeshita Y., Oma Y., Ishiura S. Overexpression of human myotonic dystrophy protein kinase in Schizosaccharomyces pombe induces an abnormal polarized and swollen cell morphology. J Biochem (Tokyo) 2003;134(4):537-42.
45. Beffy P., Barsanti C., Del Carratore R., Simi S., Benedetti P.A., Benzi L., Prelle A., Ciscato P., Simili M. Expression and localization of myotonic dystrophy protein kinase in human skeletal muscle cells determined with a novel antibody: possible role of the protein in cytoskeleton rearrangements during differentiation. Cell Biol Int 2005;29(9):742-53.

Chapter 4

MEF2 inactivation fails to protect Muscle LIM Protein (MLP) deficient mice from dilated cardiomyopathy

Ralph J. van Oort, Roel van der Nagel, Leon J. De Windt

ABSTRACT

Muscle LIM Protein (MLP) knockout mice have been shown to exhibit many features of human dilated cardiomyopathy. Although disruption of the cytoskeletal architecture, due to absence of functional MLP, likely results in impaired force transmission by individual cardiomyocytes, the mechanism that links this cytoskeletal defect with the onset of cardiac dilation and heart failure is unclear.

Because of the striking phenotypic resemblance of hearts from MLP deficient mice and mice overexpressing the transcription factor myocyte enhancer factor 2 (MEF2), we hypothesized that cardiomyopathic remodeling in MLP deficient mice involves MEF2 activation. Crossbreeding of MLP knockout mice with MEF2 reporter mice indeed indicated a dramatic increase in cardiac MEF2 activation in the absence of MLP protein.

To further examine the role of MEF2 in pathological remodeling of MLP deficient hearts, we crossbred MLP knockout mice with mice expressing a dominant-negative form of MEF2 (DNMEF2) in the heart. Histological and echocardiographic analysis, however, demonstrated no differences in cardiac morphology or function of MLP deficient hearts when MEF2 activity was inhibited.

In conclusion, MEF2 activity is enhanced in hearts of MLP knockout mice, but inhibition of MEF2 activity fails to prevent maladaptive remodeling and cardiac dysfunction of MLP deficient hearts.

INTRODUCTION

Dilated cardiomyopathy (DCM) is characterized by cardiac wall thinning and ventricular chamber dilation, accompanied by severe contractile dysfunction. A growing number of mutations in either cytoskeletal or sarcomeric genes has been described to account for the development of human DCM [1, 2]. One of the genes linked to DCM is Muscle LIM Protein (MLP), also known as cysteine rich protein 3 (CRP3) [3, 4]. MLP is a muscle specific member of the LIM-only class of the LIM domain protein family that possesses two tandem LIM domains. MLP has been originally identified in striated muscle, where it promotes myogenesis and regulates myogenic differentiation [5, 6]. Mice deficient in MLP display features of DCM and develop heart failure [7]. Furthermore, although the physiological significance is not clear, a decrease in MLP protein level has been observed in human heart failure [8]. Finally, MLP interacts and colocalizes with telethonin (T-cap), a titin interacting protein, and a human MLP mutation (W4R) associated with DCM results in a marked defect in T-cap interaction/localization, suggesting that a Z-disc MLP/T-cap

complex is a key component of the cardiomyocyte stretch sensor machinery, and that defects in this complex underlie human DCM [3].

In striated muscle, MLP has been localized at the Z-disc, where it, besides T-cap directly binds structural proteins, such as α-actinin, βI-spectrin and N-RAP, further implying a role in the stretch sensor apparatus [3, 9-11]. Impaired cytoskeletal force transmission, due to myofibrillar disorganization caused by disruption of this scaffold protein, could give a straightforward explanation for the cardiac phenotype observed in MLP knockout mice. It has been demonstrated, however, that the cardiomyopathic phenotype of these mice is related to calcium cycling defects, as a rescue occurs by crossbreeding with either phospholamban deficient or β-adrenergic receptor kinase-1 inhibitor overexpressing mice [12-14]. As calcium is a very potent secondary messenger, a decrease in MLP expression could, apart from the direct structural effects on the contractile apparatus, give rise to alterations in intracellular signaling. So far, activation of signaling pathways by reduction in MLP protein and its ramifications on the cardiac remodeling process has remained elusive.

MEF2 is a well-known downstream effector of calcium signaling and other pro-hypertrophic pathways in the cardiomyocyte [15, 16]. Recently, we and others have demonstrated that cardiac specific activation of MEF2 induces ventricular wall thinning and dilation of the heart, which resembles the phenotype of MLP knockout mice [17, 18]. Furthermore, overexpression of MEF2 in cultured cardiomyocytes induces myocyte elongation, associated with myofibril degeneration and redistribution of focal adhesion sites (Chapter 3). Interestingly, the costameric protein vinculin showed a patchy staining near the plasma membrane in cardiac myocytes upon MEF2 overexpression, a pattern earlier observed in cardiomyocytes derived from MLP deficient mice [10].

In this study, we have tested the potential activation of MEF2 in MLP knockout mice by crossbreeding these mice with MEF2 reporter mice. This demonstrated a substantial increase in MEF2 activity in both hetero- and homozygous MLP null mice compared to wildtype animals. To investigate the significance of MEF2 activity in the pathological remodeling of $MLP^{-/-}$ hearts, we crossbred MLP knockout mice with mice engineered to overexpress a dominant-negative form of MEF2 in the heart. Histological and echocardiographic analysis revealed no differences in cardiac morphology and function upon inhibition of MEF2 transcriptional activity in MLP knockout mice.

MATERIALS AND METHODS

Mice. Details on the generation of transgenic mice conditionally expressing dominant-negative MEF2 (FloxDNMEF2 mice) and mice expressing Cre recombinase under control of the 5.5-kb murine cardiac α-myosin heavy chain promoter (MHC-Cre mice) have been described previously [17, 19]. Generation of MLP-deficient mice and of MEF2 reporter (desMEF2LacZ) mice, harboring a LacZ transgene linked to the hsp68 basal promoter and three tandem copies of the MEF2 site from the desmin enhancer, has also been described elsewhere [7, 20]. Studies were performed in animals at 6 weeks of age.

Transthoracic echocardiography. Cardiac morphology and function was measured on mice anesthetized with isoflurane by noninvasive echocardiography using a Hewlett Packard Sonos 5500 instrument (Hewlett Packard) and a 15 MHz transducer (15-6L linear probe, Philips). In M-mode, the following parameters were obtained from 3 or more cardiac cycles per mouse: left ventricular posterior wall thickness, interventricular septum thickness, end-diastolic left ventricular internal diameter, end-systolic left ventricular internal diameter, and left ventricular fractional shortening.

β-galactosidase staining. Hearts were fixed in 2% paraformaldehyde/0.2% glutaraldehyde in PBS on ice for 15 minutes, followed by washing twice in PBS and immersion in PBS, containing 5 mM ferrocyanide, 5 mM ferricyanide, 2 mM $MgCl_2$, and 1 mg/ml X-gal, for 16 hours at 30˚C.

Histological analysis. Heart tissue was fixed with 4% paraformaldehyde and embedded in paraffin. Sections were stained with hematoxylin and eosin (H&E).

RNA quantification. Total RNA was isolated from heart tissue using TRIzol reagent (Invitrogen, Carlsbad, CA). One µg of RNA was reverse transcribed using M-MLV reverse transcriptase (Promega, Madison, WI). Real-time PCR using the BioRad iCycler (Bio-Rad, Hercules, CA) and fluorescence detection was performed in 96-well plates using SYBR Green and MyIQ optical software (Bio-Rad, Hercules, CA) as described in detail previously [17]. DMPK transcript quantities were normalized to the amount of ribosomal protein L7. The following oligonucleotide primer sequences were used: 5'-GGACAAGTATGTGGCCGACT (DMPK forward), 5'-CATCTTCACCACCGCTACCT (DMPK reverse), 5'-GAAGCTCATCTATGAG AAGGC (L7 forward), 5'-AAGACGAAGGAGCTGCAGAAC (L7 reverse).

Statistical analysis. The results are presented as mean ± SEM. Statistical analyses were performed with InStat 3.0 (GraphPad Software, Inc, San Diego, CA). The analyses consisted of ANOVA, followed by Tukey's posttest when group differences were detected at the 5% significance level. Statistical significance was accepted at a p value <0.05.

RESULTS

MEF2 activity is enhanced in MLP deficient hearts

MEF2 transcription factors act as transcriptional end points for several stress signals in the heart and induce dilated cardiomyopathy upon activation [15-18]. Since the cardiac phenotype of MEF2 overexpressing transgenic mice resembles the MLP knockout heart [7, 17, 18] and activation of MEF2 in isolated cardioymocytes leads to sarcomere degeneration and focal adhesion redistribution (Chapter 3), a characteristic of MLP deficient mice [10], we first examined the level of MEF2 activation in MLP knockout hearts.

To this end, we crossbred MLP knockout mice with mice harboring a MEF2-dependent LacZ reporter gene (desMEF2LacZ) [7, 20]. Mice with the correct genotypes were sacrificed at 6 weeks of age and cardiac MEF2 activity was detected by β-galactosidase staining (Fig. 1). In the presence of both MLP alleles, the MEF2-dependent LacZ transgene was expressed at background levels, consistent with the notion that MEF2 is only basally active in the postnatal heart [20, 21]. In contrast, MEF2 activity was considerably elevated in MLP heterozygous and, specifically, enlarged homozygous knockout hearts. These findings indicate that a decrease in functional MLP protein provokes MEF2 transcriptional activity.

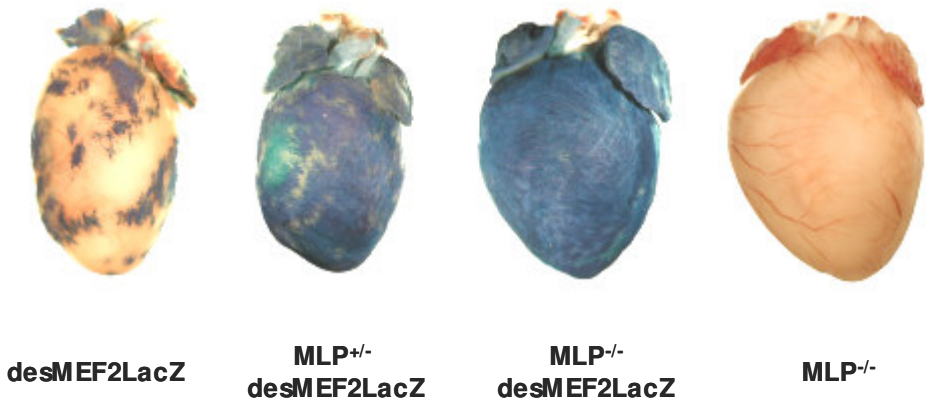

Figure 1. Enhanced MEF2 activity in MLP knockout hearts. MLP knockout mice were bred with mice harboring a MEF2-dependent LacZ reporter gene (desMEF2LacZ). Mice with the indicated genotypes were sacrificed at 6 weeks of age and hearts were stained for β-galactosidase activity. LacZ expression was detected at background levels in desMEF2LacZ control mice, but was substantially increased in $MLP^{+/-}$ and $MLP^{-/-}$ mice harboring the MEF2 reporter gene. LacZ staining was not observed in $MLP^{-/-}$ mice in the absence of the MEF2 reporter gene.

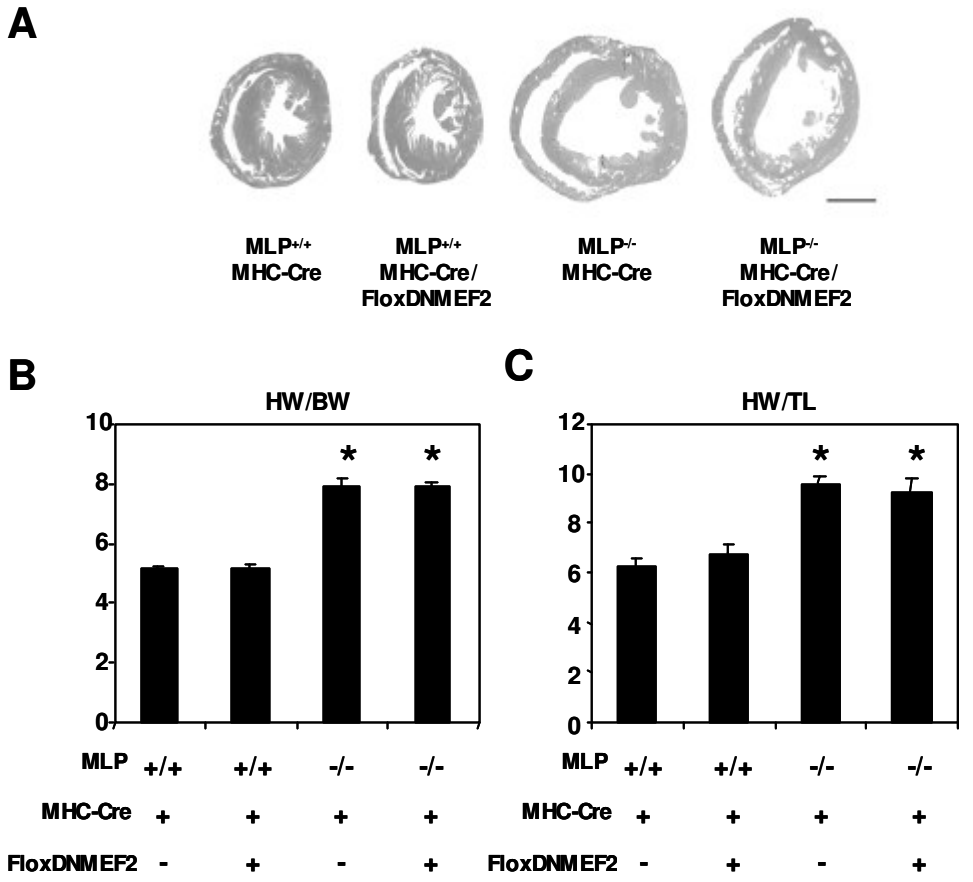

Figure 2. Inhibition of MEF2 does not prevent cardiac dilation in MLP knockout mice. **A.** H&E stained cardiac sections, cut at the midsagittal level of the heart, demonstrate ventricular wall thinning and dilation in $MLP^{-/-}$ hearts independent of MEF2 activity. **B, C.** Ratios of heart-weight-to-body-weight (HW/BW) (B) and heart-weight-to-tibia-length (HW/TL) (C) of the indicated groups show an equal increase in cardiac mass for $MLP^{-/-}$/MHC-Cre and $MLP^{-/-}$/MHC-Cre/FloxDNMEF2 hearts at 6 weeks of age. *Indicates $p<0.05$ versus corresponding $MLP^{+/+}$ group. Scale bar = 2 mm.

Inhibition of MEF2 does not prevent cardiac dilation in MLP knockout mice

To further investigate the significance of increased MEF2 activity in MLP deficient hearts, we intercrossed MLP knockout mice with MHC-Cre transgenic mice, which express Cre recombinase in postnatal cardiac muscle, and FloxDNMEF2 mice, which express a dominant-negative form of MEF2 upon activation of Cre recombinase [17, 19].

Histological analysis of hearts obtained from 6-week-old mice demonstrated no morphological difference between MLP$^{+/+}$/MHC-Cre/FloxDNMEF2 and MLP$^{+/+}$/MHC-Cre control mice (Fig. 2A). In line with earlier observations, hearts from MLP$^{-/-}$/MHC-Cre mice displayed thinning of cardiac walls and biventricular dilation [7]. These morphological changes were independent of MEF2 activity, as wall thicknesses and ventricular dimensions were indistinguishable between MLP$^{-/-}$/MHC-Cre and MLP$^{-/-}$/MHC-Cre/FloxDNMEF2 mice (Fig. 2A).

Furthermore, measurements of heart-weight-to-body-weight (HW/BW) and heart-weight-to-tibia-length (HW/TL) ratios indicated a similar increase in cardiac mass for both MLP$^{-/-}$/MHC-Cre (7.9±0.3 and 9.6±0.3 for HW/BW and HW/TL ratios, respectively; $p<0.05$) and MLP$^{-/-}$/MHC-Cre/FloxDNMEF2 mice (7.9±0.1 and 9.3±0.5 for HW/BW and HW/TL ratios, respectively; $p<0.05$), compared to MLP$^{+/+}$/MHC-Cre (5.2±0.1 and 6.3±0.3 for HW/BW and HW/TL ratios, respectively) and MLP$^{+/+}$/MHC-Cre/FloxDNMEF2 (5.2±0.1 and 6.8±0.4 for HW/BW and HW/TL ratios, respectively) control mice (Fig. 2B and C). These data demonstrate that inhibition of MEF2 activity does not prevent cardiac remodeling in MLP knockout hearts.

Table. Echocardiographic characteristics in MLP$^{+/+}$/MHC-Cre, MLP$^{+/+}$/ MHC-Cre/FloxDNMEF2, MLP$^{-/-}$/MHC-Cre and MLP$^{-/-}$/MHC-Cre/FloxDNMEF2 mice.

	MLP$^{+/+}$		MLP$^{-/-}$	
	MHC-Cre (n=11)	MHC-Cre/Flox-DNMEF2 (n=7)	MHC-Cre (n=11)	MHC-Cre/Flox-DNMEF2 (n=7)
BW (g)	20.1 ± 1.0	22.0 ± 1.4	19.3 ± 0.9	19.4 ± 1.5
IVSs (mm)	1.20 ± 0.07	1.15 ± 0.09	0.95 ± 0.09	1.05 ± 0.11
IVSd (mm)	0.67 ± 0.04	0.69 ± 0.04	0.65 ± 0.04	0.72 ± 0.07
LVPWs (mm)	1.28 ± 0.05	1.30 ± 0.06	0.93 ± 0.08 *	1.00 ± 0.11
LVPWd (mm)	0.72 ± 0.03	0.68 ± 0.05	0.66 ± 0.04	0.66 ± 0.06
ESD (mm)	1.72 ± 0.17	1.75 ± 0.22	3.08 ± 0.21 *	3.38 ± 0.17 *
EDD (mm)	3.49 ± 0.15	3.67 ± 0.23	4.19 ± 0.12 *	4.58 ± 0.15 *
FS (%)	52 ± 3	53 ± 5	27 ± 3 *	26 ± 3 *

Data are expressed as mean ± SEM. *Indicates $p<0.05$ vs. corresponding MLP$^{+/+}$ group. BW = body weight; EDD = end-diastolic diameter; ESD = end-systolic diameter; FS = left ventricular fractional shortening; IVS = intraventricular septal wall thickness; LVPW = left ventricular posterior wall thickness.

Inhibition of MEF2 does not preserve cardiac function in MLP knockout mice

Next, we measured lung-weight-to-body-weight (LW/BW) and lung-weight-to-tibia-length (LW/TL) ratios, which indicated that in both groups cardiac remodeling was associated with pulmonary edema, as LW/BW and LW/TL ratios amounted to 8.5±0.5 and 10.3±0.3 for MLP$^{-/-}$/MHC-Cre and 9.1±0.4 and 10.7±0.7 for MLP$^{-/-}$

/MHC-Cre/FloxDNMEF2 mice ($p<0.05$), compared to 7.2±0.4 and 8.6±0.5 for $MLP^{+/+}$/MHC-Cre and 6.4±0.4 and 8.3±0.6 for $MLP^{+/+}$/MHC-Cre/FloxDNMEF2 control mice (Fig. 3A and B).

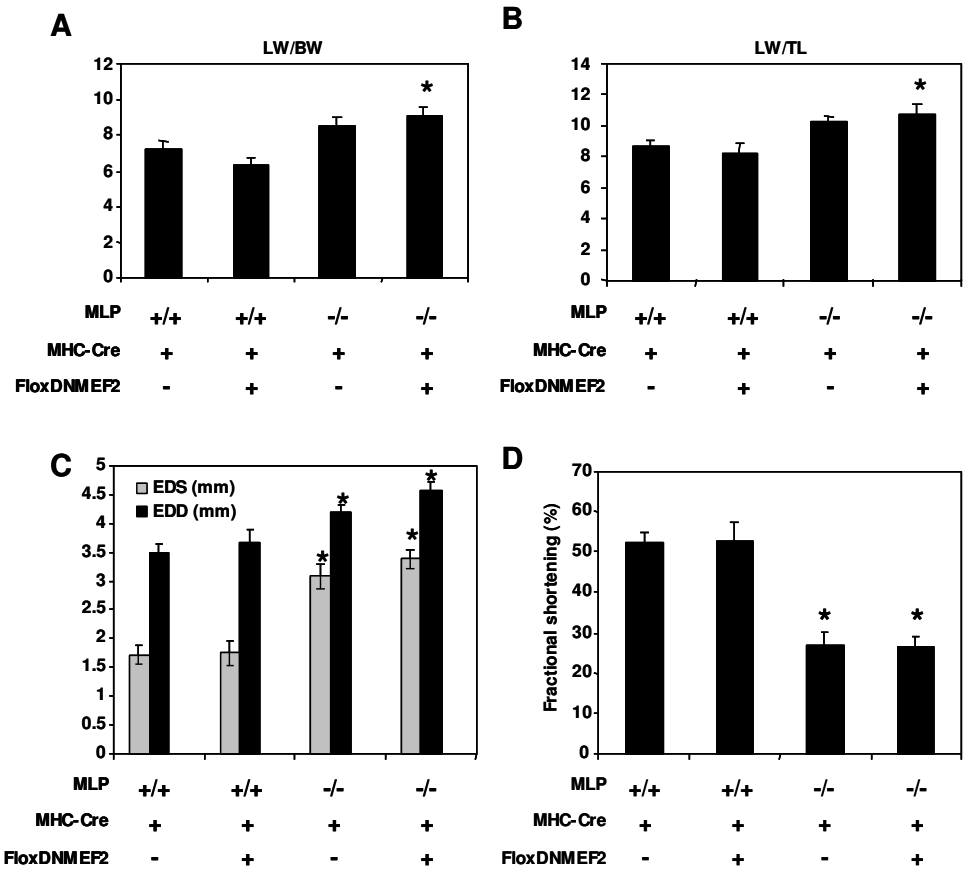

Figure 3. Inhibition of MEF2 does not preserve cardiac function in MLP knockout mice. **A, B.** Lung-weight-to-body-weight (LW/BW) (A) and lung-weight-to-tibia-length (LW/TL) (B) ratios indicate a similar degree of pulmonary congestion for both $MLP^{-/-}$/MHC-Cre and $MLP^{-/-}$/MHC-Cre/FloxDNMEF2 mice. **C.** Echocardiographic analysis of end-diastolic diameter (EDD) and end-systolic diameter (ESD) demonstrate ventricular dilation in both $MLP^{-/-}$/MHC-Cre and $MLP^{-/-}$/MHC-Cre/FloxDNMEF2 mice. **D.** Fractional shortening is decreased in both $MLP^{-/-}$/MHC-Cre and $MLP^{-/-}$/MHC-Cre/FloxDNMEF2 mice. *Indicates $p<0.05$ versus corresponding $MLP^{+/+}$ group.

Heart geometry and function was further analyzed by noninvasive echocardiography at 6 weeks of age (Table). In line with the observed histological alterations, MLP knockout hearts display severe ventricular dilation, as left ventricular end-systolic diameter (ESD) and end-diastolic diameter (EDD) in $MLP^{-/-}$/MHC-Cre mice (3.08±0.21 mm and 4.19±0.12 mm for ESD and EDD, respectively) were significantly increased compared to $MLP^{+/+}$/MHC-Cre control mice (1.72±0.17 mm and 3.49±0.15 mm for ESD and EDD, respectively; $p<0.05$; Fig. 3C). Again, MEF2 inhibition did not prevent ventricular dilation of the MLP deficient heart, as $MLP^{-/-}$/MHC-Cre/FloxDNMEF2 mice exhibited an increase in ESD and EDD similar to $MLP^{-/-}$/MHC-Cre mice (3.38±0.17 mm (ESD) and 4.58±0.15 mm (EDD), and 1.75±0.22 mm (ESD) and 3.67±0.23 mm (EDD), for $MLP^{-/-}$/MHC-Cre/FloxDNMEF2 and $MLP^{+/+}$/MHC-Cre/FloxDNMEF2 mice, respectively; $p<0.05$). Also cardiac function was affected to a similar extent in both groups, as fractional shortening (FS) dramatically decreased (27±3% and 26±3% for $MLP^{-/-}$/MHC-Cre and $MLP^{-/-}$/MHC-Cre/FloxDNMEF2 mice, respectively) compared to control mice (52±3% and 53±5% for $MLP^{+/+}$/MHC-Cre and $MLP^{+/+}$/MHC-Cre/FloxDNMEF2 mice, respectively; $p<0.05$; Fig. 3D). In conclusion, inhibition of MEF2 activity is not sufficient to prevent maladaptive remodeling and dysfunction of MLP deficient hearts.

Expression levels of myotonic dystrophy protein kinase are unchanged in MLP knockout hearts

Recently, we have identified myotonic dystrophy protein kinase (DMPK) as a direct MEF2 target gene involved in pathological remodeling of cardiomyocytes (Chapter 3). MEF2 induced elongation of cultured cardiomyocytes was associated with an increase in DMPK protein levels. Furthermore, siRNA-mediated knockdown of DMPK sufficed to inhibit cardiomyocyte elongation and sarcomere disassembly (Chapter 3).

To investigate potential alterations in DMPK expression in MLP knockout hearts, we measured cardiac DMPK transcript levels in mice from our experimental groups by real-time PCR analysis (Fig. 4). DMPK mRNA levels were similar for all different genotypes, suggesting that maladaptive remodeling of MLP knockout hearts is DMPK independent.

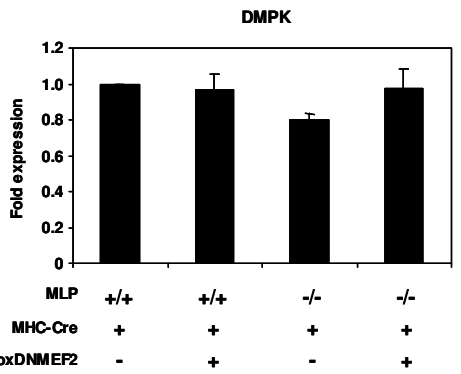

Figure 4. Real-time PCR analysis demonstrates unaffected DMPK transcript levels in the absence of MLP protein (n=4 to 6).

Conclusively, MEF2 activity is enhanced in MLP knockout mice with clear features of severe biventricular dilation, but inhibition of MEF2 activity fails to prevent the development of dilated cardiomyopathy in this mouse model. In addition, despite enhanced MEF2 activity in MLP deficient hearts, the expression level of DMPK remained unaltered. Together, our data suggest that cardiomyopathic remodeling in MLP knockout mice is independent of MEF2 activity and DMPK expression levels.

DISCUSSION

Here, we examined the involvement of MEF2 in remodeling of MLP deficient hearts. One intriguing finding of this study is the dramatic increase in cardiac MEF2 activity in heterozygous and, especially, homozygous MLP knockout mice. Disruption of the gene for MLP leads to impaired cytoskeletal organization in cardiomyocytes associated with dilated cardiomyopathy and heart failure [7]. Although the mechanistical link between disturbances of the cytoskeleton in individual cardiomyocytes and the progression to dilated cardiomyopathy is unclear, several studies have reported the involvement of impaired intracellular calcium homeostasis [12, 14, 22]. Altered intracellular calcium levels/fluctuations could provide an explanation for the observed increase in MEF2 activity, whereas MEF2 is a well-known downstream effector of calcium signaling [15, 16]. Furthermore, calsarcin-1, another Z-disc protein, has been found to interact with calcineurin and mice lacking calsarcin-1 protein are sensitized to calcineurin signaling and display an accelerated progression to cardiomyopathy [23]. Calcineurin is known to activate MEF2 transcriptional activity in the heart [17]. Loss of Z-disc integrity by MLP deficiency has also been described to result in decreased calcineurin compartmentalization, although this was thought to result in inhibition of calcineurin activity [24].

Despite the clear increase in MEF2 activity in MLP knockout hearts, inhibition of this activity did not result in rescue of the dilated cardiac phenotype nor improved cardiac function. Therefore, we conclude that the pathological cardiac remodeling in MLP deficient mice is independent of MEF2. Concordantly, expression levels of DMPK, a MEF2 transcriptional target involved in maladaptive cardiomyocyte remodeling (Chapter 3), are unchanged in hearts of MLP knockout mice. However, we cannot fully exclude that the inactivation potential of the dominant-negative transgene is insufficient to cope with the dramatic increase in MEF2 activity observed in hearts of MLP deficient mice and that MEF2 target

genes, other than DMPK, may be responsible for the onset of dilated cardiomyopathy.

Overall, MEF2 activity is enhanced in MLP knockout hearts. However, with our approach to inhibit MEF2 activity in vivo, we were unable to protect MLP deficient mice from the development of dilated cardiomyopathy.

ACKNOWLEDGEMENTS

We are grateful to Jeroen Korving for technical assistance.

REFERENCES

1. Fatkin D., Graham R.M. Molecular mechanisms of inherited cardiomyopathies. Physiol Rev 2002;82(4):945-80.
2. Ahmad F., Seidman J.G., Seidman C.E. The genetic basis for cardiac remodeling. Annu Rev Genomics Hum Genet 2005;6:185-216.
3. Knoll R., Hoshijima M., Hoffman H.M., Person V., Lorenzen-Schmidt I., Bang M.L., Hayashi T., Shiga N., Yasukawa H., Schaper W., McKenna W., Yokoyama M., Schork N.J., Omens J.H., McCulloch A.D., Kimura A., Gregorio C.C., Poller W., Schaper J., Schultheiss H.P., Chien K.R. The cardiac mechanical stretch sensor machinery involves a Z disc complex that is defective in a subset of human dilated cardiomyopathy. Cell 2002;111(7):943-55.
4. Mohapatra B., Jimenez S., Lin J.H., Bowles K.R., Coveler K.J., Marx J.G., Chrisco M.A., Murphy R.T., Lurie P.R., Schwartz R.J., Elliott P.M., Vatta M., McKenna W., Towbin J.A., Bowles N.E. Mutations in the muscle LIM protein and alpha-actinin-2 genes in dilated cardiomyopathy and endocardial fibroelastosis. Mol Genet Metab 2003;80(1-2):207-15.
5. Arber S., Halder G., Caroni P. Muscle LIM protein, a novel essential regulator of myogenesis, promotes myogenic differentiation. Cell 1994;79(2):221-31.
6. Kong Y., Flick M.J., Kudla A.J., Konieczny S.F. Muscle LIM protein promotes myogenesis by enhancing the activity of MyoD. Mol Cell Biol 1997;17(8):4750-60.
7. Arber S., Hunter J.J., Ross J., Jr., Hongo M., Sansig G., Borg J., Perriard J.C., Chien K.R., Caroni P. MLP-deficient mice exhibit a disruption of cardiac cytoarchitectural organization, dilated cardiomyopathy, and heart failure. Cell 1997;88(3):393-403.
8. Zolk O., Caroni P., Bohm M. Decreased expression of the cardiac LIM domain protein MLP in chronic human heart failure. Circulation 2000;101(23):2674-7.
9. Flick M.J., Konieczny S.F. The muscle regulatory and structural protein MLP is a cytoskeletal binding partner of betaI-spectrin. J Cell Sci 2000;113 (Pt 9):1553-64.
10. Ehler E., Horowits R., Zuppinger C., Price R.L., Perriard E., Leu M., Caroni P., Sussman M., Eppenberger H.M., Perriard J.C. Alterations at the intercalated disk associated with the absence of muscle LIM protein. J Cell Biol 2001;153(4):763-72.
11. Miller M.K., Granzier H., Ehler E., Gregorio C.C. The sensitive giant: the role of titin-based stretch sensing complexes in the heart. Trends Cell Biol 2004;14(3):119-26.
12. Minamisawa S., Hoshijima M., Chu G., Ward C.A., Frank K., Gu Y., Martone M.E., Wang Y., Ross J., Jr., Kranias E.G., Giles W.R., Chien K.R. Chronic phospholamban-

sarcoplasmic reticulum calcium ATPase interaction is the critical calcium cycling defect in dilated cardiomyopathy. Cell 1999;99(3):313-22.
13. Esposito G., Santana L.F., Dilly K., Cruz J.D., Mao L., Lederer W.J., Rockman H.A. Cellular and functional defects in a mouse model of heart failure. Am J Physiol Heart Circ Physiol 2000;279(6):H3101-12.
14. Rockman H.A., Chien K.R., Choi D.J., Iaccarino G., Hunter J.J., Ross J., Jr., Lefkowitz R.J., Koch W.J. Expression of a beta-adrenergic receptor kinase 1 inhibitor prevents the development of myocardial failure in gene-targeted mice. Proc Natl Acad Sci U S A 1998;95(12):7000-5.
15. Frey N., Katus H.A., Olson E.N., Hill J.A. Hypertrophy of the heart: a new therapeutic target? Circulation 2004;109(13):1580-9.
16. Heineke J., Molkentin J.D. Regulation of cardiac hypertrophy by intracellular signalling pathways. Nat Rev Mol Cell Biol 2006;7(8):589-600.
17. van Oort R.J., van Rooij E., Bourajjaj M., Schimmel J., Jansen M.A., van der Nagel R., Doevendans P.A., Schneider M.D., van Echteld C.J., De Windt L.J. MEF2 activates a genetic program promoting chamber dilation and contractile dysfunction in calcineurin-induced heart failure. Circulation 2006;114(4):298-308.
18. Xu J., Gong N.L., Bodi I., Aronow B.J., Backx P.H., Molkentin J.D. Myocyte enhancer factors 2A and 2C induce dilated cardiomyopathy in transgenic mice. J Biol Chem 2006;281(14):9152-62.
19. Agah R., Frenkel P.A., French B.A., Michael L.H., Overbeek P.A., Schneider M.D. Gene recombination in postmitotic cells. Targeted expression of Cre recombinase provokes cardiac-restricted, site-specific rearrangement in adult ventricular muscle in vivo. J Clin Invest 1997;100(1):169-79.
20. Naya F.J., Wu C., Richardson J.A., Overbeek P., Olson E.N. Transcriptional activity of MEF2 during mouse embryogenesis monitored with a MEF2-dependent transgene. Development 1999;126(10):2045-52.
21. Zhang C.L., McKinsey T.A., Chang S., Antos C.L., Hill J.A., Olson E.N. Class II histone deacetylases act as signal-responsive repressors of cardiac hypertrophy. Cell 2002;110(4):479-88.
22. Su Z., Yao A., Zubair I., Sugishita K., Ritter M., Li F., Hunter J.J., Chien K.R., Barry W.H. Effects of deletion of muscle LIM protein on myocyte function. Am J Physiol Heart Circ Physiol 2001;280(6):H2665-73.
23. Frey N., Barrientos T., Shelton J.M., Frank D., Rutten H., Gehring D., Kuhn C., Lutz M., Rothermel B., Bassel-Duby R., Richardson J.A., Katus H.A., Hill J.A., Olson E.N. Mice lacking calsarcin-1 are sensitized to calcineurin signaling and show accelerated cardiomyopathy in response to pathological biomechanical stress. Nat Med 2004;10(12):1336-43.
24. Heineke J., Ruetten H., Willenbockel C., Gross S.C., Naguib M., Schaefer A., Kempf T., Hilfiker-Kleiner D., Caroni P., Kraft T., Kaiser R.A., Molkentin J.D., Drexler H., Wollert K.C. Attenuation of cardiac remodeling after myocardial infarction by muscle LIM protein-calcineurin signaling at the sarcomeric Z-disc. Proc Natl Acad Sci U S A 2005;102(5):1655-60.

Chapter 5

MEF2 transcriptional activity is required for cardiac mitochondrial adaptation in pressure overload and protects against cardiac dysfunction

Ralph J. van Oort, Roel van der Nagel, Michael D. Schneider, Wim Sluiter, Martin W. Bergmann, Leon J. De Windt

Submitted

ABSTRACT

The transcription factor myocyte enhancer factor 2 (MEF2) is a downstream target for several hypertrophic signaling pathways in the heart. Using transgenic approaches, however, it has recently been demonstrated that MEF2 activity in the postnatal heart evokes cardiac dilation instead of hypertrophy, suggesting MEF2 as a valuable therapeutic target in the treatment of heart failure.

In this study, we wanted to investigate the potential benefits of MEF2 inhibition in a more physiological model of chronic pressure overload. Therefore, we subjected transgenic mice expressing a dominant negative form of MEF2 (DNMEF2) in the heart to transverse aortic constriction (TAC). Histological analysis did not indicate any differences in cardiac remodeling between DNMEF2 and control animals 5 weeks after TAC. Surprisingly, echocardiographic analysis revealed that DNMEF2 mice displayed a decrease in cardiac function compared to control animals after induction of pressure overload. Both proliferator-activated receptor-γ coactivator 1α (PGC-1α) transcript levels and citrate synthase activity were found to be decreased in DNMEF2 already at basal conditions, suggesting a decrease in mitochondrial number in the absence of active MEF2. Furthermore, mRNA levels of cytochrome c oxidase subunit VIa (Cox6a2) and the activity of mitochondrial electron transport chain complex IV were upregulated only in control and not in DNMEF2 mice after TAC, indicating an impaired adaptation to elevated cardiac loading conditions in DNMEF2 mice.

Together, these data suggest that inhibition of MEF2 transcriptional activity affects mitochondrial biogenesis and predisposes the heart to impaired mitochondrial adaptation, resulting in enhanced cardiac dysfunction following pressure overload.

INTRODUCTION

In response to stress, the heart compensates by hypertrophic growth, which frequently progresses to cardiac dilation and heart failure. The initial hypertrophic response is associated with activation of several intracellular signaling pathways [1, 2]. These pathways are interconnected and culminate in the nucleus on only a few transcriptional regulators. With the hope of revealing novel therapeutic targets in the treatment of heart failure, much effort has been dedicated to dissecting the role of these select transcription factors. One of the common downstream targets for several stress cascades in the heart is myocyte enhancer factor 2 (MEF2).

The normal adult heart exhibits only basal MEF2 transcriptional activity, which is likely required for the maintenance of the cardiomyocyte contractile apparatus and energy metabolism [3, 4]. This activity, however, is upregulated by prohypertrophic signaling cascade constituents, such as calcineurin, calcium/calmodulin-dependent protein kinase (CaMK), protein kinase C (PKC), protein kinase D (PKD), big mitogen-activated protein kinase (MAPK)-1 (BMK-1), and p38 MAPK [2, 3, 5, 6]. Furthermore, it has been demonstrated that MEF2 is implicated in a physiological model of hypertrophy, as MEF2 DNA binding activity is increased in hearts of rats subjected to pressure overload [7, 8].

Despite the considerable amount of evidence that suggest MEF2 factors to promote hypertrophic cardiac growth, this hypothesis has just recently been tested in a more direct approach. We and others have shown by overexpressing MEF2A or MEF2C in the postnatal murine heart, that MEF2 activity minimally affects cardiac growth but evokes dilated cardiomyopathy [9, 10]. Furthermore, *in vivo* inhibition of MEF2 activity resulted in minimal reduction of calcineurin induced hypertrophy, but prevented wall thinning and chamber dilation and significantly improved cardiac function [10]. These results imply that MEF2 does not trigger the hypertrophic growth response per se, but rather the molecular and genetic particulars underlying cardiac dilation and contractile loss, at least in certain experimental settings, which suggests that therapeutic MEF2 targeting may have future value to prevent chamber dilation and cardiac dysfunction in heart failure.

In this study, we tested the effects of MEF2 inhibition in cardiac hypertrophy and heart failure using a physiological model of pressure overload. To this end, conditional transgenic mice expressing dominant-negative MEF2 (DNMEF2) in the heart were subjected to transverse aortic constriction (TAC), a surgical model for pressure overload. To our surprise, DNMEF2 mice did not display an improvement in heart function in response to TAC surgery, as assessed by echocardiography. In fact, cardiac function was worsened in DNMEF2 mice, which correlated to impaired compensation for the increased energetic demand during pressure overload. In fact, in DNMEF2 mice expression levels of proliferator-activated receptor-γ coactivator 1α (PGC-1α), a dominant regulator of oxidative metabolism and mitochondrial biogenesis, and the activity of citrate synthase (CS), a reflection of mitochondrial density, were reduced at basal conditions compared to control mice. Furthermore, unlike control mice, DNMEF2 mice failed to increase cytochrome c oxidase subunit VIa (Cox6a2) transcript levels and mitochondrial electron transport chain complex IV activity after TAC surgery. The findings of this study indicate that inhibition of MEF2 transcriptional activity in the setting of pressure overload predisposes the heart to mitochondrial defects.

MATERIALS AND METHODS

Mice. Details on the generation of transgenic mice conditionally expressing DNMEF2 and mice expressing Cre recombinase under control of the 5.5-kb murine cardiac α-myosin heavy chain promoter were described previously [10, 11].

Aortic banding. Transverse aortic constriction (TAC) or sham surgery was performed in male mice, which were at least 10 weeks of age, by subjecting the aorta to a defined 27-gauge constriction between the first and second truncus of the aortic arch as described in detail previously [12].

Transthoracic echocardiography. Five weeks after surgery, cardiac remodeling and function was assessed by noninvasive echocardiography using a VisualSonics Vevo 770 high-resolution imaging system equipped with a 30 MHz RMV-707B scanning head. Echocardiographic measurements were performed on mice anesthetized with isoflurane. In M-mode, the following parameters were obtained with 3 or more readings per mouse: left ventricular posterior wall thickness, interventricular septum thickness, end-diastolic left ventricular internal diameter, end-systolic left ventricular internal diameter, left ventricular fractional shortening and ejection fraction. Doppler echocardiography was used to determine the pressure gradient between the proximal and distal sites of the transverse aortic constriction, and only mice with a pressure gradient >30 mm Hg were used in this study.

Histological analysis. Heart tissue was fixed with 4% paraformaldehyde and embedded in paraffin. Sections were stained with hematoxylin and eosin (H&E) and Sirius red.

RNA quantification. Total RNA was isolated from heart tissue using TRIzol reagent (Invitrogen, Carlsbad, CA). One μg of RNA was reverse transcribed using M-MLV reverse transcriptase (Promega, Madison, WI). Real-time PCR using the BioRad iCycler (Bio-Rad, Hercules, CA) and fluorescence detection was performed in 96-well plates using SYBR Green and MyIQ optical software (Bio-Rad, Hercules, CA) as described in detail previously [10]. Oligonucleotide primer sequences are listed in Table 1.

Measurement of mitochondrial function. Snap-frozen tissue was thawed on ice, minced in a small volume of buffer sucrose medium (250 mmol/L sucrose; 10 mmol/L HEPES, pH 7.4; 1 mmol/L EDTA), and homogenized. Citrate synthase activity of the homogenate, expressed in mU as nmol 5-thio-2-nitrobenzoate (TNB)/min per mg protein, was measured by monitoring the CoA-coupled conversion of Ellman reagent into TNB at 412 nm. The assay of complex IV activity of the homogenate was adapted from Birch-Machin and Turnbull's method [13]. The initial rate of oxidation of cytochrome C at 37°C was followed at 550 nm using 540 nm as the reference wavelength and expressed in mU as nmol oxidized

cytochrome C/min per mg protein. Cytochrome C was reduced with sodium dithionite and purified by gelfiltration on a Sephadex G-25 Medium column (PD-10). ***Statistical analysis.*** The results are presented as mean ± SEM. Statistical analyses were performed with InStat 3.0 (GraphPad Software, Inc, San Diego, CA). The analyses consisted of ANOVA, followed by Tukey's posttest when group differences were detected at the 5% significance level. Statistical significance was accepted at a p value <0.05.

Table 1. Oligonucleotide primers used in real-time PCR analysis.

Gene	Accession number	Sense oligo	Anti-sense oligo
ANF	NM_008725	TCTTCCTCGTCTTGGCCTTT	CCAGGTGGTCTAGCAGGTTC
PGC-1α	BC066868	TGTGCTGCTCTGGTTGGTGAG	CTCAAATATGTTCGCAGGCTC
Cox6a2	NM_009943	TGCCTCTAAAGGTCCGAGC	GGTGGTGATACGGGTGAAC
L7	BC086786	GAAGCTCATCTATGAGAAGGC	AAGACGAAGGAGCTGCAGAAC

RESULTS

Inhibition of MEF2 activity does not prevent pressure overload-induced cardiac hypertrophy

MEF2 transcription factors are activated by several intracellular hypertrophic signaling pathways [1]. Using transgenic mice that express a dominant-negative form of MEF2 upon activation of Cre recombinase (FloxDNMEF2 mice), we have recently demonstrated that inhibition of MEF2 transcriptional activity downstream of cardiac calcineurin signaling minimally affected the hypertrophic response, but substantially reduced cardiac dilation and improved contractility [10].

In this study, we used the same genetic loss-of-function approach to assess the role of MEF2 in pressure overload-induced cardiac remodeling, anticipating that heart-restricted MEF2 inhibition during pressure overload may also confer protection against this form of maladaptive remodeling. To this end, we subjected MHC-Cre/FloxDNMEF2 and control MHC-Cre mice to transverse aortic constriction (TAC) or sham surgery, and phenotyped mice 5 weeks after surgery. The hypertrophic response in MHC-Cre/FloxDNMEF2 after TAC was indistinguishable from that of pressure-overloaded MHC-Cre mice (Fig. 1A and B). Heart-weight-to-body-weight (HW/BW) or heart-weight-to-tibia-length (HW/TL) ratios confirmed the increase in heart weight after pressure overload for both MHC-Cre and MHC-

Cre/FloxDNMEF2 mice compared to sham-operated mice (Fig. 1C). Conclusively, inhibition of MEF2 activity does not inhibit the hypertrophic response following pressure overload.

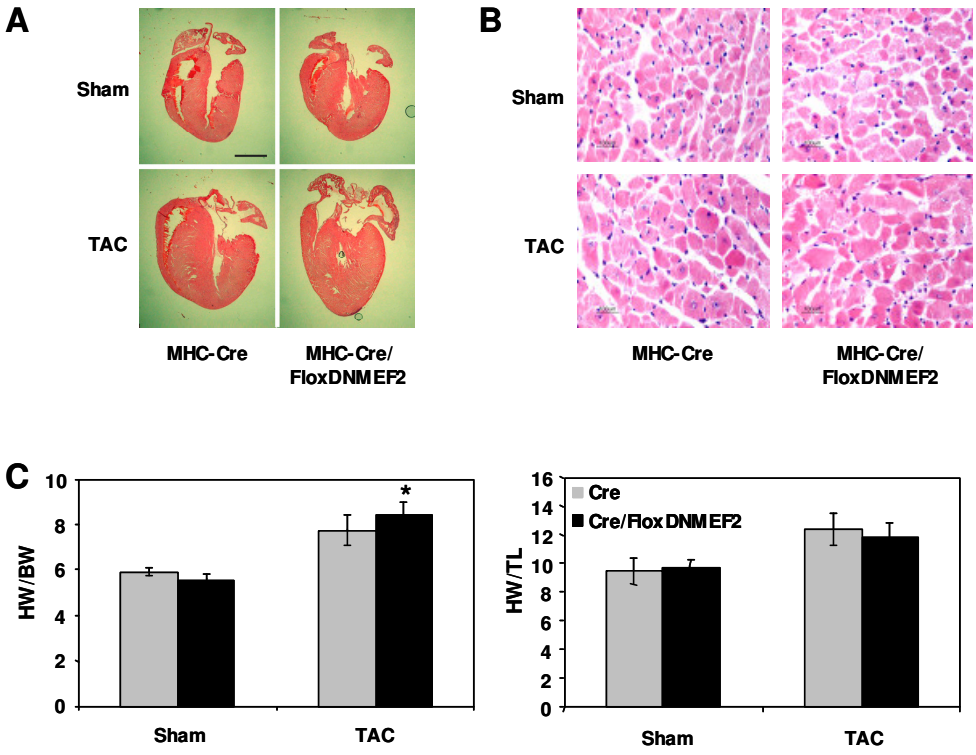

Figure 1. Inhibition of MEF2 does not prevent pressure overload induced cardiac hypertrophy. **A.** H&E stained coronal sections of the 4 experimental groups demonstrating a massive hypertrophic response in MHC-Cre and MHC-Cre/FloxDNMEF2 mice after TAC. **B.** H&E staining of cardiac sections indicating a similar increase in cardiomyocyte cross-sectional area in MHC-Cre/FloxDNMEF2 and MHC-Cre hearts after TAC. **C.** Ratios of heart weight to body weight (HW/BW) and heart weight to tibia length (HW/TL) of the indicated groups show an equal hypertrophic response for MHC-Cre and MHC-Cre/FloxDNMEF2 hearts 5 weeks after TAC. *Indicates $p<0.05$ versus corresponding sham group.

Inhibition of MEF2 activity accelerates pressure overload induced heart failure

Next, we determined the extent of interstitial fibrosis by Sirius red staining. The degree of fibrosis was similar in both groups after TAC (Fig. 2A). Also ANF

expression was found to be similarly upregulated in both groups after TAC, as assessed by real-time PCR (Fig. 2B). Furthermore, pressure overload was associated with pulmonary edema, as lung-weight-to-body-weight (LW/BW) or to tibia length (LW/TL) ratios increased to 7.2 ± 1.2 and 10.3 ± 1.8 (LW/BW) and to 11.4 ± 1.9 and 14.8 ± 3.0 (LW/TL) for MHC-Cre and MHC-Cre/FloxDNMEF2 TAC mice, respectively (Fig. 2C). The increase in these ratios for MHC-Cre/FloxDNMEF2 TAC mice tended to be higher compared to MHC-Cre TAC mice (N.S.), which may suggest that cardiac function after TAC is worse in these mice. Overall, our pressure overload regimen induced cardiac hypertrophy and cardiac dysfunction, which seemed to be worse in the absence of active MEF2.

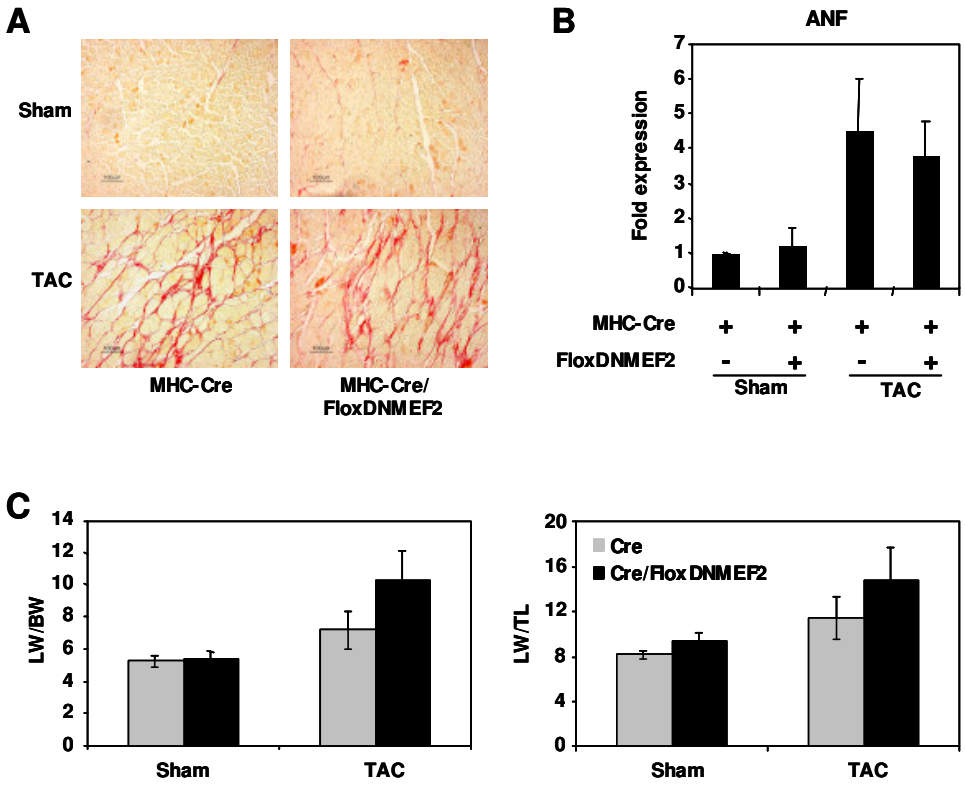

Figure 2. Inhibition of MEF2 does not rescue mice from pressure overload induced cardiac fibrosis or pulmonary congestion. **A.** Sirius red staining of cardiac sections indicating a similar degree of fibrosis in MHC-Cre/FloxDNMEF2 and MHC-Cre hearts after TAC. **B.** Real-time PCR analysis for ANF expression. **C.** Lung weight to body weight (LW/BW) and lung weight to tibia length (LW/TL) ratios indicate a similar degree of pulmonary congestion for both groups after TAC.

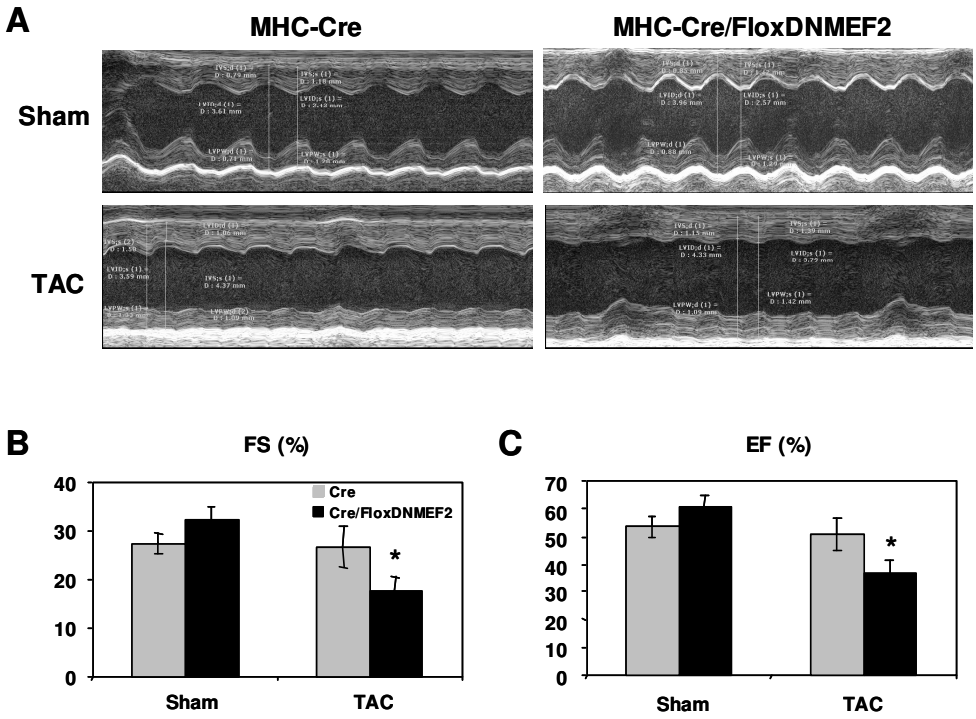

Figure 3. Inhibition of MEF2 accelerates pressure overload induced cardiac dysfunction. **A.** Representative M-mode echocardiography images of MHC-Cre and MHC-Cre/Flox-DNMEF2 mice 5 weeks after TAC or sham surgery. **B.** Fractional shortening (FS) and **C.** ejection fraction (EF) indicate left ventricular dysfunction MHC-Cre/FloxDNMEF2 mice after TAC.

Heart geometry and function was also analyzed by noninvasive echocardiography 5 weeks after TAC (Fig. 3A). In agreement with HW/BW and HW/TL ratios, thickening of ventricular walls was evident in MHC-Cre mice, as left ventricular posterior wall thickness at diastole (LVPWd) amounted to 0.98 ± 0.05 mm for MHC-Cre TAC compared to 0.75 ± 0.05 mm for MHC-Cre sham mice ($p<0.05$, Table 2). MHC-Cre/FloxDNMEF2 mice, in contrary, display signs of wall thinning instead of thickening after induction of pressure overload. During systole, both intraventricular septal wall thickness (IVS) and LVPW are significantly decreased in MHC-Cre/FloxDNMEF2 TAC mice (1.08 ± 0.05 mm and 1.10 ± 0.05 mm for IVSs and LVPWs, respectively) compared to MHC-Cre TAC mice (1.41 ± 0.08 mm and 1.32 ± 0.05 mm for IVSs and LVPWs, respectively, $p<0.05$). One could hypothesize that this difference in wall thickness is the result of inhibition of the hypertrophic response in MHC-Cre/FloxDNMEF2 TAC mice, but this is unlikely

with regard to the overall increase in heart size and weight in both groups after TAC (Fig. 1). Furthermore, one would expect preserved cardiac function in MHC-Cre/FloxDNMEF2 TAC mice if the hypertrophic response would have been inhibited, as wall thicknesses in these mice were comparable to sham control mice. However, geometric changes of the heart were accompanied by an impaired cardiac function in MHC-Cre/FloxDNMEF2 after TAC, as both fractional shortening (FS) and ejection fraction (EF) were significantly lower (18 ± 3% and 37 ± 5% for FS and EF, respectively) compared to MHC-Cre/FloxDNMEF2 sham mice (32 ± 3% and 61 ± 4% for FS and EF, respectively, $p<0.05$, Fig. 3B and C).

Overall, these results indicate that inhibition of MEF2 activity does not prevent the development of cardiac hypertrophy and heart failure during pressure overload, and suggests accelerated adverse adaptation to pressure overload when MEF2 transcriptional activity was inhibited.

Table 2. Echocardiographic characteristics in MHC-Cre and MHC-Cre/Flox-DNMEF2 mice after sham operation and after transverse aortic constriction (TAC).

	Sham		TAC	
	MHC-Cre (n=5)	MHC-Cre/Flox-DNMEF2 (n=5)	MHC-Cre (n=8)	MHC-Cre/Flox-DNMEF2 (n=8)
BW (g)	30.1 ± 3.8	33.8 ± 2.3	30.6 ± 2.2	25.6 ± 1.7
IVSs (mm)	1.13 ± 0.09	1.32 ± 0.08	1.41 ± 0.08	1.08 ± 0.05 †
IVSd (mm)	0.83 ± 0.06	0.92 ± 0.06	1.01 ± 0.05	0.84 ± 0.05
LVPWs (mm)	1.15 ± 0.09	1.21 ± 0.04	1.32 ± 0.05	1.10 ± 0.05 †
LVPWd (mm)	0.75 ± 0.05	0.85 ± 0.02	0.98 ± 0.05 *	0.87 ± 0.05
ESD (mm)	2.89 ± 0.15	2.60 ± 0.20	3.00 ± 0.29	3.44 ± 0.18
EDD (mm)	3.97 ± 0.13	3.82 ± 0.17	4.01 ± 0.24	4.16 ± 0.11
FS (%)	27 ± 2	32 ± 3	27 ± 4	18 ± 3 *
EF (%)	54 ± 4	61 ± 4	51 ± 6	37 ± 5 *
AoPg (mm Hg)	3 ± 1	3 ± 1	48 ± 3 *	42 ± 2 *

Data are expressed as mean ± SEM. *Indicates $p<0.05$ vs. corresponding sham group. †Indicates $p<0.05$ vs. MHC-Cre TAC. AoPg = aortic pressure gradient; BW = body weight; EDD = end-diastolic diameter; EF = ejection fraction; ESD = end-systolic diameter; FS = left ventricular fractional shortening; IVS = intraventricular septal wall thickness; LVPW = left ventricular posterior wall thickness.

Inhibition of MEF2 during pressure overload causes mitochondrial defects

Cardiac hypertrophy is thought to primarily be a compensatory reaction to match the increased workload imposed upon the heart [14]. In this compensation

process mitochondrial energy supply should be able to match the increased energy demand [15]. During pathological hypertrophy, however, mitochondrial adaptation is inadequate, which may contribute to cardiac decompensation [15]. As MEF2 is known to regulate the expression of genes involved in energy metabolism and of several nuclear encoded mitochondrial genes, we hypothesized that the accelerated decompensation observed in pressure overloaded MHC-Cre/FloxDNMEF2 mice may be caused by impaired mitochondrial adaptation.

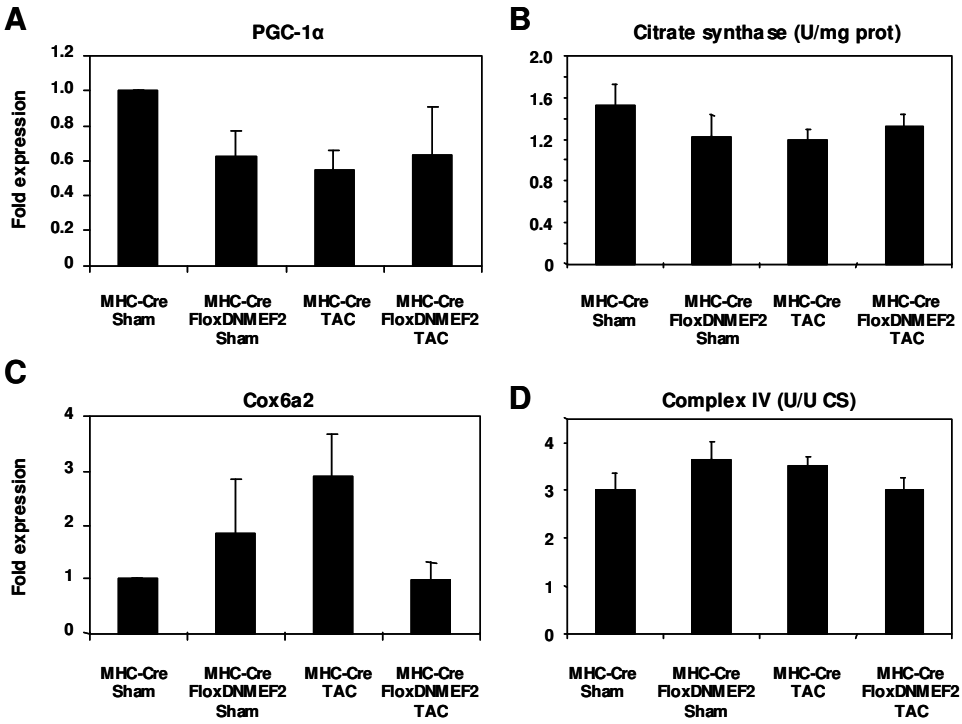

Figure 4. Inhibition of MEF2 during pressure overload results in impaired mitochondrial adaptation. **A.** Verification of PGC-1α transcript levels by real-time PCR detection. **B.** Citrate synthase assay on hearts from MHC-Cre and MHC-Cre/FloxDNMEF2 mice after TAC or sham surgery. **C.** Verification of PGC-1α transcript levels by real-time PCR detection. **D.** Measurements of respiratory chain complex IV activity. Complex IV activity is standardized for the amount of mitochondria (citrate synthase).

One of the genes described to be regulated by MEF2 is PGC-1α, a dominant regulator of oxidative metabolism and mitochondrial biogenesis [15-17]. In PGC-1α knockout mice, it has been demonstrated that repression of PGC-1α contributes to the development of heart failure after TAC [18]. By real-time PCR, we determined

PGC-1α mRNA levels in the hearts of mice from our experimental groups (Fig. 4A). As previously described, expression levels of PGC-1α are decreased after TAC. Interestingly, PGC-1α transcript levels in MHC-Cre/FloxDNMEF2 sham mice already show a 40% reduction compared to MHC-Cre sham mice. We interpret that the basal decrease in PGC-1α expression may affect mitochondrial homeostasis in MHC-Cre/FloxDNMEF2 mice, making these animals predisposed to development of cardiac decompensation. Indeed, basal mitochondrial density in sham operated MHC-Cre/FloxDNMEF2 mice is decreased compared to sham operated MHC-Cre control mice, as indicated by the level of mitochondrial matrix enzyme citrate synthase (CS) (Fig. 4B).

In further support of this notion, we found differences in expression levels of cytochrome c oxidase subunit VIa (Cox6a2) (Fig. 4C). MEF2 has been reported to regulate the expression of this muscle specific subunit of cytochrome c oxidase (COX), which forms the terminal enzyme complex of the mitochondrial electron transport chain (complex IV) [19]. Lack of this COX subunit is sufficient to cause cardiac dysfunction [19, 20]. After TAC, Cox6a2 expression levels increase in MHC-Cre, but not in MHC-Cre/FloxDNMEF2 mice. We also measured the complex IV activity in the heart of these animals. Corrected for the number of mitochondria present in the tissue (i.e. the CS activity), complex IV activity is increased in MHC-Cre mice after TAC, but this increase is not observed in MHC-Cre/FloxDNMEF2 TAC mice (Figure 4D).

Taken together, postnatal inhibition of MEF2 transcriptional activity in the heart affects mitochondrial biogenesis, making the heart more prone to decompensation.

DISCUSSION

Earlier work has demonstrated that MEF2 is involved in the development of postnatal heart disease. Although MEF2 was believed to be a prohypertrophic transcription factor, our recent data have demonstrated that MEF2 activation is more likely involved in provoking cardiac dilation instead of hypertrophy [9, 10]. It was, however, unknown if the heart is able to withstand stress induced by a pathophysiological trigger, such as pressure overload, when MEF2 transciptional activity is inhibited. The results of this study demonstrate a protective role for MEF2 transcription factors in the response of the heart to pressure overload related to their role in adapting energy metabolism in the stressed myocardium.

A striking observation was the decrease in cardiac function in DNMEF2 mice at 5 weeks of pressure overload, when compared to TAC control animals. To characterize this phenomenon, we assessed changes in PGC-1α transcript levels,

demonstrating a decrease in PGC-1α expression after TAC and a lower level of PGC-1α transcripts in sham-operated DNMEF2 mice when compared to wildtype counterparts. Normally, PGC-1α expression is upregulated in response to increased energy demand. In skeletal muscle, swimming exercise results in activation of PGC-1α expression [21]. However, earlier studies have already described a decreased PGC-1α expression in response to aortic banding [16, 18, 22, 23], or in other models for cardiac disease [24, 25]. Furthermore, it has been demonstrated that MEF2 binds to and activates the PGC-1α promoter, especially when coactivated with PGC-1α itself [24, 26]. Disruption of this autoregulatory loop by inhibition of MEF2 transcriptional activity would be a plausible explanation for the lower PGC-1α transcript levels observed in our DNMEF2 mice at basal conditions. The basal reduction in PGC-1α expression is likely to accelerate heart failure development in DNMEF2 mice after aortic banding, as it has been shown that a certain threshold level of PGC-1α is critical for the heart to cope with enhanced stress [17, 18]. As PGC-1α is known to be the key regulator of mitochondrial biogenesis, the impaired cardiac adaptation could be caused by a decrease in functional mitochondria. In line, CS activity measurements support this notion.

Further investigation of mitochondrial function demonstrated enhanced activity of the electron transport chain, as measured by Cox6a2 expression and complex IV activity, in control mice after TAC. We interpret this upregulation as a compensatory response for the decline in mitochondrial number, which could not be observed in the setting of MEF2 inhibition. Indeed, expression of Cox6a2, a muscle specific subunit of complex IV, has been found to be regulated by MEF2 [19]. In line, gene ablation of this COX isoform results in spontaneous cardiac dysfunction in mice [20]. In contradiction to our findings, other studies have shown a decrease in activity of the electron transport chain and a decline in expression of different COX subunits associated with reduced PGC-1α expression after cardiac stress induction [18, 22, 25]. A possible explanation for this divergence lies in the duration of cardiac stress. Where we have chosen to perform genetic and functional analysis 5 weeks after stress initiation, a time point at which the heart may exhibit a mixture of both adaptive and maladaptive remodeling, analysis in the other studies was undertaken at 2 or even 6 months after aortic banding, when cardiac decompensation is more pronounced.

The results of this study are in sharp contrast with our previous report, where reduced MEF2 transcriptional activity in mice overexpressing an activated form of calcineurin in the heart resulted in inhibition of maladaptive cardiac remodeling [10]. Pressure overload and the associated mechanical stress, however, triggers the release and/or expression of several growth factors and hormones, including endothelin 1, angiotensin II, insulin like growth factor, transforming growth factor-β,

fibroblast growth factor, and cardiotrophin-1, resulting in the activation of a multiplicity of intracellular signaling cascades besides calcineurin signaling [2, 27, 28]. At least three signaling pathways besides calcineurin can impinge upon MEF2 factors, including p38 MAPK, diverse forms of calcium/calmodulin-dependent protein kinase (CaMK), and certain forms of protein kinase C [2, 5, 6]. Accordingly, nature and number of MEF2 target genes downstream of cardiac calcineurin activation may differ substantially from those target genes activated in the setting of pressure overload. We postulate that in the setting of an active calcineurin transgene, any adverse metabolic effects may have a minimal role, if any, compared to the more complex setting of biomechanical stress. Furthermore, calcineurin activation has been described to induce PGC-1α expression in skeletal muscle [29]. In line, we have not observed differential expression of PGC-1α when comparing gene expression profiles between calcineurin transgenic hearts in the presence or absence of the DNMEF2 transgene [10], suggesting at least one rationale for the differential effects between this study and our earlier observations. Conclusively, data in this report demonstrate that MEF2 inhibition, although it is beneficial downstream of sole calcineurin activation, results in enhanced cardiac dysfunction due to impaired mitochondrial adaptation in the broad setting of pressure overload.

ACKNOWLEDGEMENTS

The authors would like to thank Martin Taube and Jeroen Korving for technical assistance.

REFERENCES

1. Frey N., Olson E.N. Cardiac hypertrophy: the good, the bad, and the ugly. Annu Rev Physiol 2003;65:45-79.
2. Heineke J., Molkentin J.D. Regulation of cardiac hypertrophy by intracellular signalling pathways. Nat Rev Mol Cell Biol 2006;7(8):589-600.
3. Passier R., Zeng H., Frey N., Naya F.J., Nicol R.L., McKinsey T.A., Overbeek P., Richardson J.A., Grant S.R., Olson E.N. CaM kinase signaling induces cardiac hypertrophy and activates the MEF2 transcription factor in vivo. J Clin Invest 2000;105(10):1395-406.
4. Naya F.J., Black B.L., Wu H., Bassel-Duby R., Richardson J.A., Hill J.A., Olson E.N. Mitochondrial deficiency and cardiac sudden death in mice lacking the MEF2A transcription factor. Nat Med 2002;8(11):1303-9.
5. McKinsey T.A., Olson E.N. Toward transcriptional therapies for the failing heart: chemical screens to modulate genes. J Clin Invest 2005;115(3):538-46.

6. Frey N., Katus H.A., Olson E.N., Hill J.A. Hypertrophy of the heart: a new therapeutic target? Circulation 2004;109(13):1580-9.
7. Nadruz W., Jr., Kobarg C.B., Constancio S.S., Corat P.D., Franchini K.G. Load-induced transcriptional activation of c-jun in rat myocardium: regulation by myocyte enhancer factor 2. Circ Res 2003;92(2):243-51.
8. Molkentin J.D., Markham B.E. Myocyte-specific enhancer-binding factor (MEF-2) regulates alpha-cardiac myosin heavy chain gene expression in vitro and in vivo. J Biol Chem 1993;268(26):19512-20.
9. Xu J., Gong N.L., Bodi I., Aronow B.J., Backx P.H., Molkentin J.D. Myocyte enhancer factors 2A and 2C induce dilated cardiomyopathy in transgenic mice. J Biol Chem 2006;281(14):9152-62.
10. van Oort R.J., van Rooij E., Bourajjaj M., Schimmel J., Jansen M.A., van der Nagel R., Doevendans P.A., Schneider M.D., van Echteld C.J., De Windt L.J. MEF2 activates a genetic program promoting chamber dilation and contractile dysfunction in calcineurin-induced heart failure. Circulation 2006;114(4):298-308.
11. Agah R., Frenkel P.A., French B.A., Michael L.H., Overbeek P.A., Schneider M.D. Gene recombination in postmitotic cells. Targeted expression of Cre recombinase provokes cardiac-restricted, site-specific rearrangement in adult ventricular muscle in vivo. J Clin Invest 1997;100(1):169-79.
12. Rockman H.A., Ross R.S., Harris A.N., Knowlton K.U., Steinhelper M.E., Field L.J., Ross J., Jr., Chien K.R. Segregation of atrial-specific and inducible expression of an atrial natriuretic factor transgene in an in vivo murine model of cardiac hypertrophy. Proc Natl Acad Sci U S A 1991;88(18):8277-81.
13. Birch-Machin M.A., Turnbull D.M. Assaying mitochondrial respiratory complex activity in mitochondria isolated from human cells and tissues. Methods Cell Biol 2001;65:97-117.
14. Cooper G.t. Basic determinants of myocardial hypertrophy: a review of molecular mechanisms. Annu Rev Med 1997;48:13-23.
15. Goffart S., von Kleist-Retzow J.C., Wiesner R.J. Regulation of mitochondrial proliferation in the heart: power-plant failure contributes to cardiac failure in hypertrophy. Cardiovasc Res 2004;64(2):198-207.
16. Finck B.N., Kelly D.P. PGC-1 coactivators: inducible regulators of energy metabolism in health and disease. J Clin Invest 2006;116(3):615-22.
17. Czubryt M.P., McAnally J., Fishman G.I., Olson E.N. Regulation of peroxisome proliferator-activated receptor gamma coactivator 1 alpha (PGC-1 alpha) and mitochondrial function by MEF2 and HDAC5. Proc Natl Acad Sci U S A 2003;100(4):1711-6.
18. Arany Z., Novikov M., Chin S., Ma Y., Rosenzweig A., Spiegelman B.M. Transverse aortic constriction leads to accelerated heart failure in mice lacking PPAR-gamma coactivator 1alpha. Proc Natl Acad Sci U S A 2006;103(26):10086-91.
19. Wan B., Moreadith R.W. Structural characterization and regulatory element analysis of the heart isoform of cytochrome c oxidase VIa. J Biol Chem 1995;270(44):26433-40.
20. Radford N.B., Wan B., Richman A., Szczepaniak L.S., Li J.L., Li K., Pfeiffer K., Schagger H., Garry D.J., Moreadith R.W. Cardiac dysfunction in mice lacking cytochrome-c oxidase subunit VIaH. Am J Physiol Heart Circ Physiol 2002;282(2):H726-33.
21. Baar K., Wende A.R., Jones T.E., Marison M., Nolte L.A., Chen M., Kelly D.P., Holloszy J.O. Adaptations of skeletal muscle to exercise: rapid increase in the transcriptional coactivator PGC-1. Faseb J 2002;16(14):1879-86.
22. Garnier A., Fortin D., Delomenie C., Momken I., Veksler V., Ventura-Clapier R. Depressed mitochondrial transcription factors and oxidative capacity in rat failing cardiac and skeletal muscles. J Physiol 2003;551(Pt 2):491-501.

23. Czubryt M.P., Olson E.N. Balancing contractility and energy production: the role of myocyte enhancer factor 2 (MEF2) in cardiac hypertrophy. Recent Prog Horm Res 2004;59:105-24.
24. Sano M., Wang S.C., Shirai M., Scaglia F., Xie M., Sakai S., Tanaka T., Kulkarni P.A., Barger P.M., Youker K.A., Taffet G.E., Hamamori Y., Michael L.H., Craigen W.J., Schneider M.D. Activation of cardiac Cdk9 represses PGC-1 and confers a predisposition to heart failure. Embo J 2004;23(17):3559-69.
25. van den Bosch B.J., van den Burg C.M., Schoonderwoerd K., Lindsey P.J., Scholte H.R., de Coo R.F., van Rooij E., Rockman H.A., Doevendans P.A., Smeets H.J. Regional absence of mitochondria causing energy depletion in the myocardium of muscle LIM protein knockout mice. Cardiovasc Res 2005;65(2):411-8.
26. Handschin C., Rhee J., Lin J., Tarr P.T., Spiegelman B.M. An autoregulatory loop controls peroxisome proliferator-activated receptor gamma coactivator 1alpha expression in muscle. Proc Natl Acad Sci U S A 2003;100(12):7111-6.
27. Ruwhof C., van der Laarse A. Mechanical stress-induced cardiac hypertrophy: mechanisms and signal transduction pathways. Cardiovasc Res 2000;47(1):23-37.
28. Brancaccio M., Fratta L., Notte A., Hirsch E., Poulet R., Guazzone S., De Acetis M., Vecchione C., Marino G., Altruda F., Silengo L., Tarone G., Lembo G. Melusin, a muscle-specific integrin beta1-interacting protein, is required to prevent cardiac failure in response to chronic pressure overload. Nat Med 2003;9(1):68-75.
29. Chin E.R., Olson E.N., Richardson J.A., Yang Q., Humphries C., Shelton J.M., Wu H., Zhu W., Bassel-Duby R., Williams R.S. A calcineurin-dependent transcriptional pathway controls skeletal muscle fiber type. Genes Dev 1998;12(16):2499-509.

Chapter 6

General discussion

GENERAL DISCUSSION

Although MEF2 has been described as a common end-point for several prohypertrophic signaling cascades in the heart [1-3], the direct consequences of MEF2 activation in cardiac muscle remained to be demonstrated. The aim of this thesis was to dissect the functional role of MEF2 in the development of cardiac hypertrophy and heart failure.

One central pathway that transduces intracellular prohypertrophic signals in heart muscle employs the Ca^{2+} activated phosphatase calcineurin [4]. MEF2 transcription factors are activated downstream of cardiac calcineurin activity, but the precise mechanism of this activation remained to be determined [5, 6]. In this thesis, we demonstrated that MEF2 transcriptional activity in the heart is induced by recruiting the well-described calcineurin target NFAT (Chapter 2), a process earlier identified in T-cells [7]. This observation is reminiscent of the cooperative interaction between MEF2 proteins and myogenic basic helix-loop-helix factors in skeletal muscles [8] and between MEF2 proteins and GATA factors in cardiac muscles [9], and it suggests that MEF2 factors interact with a range of transcription factors to optimize gene expression. Given the overlapping expression patterns of MEF2 and NFAT factors in smooth muscle, skeletal muscle, cardiac muscle, and the central nervous system, the NFAT/MEF2-dependent pathway described in this work suggests the existence of this molecular paradigm for Ca^{2+}/calmodulin signaling in excitable tissue.

We analyzed MEF2 transcription factor function in adult cardiac muscle, starting from the premise that MEF2 would be primarily involved in the initial hypertrophic remodeling phase of the heart muscle [10]. However, a Cre/LoxP-dependent approach to antagonize cardiac MEF2 transcriptional activity prevented calcineurin induced ventricular chamber dilation and cardiac dysfunction, with minor effects on cardiac growth (Chapter 2). Furthermore, transgenic mice overexpressing MEF2A in the heart displayed ventricular chamber dilation, an observation recently confirmed by others [11]. These results are in line with our data obtained from *in vitro* experiments, as we observed an elongated morphology of cultured cardiomyocytes associated with disassembly of myofibril components, which affected both M-band and Z-disc components, and redistribution of focal adhesion sites upon increasing MEF2 transcriptional activity (Chapter 3).

Many cardiomyopathic conditions share the common characteristic of myofibril degeneration, which contrasts the promotion of sarcomere organization during early phases of cardiac hypertrophy [12-14]. Alterations in myofibrillar architecture and focal adhesion sites are also observed in cardiomyocytes from MLP knockout mice and tropomodulin-overexpressing transgenic mice, two models with severe chamber dilation [15]. Cardiomyocytes from these mice present striking alterations

of their cell-matrix as well as their cell-cell contacts. Isolated myocytes from these cardiomyopathic models elicit a more irregular shape compared with their wild-type counterparts [16], which may serve to increase the number of focal contacts between neighboring cells. Specifically, the costameric protein vinculin showed patchy staining near the plasma membranes in MLP null cardiomyocytes compared with the regular well-ordered striations that are observed at the membrane of wildtype cardiomyocytes [16]. These differences in vinculin subcellular distribution resemble the changes observed in our study on vinculin localization in hypertrophic and elongated myocytes following MEF2 activation. Increased expression of extracellular matrix components, and a general upregulation of vinculin has also been described in patients with DCM [13, 17], suggesting that this phenomenon might not be restricted to mouse models for this disease.

Although overexpression of (truncated mutants of) transcription factors harbors the risk of unwanted transcriptional squelching, the consistency in opposite phenotypes we observed using our combinatorial dominant-negative versus gain-of-function models for MEF2 transcriptional activity justifies the overall conclusions drawn in this thesis. These results suggest that MEF2 promotes symptoms that are more compatible with later manifestations of cardiac disease, which extend beyond and stem from initial pathological cardiac growth, namely chamber dilation, mechanical dysfunction, and end-stage heart failure. This conclusion is further underlined by microarray analyses described in Chapter 2 and 3, which were performed to gain mechanistic insights into the cardiomyopathic remodeling processes. Namely, the classification profiles of MEF2 target genes secondary to cardiac calcineurin stress signaling correlate well with those observed in gene chip analysis of human end-stage idiopathic dilated cardiomyopathy [18] and with the most characteristic pathological features of human end-stage dilated cardiomyopathy, which include a dynamic redistribution of cytoskeletal structures, extensive fibrosis, and extracellular alterations in mitochondria number and morphology [13]. In contrast, the classification profiles of MEF2 target genes identified revealed surprisingly little overlap with those observed with massive hypertrophic remodeling in early pressure overload (http://cardiogenomics.med.harvard.edu). The mere existence of a genetic pathway specifically underlying ventricular dilation will be of fundamental clinical and therapeutic interest.

One very interesting gene identified in this thesis by microarray analysis, using an inducible MEF2 activity assay in a novel cardiomyocyte cell line [19] to screen for early target genes, is myotonic dystrophy protein kinase (DMPK). We demonstrated that DMPK is a direct transcriptional target of MEF2 and, more importantly, that knockdown of DMPK expression was sufficient to inhibit cardiomyocyte elongation and sarcomere disassembly in response to elevated MEF2 activity (Chapter 3). The progression of the inherited neuromuscular disease

myotonic dystrophy 1 involves an expansion of untranslated CTG repeats in the 3' prime UTR of *dmpk*, which is believed to result in a pathological accumulation of RNA in the nucleus [20, 21]. However, the cardiac DM1 pathology may be more directly due to increased DMPK protein levels, rather than RNA toxicity [22]. In line, transgenic overexpression of DMPK in murine muscle evokes a heart failure phenotype associated with extensive myocyte disarray and interstitial fibrosis [23]. In this thesis, we identify DMPK as a direct transcriptional target of MEF2, promoting myocyte elongation, myofibril degeneration and polarized focal adhesion redistribution, changes of the heart muscle, which are characteristic of dilated cardiomyopathy, and we postulate that DMPK may serve as a promising therapeutic target for cardiomyopathic conditions.

Given the similarities between the aspects of MEF2 induced cardiomyocyte remodeling and the cardiac phenotype of MLP knockout mice [16, 24], we examined the activation levels of MEF2 in MLP deficient hearts (Chapter 4). Expression of a MEF2 reporter transgene [25] was significantly enhanced in the absence of MLP protein. Although the molecular mechanism underlying this activation is unclear, plausible explanations do exist. Disruption of the gene for MLP leads to impaired cytoskeletal organization in cardiomyocytes [24]. Although the mechanistical link between disturbances of the cytoskeleton in individual cardiomyocytes and the progression to dilated cardiomyopathy is unclear, several studies have reported the involvement of impaired intracellular calcium homeostasis [26-28]. This could underlie the observed increase in MEF2 activity, as MEF2 is a well-known downstream effector of calcium signaling [1, 3]. In addition, calsarcin-1 has been found to interact with calcineurin at the Z-disc and mice lacking calsarcin-1 protein are sensitized to calcineurin signaling and display an accelerated progression to cardiomyopathy [29]. Calcineurin is known to activate MEF2 transcriptional activity in the heart [30]. Loss of Z-disc integrity by MLP deficiency has also been described to result in decreased calcineurin compartmentalization, although this was thought to result in inhibition of calcineurin activity [31].

Since cardiac MEF2 activity was strongly enhanced in homozygous MLP knockout mice, we analyzed whether MEF2 inhibition strategies would attenuate the severe dilated cardiomyopathy in this relevant mouse model. As our approach to inhibit MEF2 activity did not result in improvement of the dilated cardiac phenotype, we conclude that pathological cardiac remodeling in MLP deficient mice is independent of MEF2. Mechanistically, expression levels of DMPK, a MEF2 transcriptional target involved in maladaptive cardiomyocyte remodeling (Chapter 3), are unchanged in hearts from MLP knockout mice. Nevertheless, we cannot fully exclude that the inactivation potential of the dominant-negative transgene is insufficient to cope with the dramatic increase in MEF2 activity observed in hearts

of MLP deficient mice and that MEF2 target genes, other than DMPK, may be responsible for the onset of dilated cardiomyopathy in the MLP deficient myocardium.

Next, we tested whether MEF2 would be involved in the genesis of dilation and severe cardiac dysfunction following a pathophysiological trigger, such as sustained biomechanical stress (Chapter 5). Therefore, we used our *in vivo* MEF2 inhibitory strategy in pressure overload conditions (TAC). Unexpectedly, we observed a clear decrease in cardiac function in DNMEF2 mice at 5 weeks of pressure overload. Examination of PGC-1α transcript levels provided mechanistical insights into this phenomenon, as this demonstrated a decrease in PGC-1α expression after TAC and a lower level of PGC-1α transcripts in sham-operated DNMEF2 mice when compared to wildtype counterparts. PGC-1α expression is often upregulated in response to increased energy demand. In skeletal muscle, for example, swimming exercise results in activation of PGC-1α expression [32]. Nevertheless, earlier studies have reported decreased PGC-1α expression in response to aortic banding or in other models for cardiac disease [33-38]. MEF2 is known to bind and activate the PGC-1α promoter, especially when coactivated with PGC-1α itself [39]. Disruption of this autoregulatory loop by inhibition of MEF2 transcriptional activity would be a plausible explanation for the lower PGC-1α transcript levels observed in our DNMEF2 mice at basal conditions. Furthermore, this basal reduction in PGC-1α expression can explain the accelerated heart failure development in DNMEF2 mice after aortic banding, as it has been shown that a certain threshold level of PGC-1α is critical for the heart to cope with enhanced stress [34, 40]. As PGC-1α is known to be the key regulator of mitochondrial biogenesis, the impaired cardiac adaptation in DNMEF2 mice could be caused by a decrease in functional mitochondria.

Conclusively, data in Chapter 5 demonstrate that MEF2 inhibition, although it is clearly beneficial downstream of exclusive calcineurin activation, results in enhanced cardiac dysfunction due to impaired mitochondrial adaptation in the broad setting of pressure overload, and questions the use of MEF2 as a therapeutic target for cardiac disease.

REFERENCES

1. Frey N., Katus H.A., Olson E.N., Hill J.A. Hypertrophy of the heart: a new therapeutic target? Circulation 2004;109(13):1580-9.
2. McKinsey T.A., Olson E.N. Toward transcriptional therapies for the failing heart: chemical screens to modulate genes. J Clin Invest 2005;115(3):538-46.
3. Heineke J., Molkentin J.D. Regulation of cardiac hypertrophy by intracellular signalling pathways. Nat Rev Mol Cell Biol 2006;7(8):589-600.

4. Wilkins B.J., Molkentin J.D. Calcium-calcineurin signaling in the regulation of cardiac hypertrophy. Biochem Biophys Res Commun 2004;322(4):1178-91.
5. Zhang C.L., McKinsey T.A., Chang S., Antos C.L., Hill J.A., Olson E.N. Class II histone deacetylases act as signal-responsive repressors of cardiac hypertrophy. Cell 2002;110(4):479-88.
6. Passier R., Zeng H., Frey N., Naya F.J., Nicol R.L., McKinsey T.A., Overbeek P., Richardson J.A., Grant S.R., Olson E.N. CaM kinase signaling induces cardiac hypertrophy and activates the MEF2 transcription factor in vivo. J Clin Invest 2000;105(10):1395-406.
7. Youn H.D., Chatila T.A., Liu J.O. Integration of calcineurin and MEF2 signals by the coactivator p300 during T-cell apoptosis. Embo J 2000;19(16):4323-31.
8. Molkentin J.D., Olson E.N. Combinatorial control of muscle development by basic helix-loop-helix and MADS-box transcription factors. Proc Natl Acad Sci U S A 1996;93(18):9366-73.
9. Morin S., Charron F., Robitaille L., Nemer M. GATA-dependent recruitment of MEF2 proteins to target promoters. Embo J 2000;19(9):2046-55.
10. Olson E.N., Schneider M.D. Sizing up the heart: development redux in disease. Genes Dev 2003;17(16):1937-56.
11. Xu J., Gong N.L., Bodi I., Aronow B.J., Backx P.H., Molkentin J.D. Myocyte enhancer factors 2A and 2C induce dilated cardiomyopathy in transgenic mice. J Biol Chem 2006;281(14):9152-62.
12. Mann D.L., Urabe Y., Kent R.L., Vinciguerra S., Cooper G.t. Cellular versus myocardial basis for the contractile dysfunction of hypertrophied myocardium. Circ Res 1991;68(2):402-15.
13. Schaper J., Froede R., Hein S., Buck A., Hashizume H., Speiser B., Friedl A., Bleese N. Impairment of the myocardial ultrastructure and changes of the cytoskeleton in dilated cardiomyopathy. Circulation 1991;83(2):504-14.
14. Beltrami C.A., Finato N., Rocco M., Feruglio G.A., Puricelli C., Cigola E., Sonnenblick E.H., Olivetti G., Anversa P. The cellular basis of dilated cardiomyopathy in humans. J Mol Cell Cardiol 1995;27(1):291-305.
15. Sussman M.A., Welch S., Cambon N., Klevitsky R., Hewett T.E., Price R., Witt S.A., Kimball T.R. Myofibril degeneration caused by tropomodulin overexpression leads to dilated cardiomyopathy in juvenile mice. J Clin Invest 1998;101(1):51-61.
16. Ehler E., Horowits R., Zuppinger C., Price R.L., Perriard E., Leu M., Caroni P., Sussman M., Eppenberger H.M., Perriard J.C. Alterations at the intercalated disk associated with the absence of muscle LIM protein. J Cell Biol 2001;153(4):763-72.
17. Wilke A., Schonian U., Herzum M., Hengstenberg C., Hufnagel G., Brilla C.G., Maisch B. [The extracellular matrix and cytoskeleton of the myocardium in cardiac inflammatory reaction]. Herz 1995;20(2):95-108.
18. Grzeskowiak R., Witt H., Drungowski M., Thermann R., Hennig S., Perrot A., Osterziel K.J., Klingbiel D., Scheid S., Spang R., Lehrach H., Ruiz P. Expression profiling of human idiopathic dilated cardiomyopathy. Cardiovasc Res 2003;59(2):400-11.
19. Rybkin, II, Markham D.W., Yan Z., Bassel-Duby R., Williams R.S., Olson E.N. Conditional expression of SV40 T-antigen in mouse cardiomyocytes facilitates an inducible switch from proliferation to differentiation. J Biol Chem 2003;278(18):15927-34.
20. Davis B.M., McCurrach M.E., Taneja K.L., Singer R.H., Housman D.E. Expansion of a CUG trinucleotide repeat in the 3' untranslated region of myotonic dystrophy protein kinase transcripts results in nuclear retention of transcripts. Proc Natl Acad Sci U S A 1997;94(14):7388-93.
21. Mahadevan M., Tsilfidis C., Sabourin L., Shutler G., Amemiya C., Jansen G., Neville C., Narang M., Barcelo J., O'Hoy K., et al. Myotonic dystrophy mutation: an unstable

CTG repeat in the 3' untranslated region of the gene. Science 1992;255(5049):1253-5.
22. Mahadevan M.S., Yadava R.S., Yu Q., Balijepalli S., Frenzel-McCardell C.D., Bourne T.D., Phillips L.H. Reversible model of RNA toxicity and cardiac conduction defects in myotonic dystrophy. Nat Genet 2006;38(9):1066-70.
23. O'Cochlain D.F., Perez-Terzic C., Reyes S., Kane G.C., Behfar A., Hodgson D.M., Strommen J.A., Liu X.K., van den Broek W., Wansink D.G., Wieringa B., Terzic A. Transgenic overexpression of human DMPK accumulates into hypertrophic cardiomyopathy, myotonic myopathy and hypotension traits of myotonic dystrophy. Hum Mol Genet 2004;13(20):2505-18.
24. Arber S., Hunter J.J., Ross J., Jr., Hongo M., Sansig G., Borg J., Perriard J.C., Chien K.R., Caroni P. MLP-deficient mice exhibit a disruption of cardiac cytoarchitectural organization, dilated cardiomyopathy, and heart failure. Cell 1997;88(3):393-403.
25. Naya F.J., Wu C., Richardson J.A., Overbeek P., Olson E.N. Transcriptional activity of MEF2 during mouse embryogenesis monitored with a MEF2-dependent transgene. Development 1999;126(10):2045-52.
26. Su Z., Yao A., Zubair I., Sugishita K., Ritter M., Li F., Hunter J.J., Chien K.R., Barry W.H. Effects of deletion of muscle LIM protein on myocyte function. Am J Physiol Heart Circ Physiol 2001;280(6):H2665-73.
27. Rockman H.A., Chien K.R., Choi D.J., Iaccarino G., Hunter J.J., Ross J., Jr., Lefkowitz R.J., Koch W.J. Expression of a beta-adrenergic receptor kinase 1 inhibitor prevents the development of myocardial failure in gene-targeted mice. Proc Natl Acad Sci U S A 1998;95(12):7000-5.
28. Minamisawa S., Hoshijima M., Chu G., Ward C.A., Frank K., Gu Y., Martone M.E., Wang Y., Ross J., Jr., Kranias E.G., Giles W.R., Chien K.R. Chronic phospholamban-sarcoplasmic reticulum calcium ATPase interaction is the critical calcium cycling defect in dilated cardiomyopathy. Cell 1999;99(3):313-22.
29. Frey N., Barrientos T., Shelton J.M., Frank D., Rutten H., Gehring D., Kuhn C., Lutz M., Rothermel B., Bassel-Duby R., Richardson J.A., Katus H.A., Hill J.A., Olson E.N. Mice lacking calsarcin-1 are sensitized to calcineurin signaling and show accelerated cardiomyopathy in response to pathological biomechanical stress. Nat Med 2004;10(12):1336-43.
30. van Oort R.J., van Rooij E., Bourajjaj M., Schimmel J., Jansen M.A., van der Nagel R., Doevendans P.A., Schneider M.D., van Echteld C.J., De Windt L.J. MEF2 activates a genetic program promoting chamber dilation and contractile dysfunction in calcineurin-induced heart failure. Circulation 2006;114(4):298-308.
31. Heineke J., Ruetten H., Willenbockel C., Gross S.C., Naguib M., Schaefer A., Kempf T., Hilfiker-Kleiner D., Caroni P., Kraft T., Kaiser R.A., Molkentin J.D., Drexler H., Wollert K.C. Attenuation of cardiac remodeling after myocardial infarction by muscle LIM protein-calcineurin signaling at the sarcomeric Z-disc. Proc Natl Acad Sci U S A 2005;102(5):1655-60.
32. Baar K., Wende A.R., Jones T.E., Marison M., Nolte L.A., Chen M., Kelly D.P., Holloszy J.O. Adaptations of skeletal muscle to exercise: rapid increase in the transcriptional coactivator PGC-1. Faseb J 2002;16(14):1879-86.
33. Garnier A., Fortin D., Delomenie C., Momken I., Veksler V., Ventura-Clapier R. Depressed mitochondrial transcription factors and oxidative capacity in rat failing cardiac and skeletal muscles. J Physiol 2003;551(Pt 2):491-501.
34. Arany Z., Novikov M., Chin S., Ma Y., Rosenzweig A., Spiegelman B.M. Transverse aortic constriction leads to accelerated heart failure in mice lacking PPAR-gamma coactivator 1alpha. Proc Natl Acad Sci U S A 2006;103(26):10086-91.
35. Czubryt M.P., Olson E.N. Balancing contractility and energy production: the role of myocyte enhancer factor 2 (MEF2) in cardiac hypertrophy. Recent Prog Horm Res 2004;59:105-24.

36. Finck B.N., Kelly D.P. PGC-1 coactivators: inducible regulators of energy metabolism in health and disease. J Clin Invest 2006;116(3):615-22.
37. Sano M., Wang S.C., Shirai M., Scaglia F., Xie M., Sakai S., Tanaka T., Kulkarni P.A., Barger P.M., Youker K.A., Taffet G.E., Hamamori Y., Michael L.H., Craigen W.J., Schneider M.D. Activation of cardiac Cdk9 represses PGC-1 and confers a predisposition to heart failure. Embo J 2004;23(17):3559-69.
38. van den Bosch B.J., van den Burg C.M., Schoonderwoerd K., Lindsey P.J., Scholte H.R., de Coo R.F., van Rooij E., Rockman H.A., Doevendans P.A., Smeets H.J. Regional absence of mitochondria causing energy depletion in the myocardium of muscle LIM protein knockout mice. Cardiovasc Res 2005;65(2):411-8.
39. Handschin C., Rhee J., Lin J., Tarr P.T., Spiegelman B.M. An autoregulatory loop controls peroxisome proliferator-activated receptor gamma coactivator 1alpha expression in muscle. Proc Natl Acad Sci U S A 2003;100(12):7111-6.
40. Czubryt M.P., McAnally J., Fishman G.I., Olson E.N. Regulation of peroxisome proliferator-activated receptor gamma coactivator 1 alpha (PGC-1 alpha) and mitochondrial function by MEF2 and HDAC5. Proc Natl Acad Sci U S A 2003;100(4):1711-6.

SAMENVATTING

Hartfalen is een aandoening waarbij het hart niet meer in staat is om genoeg bloed te pompen om aan de behoefte van het lichaam te voldoen. Het hart reageert op stress signalen, zoals een hartinfarct of een chronisch verhoogde bloeddruk, door te groeien (hypertrofie). Hypertrofie is in eerste instantie vaak een goede aanpassing van het hart om beter te kunnen samentrekken, maar door een nog onbekend mechanisme resulteert hypertrofie in een later stadium vaak in hartfalen, waarbij de hartwanden heel dun zijn en het hart slecht klopt. Er is op dit moment echter nog niet veel bekend over de signalen in de hartspiercel die hypertrofie en hartfalen veroorzaken. Een aantal van de bekende pro-hypertrofe signalen in de hartspiercel komen samen in de kern van de cel op de transcriptie factor myocyte enhancer factor-2 (MEF2), die alleen of samen met andere transcriptiefactoren bepaalde in het DNA gelegen genen kan activeren. In dit promotieonderzoek is de rol van MEF2 en van MEF2 gereguleerde genen tijdens de ontwikkeling van hypertrofie en hartfalen onderzocht.

Een belangrijk eiwit, dat hypertrofie veroorzakende signalen doorgeeft in de spiercellen van het hart, is het door calcium geactiveerde calcineurine. Van calcineurine is bekend dat het MEF2 kan activeren, maar men weet niet hoe deze activatie plaats vindt en niet wat het effect is van deze activatie. In hoofdstuk 2 tonen we aan dat calcineurine MEF2 kan activeren door het te laten binden aan een beter bekende calcineurine-gevoelige transcriptiefactor, genaamd NFAT. Hoewel van NFAT bekend is dat activatie leidt tot een hypertrofe respons van het hart, bleek dit voor MEF2 niet het geval. Remming van MEF2 activiteit in genetisch gemodificeerde muizen met extra actief calcineurine resulteerde niet in de remming van hypertrofie. Wel bleek MEF2 remming de ontwikkeling van hartfalen tegen te gaan in deze muizen. MEF2 remming verminderde namelijk de verwijding van de hartkamers (dilatatie) en het dunner worden van de hartwand. Door middel van MRI analyse hebben we laten zien dat MEF2 remming ook leidt tot een verbeterde hartfunctie in calcineurine muizen. Het feit dat MEF2 nauwelijks betrokken lijkt te zijn bij de ontwikkeling van hypertrofie, maar wel een rol speelt tijdens de overgang naar hartfalen werd bevestigd in muizen met meer MEF2 in het hart. De hartjes van deze muizen waren niet hypertroof, maar hadden wel verwijde kamers en dunne wanden.

In hoofdstuk 3 hebben we het effect van MEF2 activatie in individuele hartspiercellen verder onderzocht. In deze studie hebben we MEF2 geactiveerd in gekweekte hartspiercellen. Deze cellen vertoonden na 2 dagen dezelfde karakteristieken als cellen in falende harten; de cellen waren langer en dunner en vertoonden afbraak van de sarcomeer, een onderdeel van de cel dat nodig is voor het samentrekken van de spier. Met behulp van de microarray techniek hebben we

geanalyseerd welke genen door MEF2 geactiveerd worden. Eén van de direct door MEF2 geactiveerde genen die we gevonden hebben is DMPK. Van dit eiwit is bekend dat het een rol speelt in het ontstaan van een specifieke skeletspier aandoening. Het tegen houden van nieuwe DMPK aanmaak in de gekweekte hartspiercellen bleek de door MEF2 veroorzaakte elongatie en sarcomeer afbraak te remmen. DMPK speelt dus waarschijnlijk een belangrijke rol in de pathologische verandering van hartspiercellen tijdens hartfalen.

Vanwege de sterke gelijkenis tussen hartjes van MEF2 transgene muizen en van muizen die het eiwit MLP missen (de MLP knockout muis), een model voor een erfelijke vorm van hartfalen, hebben we in hoofdstuk 4 onderzocht of MEF2 een rol zou kunnen spelen in erfelijke vormen van hartfalen. Door MLP knockout muizen te kruisen met zogeheten MEF2 reporter muizen hebben we aangetoond dat MEF2 activiteit inderdaad erg verhoogd is in de afwezigheid van MLP. Echocardiografie liet echter zien dat remming van MEF2 activiteit niet leidt tot verminderde dilatie of tot functie verbetering van het hart in MLP knockout muizen.

Daar een chronisch verhoogde bloeddruk een risicofactor is voor de ontwikkeling van hartfalen hebben we in hoofdstuk 5 onderzoek gedaan naar de effecten van MEF2 remming in een muismodel voor verhoogde bloeddruk. In tegenstelling tot de positieve effecten van MEF2 remming in de calcineurine muis, resulteerde MEF2 remming niet in functie verbeteringen van het hart tijdens verhoogde bloeddruk. Het functioneren van deze hartjes bleek zelfs iets slechter te zijn na MEF2 inactivatie. Verder onderzoek toonde aan dat dit zou kunnen komen omdat afwezigheid van MEF2 activiteit de nodige aanpassingen in energie huishouding in het hart tegenwerkt, in het geval van aanhoudende hoge bloeddruk.

Samenvattend hebben we in dit proefschrift aangetoond dat MEF2 activatie in het hart niet verantwoordelijk is voor het ontstaan van hypertrofie van het hart, maar direct kan leiden tot de ontwikkeling van hartfalen. MEF2 remming lijkt echter niet de beste therapie tegen hartfalen, omdat een basale MEF2 activiteit nodig is voor enkele gunstige aanpassingen van het hart tijdens stress. Verder onderzoek zou zich moeten richten op het onderscheiden van ‘goede’ en ‘slechte’ door MEF2 geactiveerde genen. Toekomstige therapeutische strategieën zouden gebruik kunnen maken van remming van de ‘slechte’ MEF2 gereguleerde genen, zoals wellicht DMPK.

DANKWOORD

Vier jaar klinkt lang? Dat is het niet als je in die tijd een proefschrift bij elkaar wilt pipetteren. Dit waren mijn kortste vier jaren tot nu toe. Kijk ik echter terug naar mijn eerste dag in het Hubrecht en naar de dag van vandaag, dan snap ik juist weer niet dat daar slechts vier jaar tussen zit. Ik heb in deze periode meer geleerd dan ik voor mogelijk hield en ook nog eens een hoop lol gehad. Ik ben dan ook een groot aantal mensen dankbaar voor het feit dat mijn promotietijd zo leuk en leerzaam was.

Mijn eerste dank gaat uit naar mijn dagelijkse begeleider en leermeester. Leon, jij hebt er met jouw ongekende wetenschappelijke kennis, inzicht, ideeën, advies, en hulp voor gezorgd dat deze tijd zo effectief was. De lessen waren een heel enkele keer hard en begonnen, zoals je het zelf noemde, met een duik in de grote, diepe, onbekende oceaan, maar ik had op geen enkele manier meer kunnen leren dan nu. Het beloofde shirt heb ik nooit gehad, maar het motto zal me bij blijven: 'Just do it!'. Hans, bedankt dat jij, iemand die ik in wetenschappelijk opzicht zeer respecteer, mijn promotor wil zijn.

Heel veel dank gaat uit naar mijn labgenoten. Eva en Vanessa, jullie hebben mij de eerste tijd op het lab enorm wegwijs gemaakt. Vanessa, succes met je eigen promotie en ook in Houston hebben we wel een slaapplekje voor je! Roel, dat je met zulke letterlijk grote knuisten zulke letterlijk kleine (maar figuurlijk grote) dingen voor elkaar krijgt. Logistiek gezien vormden we een perfect duo; ik alle echo-benodigdheden, jij de pizza. Bedankt voor je hulp en enorme inzet. Joost en Melany, ik heb erg veel geluk gehad met zulke studenten. Jullie hebben me enorm geholpen. Joost, ik ben blij dat je je plekje hebt gevonden. Melany, succes met deze keuze. Anne, Anne-Sophie, Hamid, Meriem, Paula, Bart, Mara, Stephanos, bedankt voor al jullie hulp en gezelligheid in en buiten het lab. Eerst voor een deel ook nog op de kamer, later alleen op het lab, maar aan een goede sfeer hebben de 'Bakkertjes'; Ruben, Manon, Sonja, Jeroen, Emma, Kelly, Anne, Karel, Linda, Kristy, ook flink bijgedragen. Bedankt!

Ook buiten ons lab zijn er in het Hubrecht zoveel mensen, die het werk, op welke manier dan ook, veel makkelijker dan wel aangenamer hebben gemaakt. Iedereen op de eerste verdieping bedankt voor alle raad en reagentia. Jeroen, bedankt voor al je hulp wat betreft de transgene muizen en histologie. Alle dierverzorgers, hartelijk dank voor jullie inzet. Ook Janny en iedereen van de administratie, civiele dienst, automatisering en mediabereiding, bedankt. Natuurlijk wil ik ook iedereen, met of zonder bijnaam, bedanken voor alle lol tijdens de vrijdagmiddag- en andere borrels.

Een deel van het werk heeft plaats gevonden in het GDL. Ik wil Cees van Echteld bedanken voor deze mogelijkheid, Maurits voor zijn mooie MRI werk, en Marcel en Kees voor alle nuttige dingetjes en de koffie.

I'm very grateful to Elisabeth Ehler for her excellent help with confocal microscopy, for letting me happily wash 18 dishes full of little bastard cells at one go, and for the nice time in London.

Many thanks to Martin Bergmann and Martin Taube for all the help with echocardiography, and to everyone in the Bergmann group for the great time in Berlin.

Gelukkig zijn er ook mensen in mijn leven die niets met het werk te maken hebben, maar met wie ik in de Kuil of de Kooi een balletje kan trappen, een spelletje kan spelen, friet gyros met extra knoflooksaus kan eten, lekker kan eten, goed slechte films kan kijken, naar Lowlands kan, een hengeltje uit kan gooien, naar een concert kan, in het park kan hangen, op de bank kan hangen, naar de kroeg kan, naar een voetbalwedstrijd kan, naar de sauna kan, heerlijk slap kan ouwehoerrrrren, het veel te laat kan maken, en altijd een biertje kan drinken. Atze, Bert, Elias, Elize, Hannah, Hanneke, Jeroen, Joris, Leon, Mark, Mathilde, Mirjam, Nynke, Paul, Sander, laten we dit vooral blijven doen!

Ik zou nooit op dit punt aangekomen zijn zonder mijn familie. De Papa en de Mama, bedankt voor jullie onvoorwaardelijke liefde, steun, vertrouwen, en gegeven vrijheid. Masja, kusje van je grote broer. Martijn, DMK! Oma, bedankt voor alles en voor de gehaktballen. Opa, je blijft mijn beste vriend. Schoonfamilie, bedankt voor alle goede en leuke dingen.

Lieve Anita, ik kan niet omschrijven hoeveel jij voor mij betekent. Heb ik net mijn kortste 4 jaren achter de rug, ben ik nu begonnen aan mijn langste 3 maanden. Op dit moment mis ik je verschrikkelijk en kijk ik heel erg uit naar onze tijd samen in Houston. Daarna zien we wel weer en is alles goed, zolang we maar samen zijn.

Dus.

Ralph

CURRICULUM VITAE

Ralph Jeroen van Oort werd geboren op 25 april 1977 te Zoelen. In 1995 behaalde hij het VWO (Gymnasium) diploma op het GSG Lingecollege te Tiel, en ging hij Medische Biologie studeren aan de Universiteit Utrecht. In het kader van deze studie deed hij 2 onderzoeksstages. Zijn eerste stage was bij het Rudolf Magnus Instituut voor Neurowetenschappen in Utrecht, onder begeleiding van Dr. Govert Hoogland en Dr. Pierre de Graan. Zijn tweede stage werd uitgevoerd in het Interuniversitair Oogheelkundig Instituut in Amsterdam, onder begeleiding van Dr. Bob Nunes Cardozo en Dr. Maarten Kamermans. In april 2002 behaalde hij het doctoraal examen. In datzelfde jaar is hij begonnen als onderzoeker in opleiding in het Hubrecht Laboratorium onder begeleiding van Dr. Leon de Windt. De resultaten van dat onderzoek staan beschreven in dit proefschrift. Vanaf februari 2007 zal Ralph werkzaam zijn als postdoctoraal onderzoeker in de groep van Dr. Xander Wehrens van de afdeling Molecular Physiology and Biophysics van het Baylor College of Medicine in Houston.

LIST OF PUBLICATIONS

Hoogland G., **van Oort R.J.**, Proper E.A., Jansen G.H., van Rijen P.C., van Veelen C.W., van Nieuwenhuizen O., Troost D., de Graan P.N. Alternative splicing of glutamate transporter EAAT2 RNA in neocortex and hippocampus of temporal lobe epilepsy patients. *Epilepsy Res*. 2004;59(2-3):75-82.

van Oort R.J., De Windt L.J. TOLL-erating cardiac hypertrophy following pressure overload. *Cardiovasc Res*. 2005;68(2):178-9.

van Oort R.J.*, van Rooij E.*, Bourajjaj M., Schimmel J., Jansen M.A., van der Nagel R., Doevendans P.A., Schneider M.D., van Echteld C.J., De Windt L.J. MEF2 activates a genetic program promoting chamber dilation and contractile dysfunction in calcineurin-induced heart failure. *Circulation*. 2006;114(4):298-308. **authors contributed equally*

van Empel V.P.M., Bertrand A.T., **van Oort R.J.**, van der Nagel R., Engelen M., van Rijen H.V., Doevendans P.A., Crijns H.J.H., Ackerman S.L., Sluiter W., De Windt L.J. EUK-8, a superoxide dismutase and catalase mimetic, reduces oxidative stress and ameliorates pressure overload-induced heart failure in the harlequin mouse mutant. *J Am Coll Cardiol*. 2006;48(4):824-832.

van Oort R.J., Bourajjaj M., Schimmel J., van Oostrom M.C., van der Nagel R., Rybkin I.I., Bassel-Duby R., Olson E.N., Ehler E., De Windt L.J. MEF2 activates DMPK expression promoting cardiomyocyte elongation and sarcomere degeneration. *Submitted.*

van Oort R.J., van der Nagel R., Schneider M.D., Sluiter W., Bergmann M.W., De Windt L.J. MEF2 transcriptional activity is required for cardiac mitochondrial adaptation in pressure overload and protects against cardiac dysfunction. *Submitted.*